

**SIGNALING FROM MATRIX ELASTICITY AND TGF- β 1 TO CELLS OF
THE CARDIAC VALVE**

by

HUAN WANG

B.S., Zhejiang University 2006

A thesis submitted to the
Faculty of the Graduate School of the
University of Colorado in partial fulfillment
Of the requirement for the degree of
Doctor of Philosophy
Department of Molecular, Cellular and Developmental Biology
2012

This thesis entitled:
Signaling from Matrix Elasticity and TGF- β 1 to Cells of the Cardiac Valve
written by Huan Wang
has been approved for the Department of Molecular, Cellular and Developmental Biology

Leslie A. Leinwand, Ph.D.

Kristi S. Anseth, Ph.D.

Rui Yi, Ph.D.

Bradley B. Olwin, Ph.D.

Xuedong Liu, Ph.D.

Norm Pace, Ph.D.

Date _____

The final copy of this thesis has been examined by the signatories, and we
Find that both the content and the form meet acceptable presentation standards
Of scholarly work in the above mentioned discipline.

Wang, Huan (Ph.D., Molecular, Cellular and Developmental Biology)

Signaling from Matrix Elasticity and TGF- β 1 to Cells of the Cardiac Valve

Thesis directed by Professor Kristi Anseth and Professor Leslie Leinwand

ABSTRACT

Coordinated movement of cardiac valves controls unidirectional flow of the blood with every heart beat. Cardiac valves are composed of thin, pliable leaflets that withstand compressive tension, fluid shear stress, and bending stress as blood flows through them. The structure and the mechanical properties of the valves render them durable during the lifetime of human beings. However, changes in hemodynamic environment, inflammatory responses, and congenital valvular defects can all cause valves to undergo irreversible structural changes, one of which is calcific aortic stenosis (CAS). CAS affects 2-3% of the population over 65 years old in the western world, and the only effective treatment is valve replacement surgery. CAS is characterized by tissue stiffening and the formation of calcified nodules, the development of which is associated with abnormal differentiation of resident fibroblasts known as valvular interstitial cells (VICs). Upon tissue injury, VICs are activated to myofibroblasts which deposit excessive collagen and stiffen the matrix. Understanding how the pathogenic phenotype of VICs is regulated by cues from the matrix may lead to new therapeutic treatments for CAS. In this thesis, I examined how matrix elasticity and TGF- β 1 regulate VIC phenotypes. First, I characterized the VIC population from porcine aortic valves and showed that this population is relatively homogeneous. When I cultured these primary cells on different substrates, I found that

poly(ethylene glycol) hydrogels mimicked the native valve matrix better than tissue culture polystyrene plates with respect to preserving the quiescent fibroblast phenotype. At the level of signaling, I demonstrated that this is mediated through an elasticity-regulated PI3K/AKT pathway. Additionally, I showed that reduced matrix rigidity redirected activated valvular myofibroblasts into dormant fibroblasts without inducing significant apoptosis. Finally, I examined the effect of TGF- β 1 on VIC gene expression over time with microarray-based gene expression profiling and found that TGF- β 1 up-regulated cell-cell contact proteins (e.g., OB-cadherin, N-cadherin) in order to regulate valvular myofibroblast activation. Collectively, my thesis work revealed novel mechanosensing mechanisms employed by VICs to respond to matrix elasticity and explored the complex interactions among multiple extracellular cues, including matrix elasticity, TGF- β 1 and cell-cell adhesion, to direct the cellular fate of VICs.

To My Parents,

My Husband Luda Wang,

And My Dear Son Leo Wang

Acknowledgement

I would like to thank Prof. Leslie Leinwand and Prof. Kristi Anseth for being very supportive and considerate advisors. Thank both of you for your advice on how to tackle research problems and for your effort in editing my writings, including my first publication and my thesis. You have taught me not only on how to be a good scientist, but also on how to be an open-minded, honest and kind person (who can also be competitive). I also want to thank my committee members for their help during the journey of my dissertation. Thank Prof. Bradley Olwin for having faith in my projects (as what I always do) and encouraging me to delve deeper into scientific problems. I appreciate the resources on microarray analysis from the Olwin lab. I also want to thank Prof. Rui Yi for good discussion on how to improve my flow cytometry and about future career. Thank Prof. Xuedong Liu for insightful advice on TGF- β 1 signaling. And, thank both Prof. Norm Pace and Prof. Bradley Olwin for pushing me to publish my work early and to graduate in a timely manner.

I had the opportunity to work with many great undergraduate students, graduate students and postdoctoral researchers. First, I would like to thank my close collaborators, April Kloxin, Sarah Haeger, Mark Tibbitt and Steve Langer. Thank you for working as a team with me to tackle problems and teach me with your expertise. I have learnt a lot on data analysis and experimental design from April Kloxin and Sarah Haeger. I appreciate Mark Tibbitt and Steve Langer for being very patient teachers on polymer synthesis and virus production. I value our collaboration and friendship, which has benefited me greatly over the time of working with you. I also want to thank Tyler Menge for his dedication to undergraduate research with me. Thank the following colleagues for being good mentors in providing assistance with experiments and

scientific advice: Julie Benton, Peter Mariner, Helen Marshall, Nicholas Farina, Crystal Pulliam, Theresa Nahreini, Doug Chapnick, Yuming Han, Brooke Harrison, Jason Magida, Kristen Barthel, Eunhee Chung, Ina Weidenfeld, Chris Haines, Fan Yeung, Ada Buvoli, Massimo Buvoli, Daniel Alge, Josh McCall, Chun Yang, Malar Azagarsamy, Jennifer Leight, Sarah Gould, and Kelly Mabry. I want to especially thank Kristen Barthel, Eunhee Chung, Ina Weidenfeld, Fan Yeung, Jason Magida, Daniel Alge, Chun Yang and Ada Buvoli for being good friends and listeners. Finally, I want to thank Zhaojie Zhang, Qinghua Zhou, Ann Robinson, Sandy Duff, Janice Jones, Emi Tokuda, Kyle Kyburz, Balaji Sridhar for being my friends and being there for me during my thesis study. Without all of your help, my work would not be possible. And because of you, my long journey in graduate school seems short and is full of color and emotion.

CONTENTS

Chapter

I.	INTRODUCTION	1
1.1	Cardiac Valve Formation, Structure, Function and Diseases	5
1.2	Valvular Interstitial Cells (VICs) Mediate Valve Homeostasis and Pathology	8
1.3	VIC Differentiation is Regulated by Chemical, Physical and Biological Cues ..	12
1.4	Poly(ethylene glycol) Hydrogels as Novel Scaffolds for Culturing VICs and Understanding their Functions	17
1.5	Summary of the Thesis	22
II.	CHARACTERIZATION OF PORCINE AORTIC VALVULAR INTERSTITIAL CELLS	25
2.1	Introduction.....	25
2.2	Materials and Methods.....	27
2.3	Results and Discussion	29
2.3.1	Aortic and Pulmonary VICs Express very Low or None of the Lineage-specific Cell Surface Markers, But Small Percentages Express Stem Cell Markers.....	29
2.3.2	The Aortic ABCG2 ⁺ VICs Were Characterized for their Differentiation Potential <i>In Vitro</i>	32
2.4	Conclusion	37
III.	POLY(ETHYLENE GLYCOL) HYDROGELS PRESERVE NATIVE PHENOTYPES OF VALVULAR INTERSTITIAL CELLS THROUGH AN ELASTICITY-REGULATED PI3K-AKT PATHWAY	38
3.1	Introduction	38

3.2	Materials and Methods	42
3.3	Results	47
3.3.1	Culture on Polystyrene Plates Changes the Whole-Genome Transcriptional Profile of VICs.....	47
3.3.2	Microarray Data Are Validated Consistently by qRT-PCR.....	49
3.3.3	Soft PEG Hydrogels Preserve Native Phenotypes of VICs Better Than Plastic Plates	50
3.3.4	Soft PEG Hydrogels Prevent Valvular Myofibroblast Activation through an Elasticity-regulated PI3K-AKT Pathway, But Not the FAK or the P38 MAPK Pathways	52
3.3.5	PI3K Inhibition Prevents Myofibroblast Differentiation on Stiff Substrates	54
3.3.6	Inhibition of AKT Partially Inhibits Myofibroblast Differentiation in VICs Cultured on TCPS.....	56
3.3.7	Constitutively Active PI3K Promotes Calcific Nodule Formation in VICs Cultured on TCPS.....	58
3.4	Discussion.....	60
IV.	REDIRECTING VALVULAR MYOFIBROBLASTS INTO DORMANT FIBROBLASTS THROUGH LIGHT-MEDIATED REDUCTION IN SUBSTRATE MODULUS.....	69
4.1	Introduction	69
4.2	Materials and Methods	72
4.3	Results	77
4.3.1	Primary Valvular Myofibroblasts Deactivate in Response to Substrate Modulus Reduction.....	78
4.3.2	The Decrease in the Proportion of Valvular Myofibroblasts is Not Due to Apoptosis.....	81

4.3.3	Valvular Myofibroblasts Transform into a Less Proliferative Fibroblast Phenotype on Softer Substrates	83
4.3.4	Deactivated Fibroblasts on Stiff-to-soft Gels Maintain Responsiveness to a Proliferative Stimulus or TGF- β 1	85
4.3.5	Rat Pulmonary Myofibroblasts also De-Activate with Reduction in Substrate Modulus	87
4.4	Discussion.....	88
4.5	Conclusion.....	96
V.	TGF-β1 UP-REGULATES OB-CADHERIN EXPRESSION TO INHIBIT VALVULAR MYOFIBROBLAST DIFFERENTIATION.....	98
5.1	Introduction	98
5.2	Materials and Methods	101
5.3	Results	105
5.3.1	TGF- β 1 Induces Common and Distinct Gene Expression Changes Globally in VICs after 8 and 24 Hours	105
5.3.2	Microarray Data are Validated	106
5.3.3	Ingenuity Pathway Analyses Reveal Significantly Regulated Signaling Pathways.....	108
5.3.4	Numbers of Gene Probes Commonly and Distinctly Regulated by TGF- β 1 and TCPS	110
5.3.5	TGF- β 1 Up-regulates the Expression of CDH2 (N-cadherin) and CDH11 (OB-cadherin) in VICs	111
5.3.6	Knocking Down both OB-CDH and NCDH Promotes Valvular Myofibroblast Differentiation.....	113
5.3.7	Overexpressing OB-CDH Inhibits Valvular Myofibroblast Differentiation.....	115

5.4 Discussion.....	116
5.5 Conclusion.....	121
VI. CONCLUSIONS AND RECOMMENDATIONS.....	123
6.1 Summary.....	123
6.2 Future Directions	125
6.2.1 As an Important Cellular Determinant of Valvular Diseases, What Are VICs Really?.....	125
6.2.2 Multi-factorial Interactions of Extracellular Cues (Matrix Elasticity, TGF β 1, Cadherins, Binding Epitopes, etc.): the More the Merrier? .	126
6.2.3 The Microarrays: from the Finish Line to A New Starting Line	129
Bibliography	131

LIST OF TABLES

Table

2.1	Aortic and Pulmonary VICs Express Similar Cell Surface Markers.....	31
3.1	Gene Primer Sequences for qRT-PCR.....	45

LIST OF FIGURES

Figure

1.1	Structure and Function of Cardiac Valves.....	7
1.2	VICs Differentiate into Pathogenic Phenotypes, including Myofibroblasts and Osteoblast-like Cells, during Valve Diseases.....	10
1.3	Cells Receive Chemical, Physical and Biological Cues from their Microenvironment and these Signals Regulate Myofibroblastic Differentiation Coordinately.....	12
1.4	Formation of Photodegradable Hydrogels.....	20
1.5	Thesis Outline.....	24
2.1	Aortic VICs Are Mostly Negative for CD31, CD105, CD45 and Thy-1.....	30
2.2	A Small Fraction of VICs Express Stem Cell Markers ABCG2 and NG2.....	33
2.3	Morphology of the ABCG2 ⁺ VICs and the ABCG2 ⁻ VICs Grown on Tissue Culture Plates.....	34
2.4	Both ABCG2 ⁺ VICs and ABCG2 ⁻ VICs Differentiate into Osteoblast-like Cells But Not Adipocytes.....	36
3.1	Culture on Plastic Plates Changes the Whole-Genome Transcriptional Profile of VICs Isolated from Porcine Aortic Valves.....	49
3.2	qRT-PCR Validation of Microarray.....	50
3.3	Soft PEG Hydrogels Preserve Native Phenotypes of VICs Better Than Plastic Plates.....	51
3.4	Soft PEG Hydrogels Prevent Myofibroblast Activation through an Elasticity-regulated PI3K-AKT Pathway, But Not the FAK or the P38 MAPK Pathways.....	53
3.5	PI3K Inhibition Prevents Myofibroblast Differentiation on Stiff Substrates.....	55
3.6	Inhibition of AKT Partially Inhibits Myofibroblast Differentiation in VICs Cultured on TCPS.....	57

3.7	Constitutively Active PI3K Promotes Calcific Nodule Formation in VICs Cultured on TCPS	59
4.1	Cell Fate in Response to Substrate Modulus Reduction	78
4.2	Reduced Myofibroblast Activation in Response to Lowering Substrate Modulus ..	80
4.3	Decreased Number of Myofibroblasts on Stiff-to-soft Gels was not Due to Apoptosis.....	82
4.4	VICs Switch to a Less Activated and Less Proliferative Fibroblast Phenotype on Softer Substrates.....	84
4.5	Deactivated VICs on Stiff-to-soft Gels Enter the Cell Cycle with Proliferative Stimulus and Activate the Myofibroblast Gene Program in Response to TGF- β 1 ..	86
4.6	Rat Pulmonary Myofibroblasts De-Activated with Reduction in Substrate Modulus.....	88
5.1	Global Gene Expression of Porcine VICs in Response to TGF- β 1 over Time	106
5.2	qRT-PCR Validation of Microarray.....	107
5.3	Expression Pattern of Known TGF- β 1-responsive Genes in the Microarrays	108
5.4	Ingenuity Pathway Analyses for Microarray Data	109
5.5	Numbers of Gene Probes Commonly and Distinctly Regulated by TGF- β 1 and TCPS	110
5.6	TGF- β 1 Up-regulates Expression of CDH2 (NCDH) and CDH11 (OB-CDH) in VICs	112
5.7	Knocking down both OB-CDH and NCDH Promotes Valvular Myofibroblast Differentiation	114
5.8	Overexpression of OB-CDH Inhibits Valvular Myofibroblast Differentiation	116
6.1	Gene Expression of VICs in Response to TGF- β 1 when Cultured on Stiff or Soft	

	Hydrogels	127
6.2	OB-CDH mRNA Levels for VICs Cultured on Different Substrates	128

CHAPTER I

INTRODUCTION

Aortic valves have a trileaflet structure that is quite robust in controlling directed blood flow during cardiac cycles over a long period of time. As the left ventricle contracts and blood pressure builds up, the aortic valve opens, allowing blood flow up to 1.2 m/s and experiencing high fluid shear stresses (64–71 dyn/cm²) and bending stretch (up to 14.5%) [1]. As blood flow decelerates and the pressure drops in the ventricle, the aortic valve closes and occludes the orifice between the left ventricle and the aorta, withstanding back pressure and circumferential/axial stretch [1]. During an average human life span (~70 years), the aortic valve opens and closes ~3 billion times [2]. The structure of the valves imparts their strength and durability to withstand these repetitive mechanical challenges.

The aortic valve leaflets are ~500µm thick and are comprised of three layers defined by varying their ECM protein compositions, each rich in collagen, proteoglycan or elastin [3]. The valve structure can be affected by genetic mutations or metabolic diseases. For example, about 1-2% of all live births have bicuspid aortic valves, some of which have been associated with mutations in Notch1 [4, 5]. A majority of people born with bicuspid valves will develop calcific aortic stenosis (CAS), which is characterized by leaflet stiffening and formation of calcific nodules, and advanced CAS typically requires surgery to replace the diseased valves. In addition, endothelial damage induced by bacterial infection and other risk factors, including hypertension, old age, high serum lipid levels, height and smoking, are all associated with destruction of

normal valvular structure and development of CAS [6-8]. Mild CAS, or aortic sclerosis, is present in ~29% of adults over 65 years of age, while severe CAS is present in ~2% of the same age group [6, 9]. Unfortunately, there is no effective non-surgical treatment for end-stage CAS, and about 99,000 inpatient valve surgeries are performed each year in the United States, costing billions of dollars [10]. These statistics underscore the importance of better understanding the mechanisms of CAS disease progression so that early intervention and new drug treatments can be developed.

Proper structure and function of aortic valves are controlled by interactions between the valvular matrix, its cells, and the surrounding hemodynamic environment [1]. Valvular interstitial cells (VICs) are the main cell population residing in valves and they play critical roles in maintaining valve structure and function [11, 12]. During valve development, VICs are activated to a more synthetic and contractile phenotype and contribute to the formation and the remodeling of ECM [13]. VICs from healthy adult valves are mainly composed of fibroblasts with a small fraction of myofibroblasts and progenitor cells [12].

VICs also contribute to disease progression. In sclerotic valves, VICs are activated to myofibroblasts, which secrete excessive ECM degradative enzymes (e.g., matrix metalloproteinase, or MMPs) and collagen, leading to deterioration of the original valve structure and tissue thickening [14-16]. VICs can also differentiate into osteoblast-like cells to mediate bone matrix formation in CAS. However, during disease progression, not only are cells changing their surrounding matrix, but the matrix is also feeding back to regulate cellular functions. The gradual accumulation of stiffened collagen-rich matrix in valve sclerosis or calcified matrix in CAS, in turn, reinforces the differentiation of VICs into myofibroblasts and osteoblasts,

respectively [17-19]. To better understand this intricate interplay between cells and matrix, we believe that it is important to study VICs on tissue-mimicking matrix substrates with user-defined properties rather than on the ultra-stiff, non-physiologic tissue culture plastic. These types of synthetic extracellular matrices should allow one to study the pathogenic differentiation of VICs in a more physiologically relevant environment *in vitro*.

One versatile material for fabricating such a matrix environment for the culture of cells is based on poly(ethylene glycol) (PEG) hydrogels. PEG materials are polymer networks that resist non-specific adsorption of proteins and possess a soft tissue-like water content and elasticity [20-23]. Elasticity (E) measures the degree of deformation of a material in response to an applied force and relates to the stiffness of the material. Recent studies have shown that elasticity can direct cellular functions, such as stem cell differentiation [24] and renewal [25], independent of soluble growth factors. For example, soft matrices that more closely mimic the stiffness of brain with E around 0.1-1kPa have been found to promote neurogenic differentiation of human mesenchymal stem cells, while rigid matrices that mimic collagenous bone (E , 25-40kPa) have been found to promote osteogenesis [24]. In a second example, muscle satellite cells were observed to retain a higher self-renewal capacity when cultured on hydrogels with a muscle-like E (~10kPa) than on plastic plates (E , ~3GPa) [25]. Collectively, these results suggest that certain cell types need to be cultured on substrates with more physiologically relevant E , so their functions are not biased by the super-physiologically stiff tissue culture plastic plates (E , ~3 GPa).

Utilizing PEGs with different molecular weights or structures, hydrogels can be synthesized with a wide range of E (from ~0.1kPa to 100s of kPa) to more closely match those

found in native tissues. Further, the PEG macromolecule can be modified with photolabile groups (e.g., nitrobenzyl ether group) to manufacture photo-degradable hydrogels, making it possible to reduce *E in situ* and monitor cellular responses to changes in mechanical properties in real time [26]. This thesis work exploits PEG hydrogels to study the effect of substrate elasticity on VIC properties. For example, I study how soft PEG gels (E , $\sim 7\text{kPa}$) might the mimic the endogenous niche of VICs and preserve their native fibroblast phenotype of VICs, compared with the plastic plates or stiff hydrogels (E , $\sim 32\text{kPa}$, Chapter III). Additionally, I utilize the photolabile, softening PEGs to study the influence of dynamic changes in E on redirecting activated myofibroblasts into less proliferative fibroblast cell fate (Chapter IV). The ultimate goal is to build a home, rather than just a house, for cells so that we can improve our understanding of the signaling pathways regulating VIC differentiation, proliferation and apoptosis in response to microenvironmental cues and eventually manipulate VICs at the molecular level for valve disease management and/or tissue regeneration *in vitro* [23].

This introduction first presents current knowledge on the development, structure, function and diseases of cardiac valves, focusing on the most prevalent valvular disease, CAS. The functions and pathogenic differentiation of resident VICs in valves are reviewed and associated with valvular maintenance and CAS progression. Based on previous studies, chemical cues (e.g., TGF- $\beta 1$), physical cues (e.g., elasticity) and biological cues (e.g., cell-cell adhesion) are all known to regulate the disease-associated VIC differentiation. However, to understand this regulation, VICs ought to be cultured in a tissue-mimicking environment, such as hydrogels synthesized from PEG. The advantages of using PEG hydrogels as a culturing substrate for understanding cellular functions and differentiation are reviewed in the final section.

1.1 Cardiac Valve Formation, Structure, Function and Diseases

The heart is the first functioning organ as the human embryo develops. During heart morphogenesis, endocardial cushions, or cardiac valve primordia, form in the outflow tract and atrioventricular canal regions of the primitive heart tube [27]. The endocardial cells surrounding the cardiac cushions undergo endothelial-to-mesenchymal transdifferentiation (EMT), proliferate, and secrete extracellular matrix (ECM) related proteins necessary to build and remodel the cardiac valves [28]. This is a highly coordinated process regulated by signaling molecules temporally and spatially [29]. For example, BMPs, TGF- β s, Notch and ECM proteins, such as hyaluronan and versican, regulate the specification of the endothelial cells to initiate cardiac cushions and the EMT process [30-35]. As the cushion grows, a number of signaling pathways, including VEGF signaling, BMP signaling and ErbB signaling, are activated to promote cell proliferation [28]. During valve stratification into its layered matrix structure, Notch signaling is specifically activated on the flow side, or ventricularis side, of the aortic valves, whereas Wnt signaling is activated in the fibrosa layer [29]. These distinct pathways regulate local cells to express specific ECM proteins for modeling valve structure [36]. To ensure controlled development of the valves, Smad6 functions as an inhibitor of BMP signaling to prevent excessive EMT, and apoptotic mechanisms are involved to control cell number in the valves [37, 38]. The complex developmental process of cardiac valves initiated from a group of endothelial cells is still being investigated, and one critical question is how these signaling pathways crosstalk and systematically regulate cellular transdifferentiation, proliferation, apoptosis and tissue production and organization.

The multiplex regulation of cardiac valve formation reflects the importance of these

tissues in the heart. The function of cardiac valves is conserved from fish to human, and controls uni-directional flow of blood by passively opening and closing in response to differential pressure [39, 40]. Humans have four chambered hearts and four different cardiac valves: two semilunar valves (pulmonary valve and aortic valve) and two atrioventricular valves (tricuspid valve and mitral valve) (Figure 1.1A). The aortic valve gates the supply of oxygenated blood from the left ventricle to the whole body, and the aortic valve is most prone to disease; thus, this thesis focuses on understanding the biology of cells isolated from aortic valves. During systole when the ventricle contracts, aortic valves open with blood flowing through at a speed of up to ~ 1.2 m/s [1]. The valves close as the blood flow decelerates during the relaxation of ventricle, or diastole. Within the working cycles of the valves, they experience a number of mechanical forces, including fluid shear stress, tensile stretch, bending stretch and pressure as depicted by the arrows in Figure 1.1B [1]. For normal aortic valves, shear stress peaks at $64\text{--}71$ dyn/cm² in the ventricular side during systole [41], and tensile strain reaches 11% circumferentially and 25% radially during diastole [42]. Aortic valves must function in this complex hemodynamic environment, and this often necessitates equally complex responses from the resident cell populations to maintain valve homeostasis. Meanwhile, the hemodynamic environment is important for proper valve development, maintenance of structure, and is often a measure of disease progression.

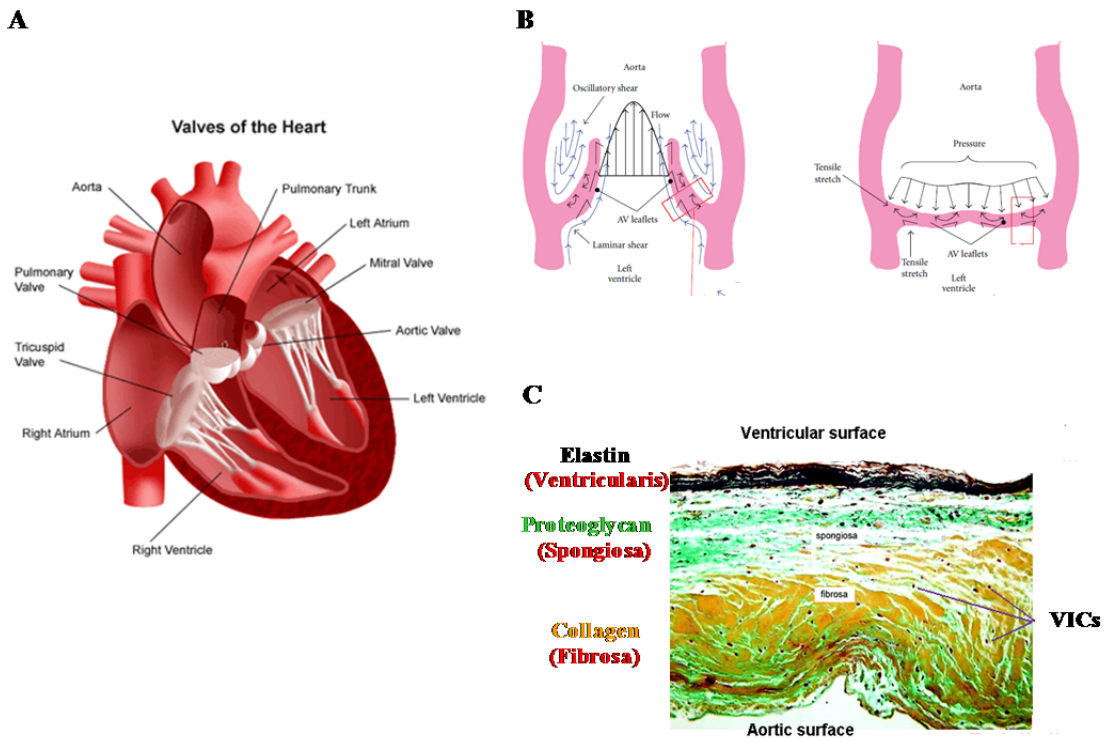


Figure 1.1 Structure and Function of Cardiac Valves. (A) shows the locations of cardiac valves in human hearts (picture adapted from <http://stemcellumbilicalcordblood.com>). The various mechanical stresses applied on the valves are depicted by arrows in (B) [1]. (C) shows the layered ECM structure of aortic valves, with elastin-, proteoglycan- and collagen- rich layers [43].

Native valve tissue is a thin compliant material designed for its function. If one more closely examines the architecture of an aortic valve leaflet, histological sections clearly show three distinct layers of ECM, consisting mainly of collagen, proteoglycan and elastin (Figure 1.1C). These ECM proteins impart unique macroscopic mechanical properties to valves, enabling them to withstand tension when closed and bend to open. In particular, the elastin fibers on the flow side of the valves (i.e., ventricularis) are elastic, extending when valves open and recoiling when valves close. Proteoglycans are mainly distributed in the middle layer of the valves, the spongiosa, and serve as a cushion for absorbing tension and for mediating movements between

the top and the bottom layers. Finally, the fibrosa layer contains collagen fibers, which confer stiffness and strength to the valves. When the normally compliant valvular structure is disrupted, for example, in the CAS, blood regurgitation back into left ventricles or insufficient blood supply can occur.

CAS is a life threatening disease and affects 2-3% of people over 65 years old in the western world [9]. It is characterized by progressive thickening of the valve leaflets, formation of calcific nodules or even lamellar or endochondral bone, and new vascularization [6]. The pathology of valve calcification has similarities with the formation of calcified plaques in the atherosclerosis of blood vessels, where inflammation, oxidative stress, lipid overload, apoptosis and trans-differentiation of resident cells all contribute to abnormal calcium deposition in these soft tissues [44]. However, clinical trials based on lipid-lowering drugs derived from statins showed no effect in halting the progression of valve calcification or induce its regression [45]. This indicates that targeting multiple aspects of the disease in the right temporal manner may be necessary for treating CAS. For a long time, CAS was viewed as a degenerative disease, as valves wear and tear. However, numerous studies argue that the pathogenic differentiation of resident VICs into myofibroblasts and osteoblast-like cells drives cell-mediated fibrosis, calcification or even bone formation in diseased valves [2, 46-50].

1.2 Valvular Interstitial Cells (VICs) Mediate Valve Homeostasis and Pathology

Cardiac valves are composed of a layer of endothelial cells on their surface and VICs throughout the bulk of their leaflets. VICs are fibroblast-like cells acting as tissue builders by secreting matrix proteins, including collagen I, fibronectin 1, elastin, etc. [51, 52], and matrix remodeling enzymes, including various matrix metalloproteinases (MMPs) and their inhibitors

[53, 54]. During remodeling and stratification of fetal human valves, VICs have a higher level of proliferation and apoptosis, and secrete more matrix-remodeling enzymes [13]. In adult valves, VICs continue to play critical roles in tissue homeostasis and repair. Aikawa *et al.* showed that most VICs are quiescent in normal adult valves [11, 13]. However, with disease or tissue injury, VICs can be activated to proliferate, to remodel the matrix and to acquire different pathogenic phenotypes, including the myofibroblasts and the osteoblast-like cells [6, 55, 56]. In sclerotic valves or mild CAS, VICs are activated to myofibroblasts, which are more contractile and secrete higher level of ECM proteins and degradative enzymes [15, 16, 19]. However, in severe CAS, osteoblastic differentiation of VICs characterized by the expression of osteogenic genes, such as Cbfa1 and Osteocalcin, has been detected [6, 7, 47, 49].

Myofibroblasts have an intermediate phenotype with properties between fibroblasts and smooth muscle cells [57]. Activation of quiescent fibroblasts into myofibroblasts has been observed in tissue repair and fibrosis of various vital organs, such as skin [58], liver [59], lung [60], kidney [61] and heart [62]. This is a critical step as myofibroblasts are superior to fibroblasts in accelerating tissue repair. Myofibroblasts proliferate, migrate to wounds, express α -smooth muscle actin (α SMA) stress fibers (Figure 1.2C) to contract wounds, and produce more ECM scaffold proteins and ECM degradative enzymes to remodel the tissues around them [63, 64]. While myofibroblasts are predominant during the initial phase of tissue healing, persistence of myofibroblasts can lead to fibrosis and permanent tissue damage [65, 66]. Temporal control of the myofibroblast phenotype is crucial. It has been suggested that some myofibroblasts undergo apoptosis in granulation tissue, a structure formed towards the end of skin wound repair [67]. Apoptosis could be induced by changes in the mechanical environment, as dermal fibroblasts

cultured in an anchored 3D collagen gel initiated apoptosis upon sudden release of the gels [68]. However, it is unclear if myofibroblasts can acquire some other fates, for example, de-differentiating into quiescent fibroblasts towards the end of tissue repair. Chapter IV of this thesis studies how changing mechanics of the matrix can re-direct activated valvular myofibroblasts into fibroblasts without inducing significant apoptosis. This mechanism provides some insight as to what might be happening *in vivo* and points to another fate of myofibroblasts in response to matrix mechanical cues.

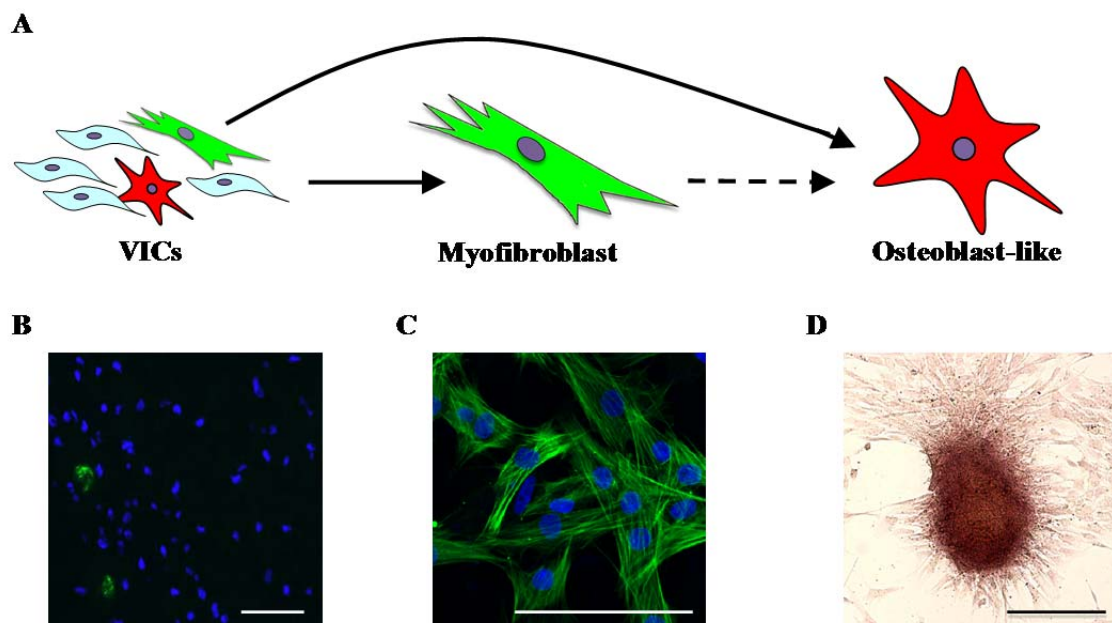


Figure 1.2 VICs Differentiate into Pathogenic Phenotypes, including Myofibroblasts and Osteoblast-like Cells, during Valve Diseases. (A) The hypothetical pathway of VICs differentiating into the pathogenic myofibroblast or osteoblast phenotypes. Native valve sections (B) or VICs cultured on plastic plates (C) were stained with α SMA (Green) and DAPI (blue). Myofibroblasts are characterized by the α SMA⁺ stress fibers as shown in (C). (D) demonstrates a calcified nodule derived from VICs and stained positive for calcium by alizarin red S (D, image in courtesy of Dr. Julie Benton) . Scale bars in (B-D) are 100 μ m.

Another pathogenic phenotype of VICs is the osteoblast-like phenotype, which has been observed in CAS. In severely calcified valves, active bone mineralization has been verified

by histological staining [7], and VICs have been shown to express proteins characteristic of osteoblasts, such as Osterix and Runx2 [69, 70]. Multiple research groups have also demonstrated that when VICs are cultured in the osteogenic media, they have elevated alkaline phosphatase activity and deposit calcium phosphates, the major inorganic matrix component in bone [49, 71-75]. This observation indicates that VICs may be a critical cellular determinant during valve disease progression. The sequence of cell differentiation into myofibroblasts and osteoblasts is still unclear (Figure 1.2A). While some propose that there are distinct sub-populations of VICs differentiating into either myofibroblasts or osteoblasts [71, 76], Benton and Anseth have provided evidence that myofibroblastic differentiation proceeds the osteogenic differentiation, since α SMA knockdown in VIC cultures, which prevents myofibroblasts formation, also blocks calcific nodule formation in VICs [77]. The two proposed sequences of differentiation are not mutually exclusive, but it is meaningful to determine which cells give rise to the pathogenic phenotypes predominantly *in vivo* and this can be benefited from clonally derived cell assays *in vitro* and lineage tracing experiments *in vivo*.

Despite the important functions of VICs, the cellular composition of valves has not been well-defined. The Magdi group compared human VICs with human mesenchymal stem cells (hMSCs) and found that these cells shared the expression of fibroblast markers, fibroblast surface antigen (FSA) and vimentin, but only a small fraction of VICs expressed smooth muscle cell markers (desmin and smooth muscle myosin) or stem cell markers (CD34, CD133, c-Kit, Stro-1, CD105) [73, 78]. Four distinct cell clones isolated from bovine VICs express integrin β 1 and type A nonmuscle myosin, but not the hematopoietic marker CD45 nor the endothelial/epithelial marker von Willebrand Factor (vWF) [71]. Collectively, this evidence

suggests that VICs are probably not hematopoietic cells (CD45⁻), not endothelial cells (vWF⁻), not smooth muscle cells (smooth muscle myosin^{low} and desmin^{low}), but fibroblasts (FSA⁺ and vimentin⁺). These work support the notion that VICs are a relatively homogeneous population and that a fraction of cells expressing stem cell markers may participate in maintaining tissue homeostasis and regeneration.

1.3 VIC Differentiation is Regulated by Chemical, Physical and Biological Cues

VICs, like most cells in their native niche, receive a spectrum of signals from their microenvironment. These cells are constantly sensing environmental cues through cell surface receptors for soluble or tethered chemical factors, through integrins to probe ECM composition and elasticity, and through cadherins for cell-cell interaction (Figure 1.3). Chemical, cell-matrix and cell-cell interactions elicit specific signaling pathways intracellularly and systematically regulate cellular functions, including proliferation, apoptosis, and differentiation.

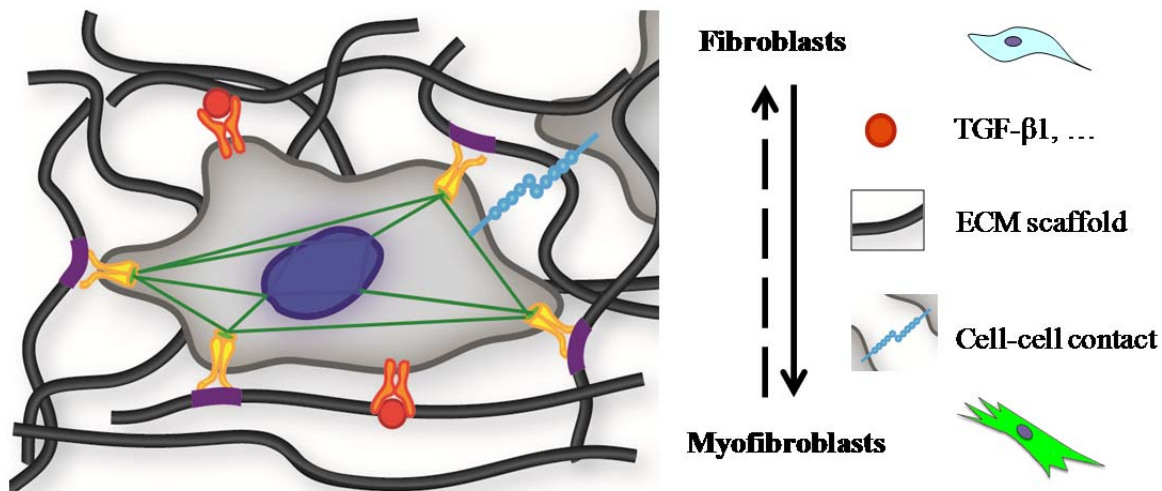


Figure 1.3 Cells Receive Chemical, Physical and Biological Cues from their Microenvironment and these Signals Regulate Myofibroblastic Differentiation Coordinately. A chemical cue and its cellular receptor (Orange), ECM scaffold (Gray), ECM scaffold peptides (Purple), Integrins (Yellow), Cell-cell contact (Light Blue), Cytoskeleton (Green), Nucleus (Blue). Image adapted from Dr. April Kloxin and Dr. Mark Tibbitt.

Chemical factors are among the first cues to be identified and studied in directing VIC phenotypes. In diseased valves, inflammation-related chemokines, such as TGF- β 1 [79], TNF- α [14] and Interleukin 1 [80] are significantly up-regulated, and *in vitro*, these factors can also promote the pathogenic myofibroblastic or osteoblastic phenotypes in VICs [48, 79, 81]. For example, TGF- β 1 is one of the most potent chemical cues in inducing the myofibroblastic phenotype, not only in VICs [81], but also in fibroblasts isolated from liver, lung, and kidney [82-85]. TGF- β 1 activates the phosphorylation of Smad2/3 and their nuclear translocation, which regulates the gene expression of α SMA, Collagen1A1 (Coll1A1) and connective tissue growth factor (CTGF) to collectively promote myofibroblastic differentiation [86-90]. TGF- β 1 can also act through non-canonical pathways, such as p38 MAPK [91], PI3K/AKT [92, 93] or Wnt/ β -catenin [19, 94] to promote myofibroblast activation. The myofibroblastic phenotype of VICs is effectively blocked by neutralizing antibodies against TGF- β 1 [81]. A number of other chemical cues have been associated with valvular diseases and VIC activation, including endothelin 1 [95], lipids [96, 97], reactive oxygen species [98, 99], etc.. These chemical signals also interact with each other. Interestingly, the FGF-2 signaling can antagonize TGF- β 1 in the myofibroblast differentiation [100], whereas Wnt signaling can synergize with TGF- β 1 in promoting valvular myofibroblast activation [19].

Matrix cues in the form of mechanical signals and physical signals have traditionally been under-appreciated in regulating cellular functions, and this is especially obvious with culturing cells on plastic plates, which are physically different from most soft tissues in elasticity and structure. Native VICs experience a number of different physical stimuli, for example, cyclic stretch during valve movement, interstitial flow, nano-topography of the matrix and constant

tension from the ECM that they attach to. Thayer and Yoganathan *et al.* have shown that stretch on valves at 15% in combination with pressure can inhibit the expression of α SMA, vimentin and Calponin (α -smooth muscle cell markers) [101], but stretch at 10%-20% induces collagen synthesis in VICs [102]. When biaxial stretch was introduced to VICs in 3D, that also decreased the expression of α SMA and vimentin [103].

More recently, substrate modulus, or elasticity, has attracted a great deal of attention in the fibrosis field in regulating disease progression. As a fibrotic lesion develops *in vivo*, there is an increase in collagen deposition and matrix stiffness, which can provide cues or a physical matrix environment for myofibroblasts to activate or stay activated [104, 105]. Microenvironment elasticity can be described by the Young's modulus (E) of a material where E is calculated based on the ratio of the stress acting on a substance to the strain produced. Elasticity has been shown to not only regulate the fate of VICs, but also fibroblasts from different tissues. When valvular, hepatic or lung fibroblasts are cultured on low modulus substrata ($E \leq 10$ kPa), they maintain an un-activated phenotype; however, when cultured on higher modulus substrata, they are activated to myofibroblasts [19, 104-106]. Further, reducing the elastic modulus of the substratum to a very low level ($E \leq 1$ kPa) promotes apoptosis in various fibroblasts [105, 107, 108]. Moreover, VICs and NIH3T3 fibroblasts grown on compliant substrata show a decrease in proliferation, compared with cells cultured on stiff substrata ($E > 15$ kPa) [107, 109]. Interestingly, Balestrini and Hinz showed that lung myofibroblasts can memorize the stiff substrate that they had been cultured on for 3 weeks and do not de-activate after being transferred to soft substrates [110].

However, most of the previous studies were performed on materials with discrete

stiffnesses. Results in Chapter IV of this thesis demonstrate that valvular myofibroblasts can de-activate to a less-proliferative fibroblast state without significant apoptosis when the substrate modulus is reduced *in situ* from ~32kPa to ~7kPa. This method avoids transferring of cells from a stiff substrate to a soft substrate and enables one to monitor cell fate in real time while dynamically changing matrix mechanical properties.

Despite the important roles of elasticity in regulating the functions and differentiation of fibroblasts [104, 105, 110, 111] and a number of other cell types, e.g. human MSCs [112] and myoblasts [113], numerous questions remain as to how the mechanical cue of elasticity is translated into intracellular signaling. Dupont *et al.* showed that YAP and TAZ, two transcriptional factors, can serve as sensors to the ECM stiffness in a Rho GTPase- and actomyosin cytoskeleton-dependent manner in MSCs and regulate their differentiation into osteoblasts on stiff substrates and into adipocytes on soft substrates [112]. As cells bind with their matrix via integrins, these transmembrane proteins are mechano-sensitive and elicit biochemical pathways intracellularly, including FAK, ERK and JNK signaling [114]. Additionally, integrins can be internalized together with BMP receptors via caveolae-dependent endocytosis on soft substrates ($E \sim 0.1$ -1kPa) to promote neuronal differentiation of bone-marrow MSCs [115]. Han and Schlunck have shown that soft substrates attenuate the persistence of TGF β 1 signaling, which acts through Smad2/3, ERK and AKT, in human trabecular meshwork cells [116]. Recently, Huang and Zhou *et al.* showed that lung fibroblasts respond to substrate stiffness through nuclear translocation of Megakaryoblastic leukemia factor-1 (MKL1) and RhoA/Rock activation on stiff substrata [117]. The PI3K/AKT pathway was activated by the mechanical cue of cyclic strain in mesangial cells [118], but has not been shown to be regulated

by substrate elasticity. Chapter III explores how VICs respond to changes in substrate modulus by modulating the activity of the PI3K/AKT pathway, which provides an underlying mechanism as to how E translates into cell signaling and regulates the myofibroblast phenotype of VICs.

Myofibroblast activation is also regulated by cell-cell contact mediated through cadherins. Masur *et al.* showed that corneal fibroblasts differentiated into myofibroblasts when plated at low density [119]. During skin wound repair, the activation of dermal fibroblasts into myofibroblasts is accompanied by increased expression of OB-cadherin (or Cadherin 11) and decreased expression of N-cadherin (or Cadherin 2) [120]. Additionally, anti-OB-cadherin, but not anti-N-cadherin, peptide inhibits the contraction of myofibroblast-populated collagen gels [120]. Interestingly, OB-cadherin bonds resist 2-fold higher forces than the N-cadherin bonds, consistent with the idea that myofibroblasts are changing adherens junctions to adapt to the mechanical challenges during wound contraction [121]. OB-cadherin is also selectively expressed by synovial fibroblasts and plays a critical role in synovial inflammation and cartilage formation [122-124]. Besides the canonical roles of cadherins in mediating cell adhesion and sorting during tissue morphogenesis [125], both OB-cadherin and N-cadherin have been shown to regulate cell invasion/migration [126-128] and osteoblast differentiation [129]. However, specific studies on the effects of these cadherins on myofibroblast differentiation have been lacking, so Chapter V of this thesis investigates this question in detail by knocking-down or over-expressing these cadherins in VICs.

Signals from chemical cues, matrix, or neighboring cells often take place at the same time, and one cell can receive a complex milieu of competing and synergistic signals. So a key question is what is their combinatorial effect? Does one kind of signal dominate, or do they act

through different but paralleled pathways in regulating cellular functions? The field is just beginning to address and better understand the complex interactions among different types of signals. For example, chemical factors are not usually presented in a soluble mature form *in vivo*. Instead, they are secreted as pre-proteins and stored in the ECM through non-covalent interactions, where ECM regulates the stability and the spatial distribution of these factors [130]. Hinz *et al.* showed that myofibroblasts can activate latent TGF- β 1 by contraction [131]. On the other hand, Merryman and Sacks have shown that cyclic stretch on VICs can inhibit the α SMA expression; however, cyclic stretch in combination with TGF- β 1 treatment induced more activation of myofibroblasts than TGF- β 1 alone, indicating that this mechanical cue can regulate cellular responses to TGF- β 1 [132]. Numerous questions remain and several interesting directions to pursue in order to better define the systematic regulatory map of VIC differentiating into myofibroblasts by various extracellular cues.

1.4 Poly(ethylene glycol) Hydrogels as Novel Scaffolds for Culturing VICs and Understanding their Functions

Traditionally, cells are cultured on polystyrene plates for studying their functions *in vitro*. However, plastic plates cannot recapitulate critical biochemical and biophysical cues presented by the native ECM, leading to changes in the cellular gene expression and functions at baseline (Chapter III, Figure 3.1A). Additionally, plastic plates only provide a 2-dimensional (2D) surface for growing cells, whereas most cell types residing in human bodies are embedded in a 3-dimensional (3D) matrix. To overcome some of these limitations associated with traditional plastic plate tissue culture, various biomaterials have been developed and range in composition from naturally-derived matrix proteins to synthetic polymers. Naturally-derived scaffold proteins

include collagen found in mammalian ECM and polysaccharides, such as alginate extracted from seaweed. While collagen and alginate resemble the native ECM and are enzymatically-degradable, they have several limitations, such as high batch-to-batch variation during isolation, immunogenicity, pathogen transmission, and uncontrolled degradation, for cell culture and tissue engineering purposes [20]. Therefore, synthetic hydrogels have become attractive as an alternative scaffold for providing defined biochemical and biophysical cues to support 2D and 3D cell survival and metabolism and for understanding specific mechanisms of cell-matrix interaction. This thesis specifically exploits one synthetic hydrogel material system for the culture of VICs.

Several types of synthetic hydrogels, including poly(peptide), poly(vinyl alcohol) (PVA) and poly(ethylene glycol)(PEG), have been developed and reported in the literature. Poly(peptide) hydrogels can be self-assembled through interactions among the peptides in neutral aqueous solution and have been used for drug delivery, tissue scaffolds, biosensors, etc. [133-135]. However, it is often hard to decouple the effects of biochemical cues inherent in the peptide sequences from the biophysical effects of the scaffold. PVA hydrogels are water-swollen polymer networks and have been developed as tissue scaffolds for chondrocytes and VICs [136-138]. PEG based hydrogels are among the most widely used synthetic gels for biological and medical applications [20, 21]. The repeating structure of PEG polymers, as shown in Figure 1.4A, renders these materials hydrophilic, biologically inert and minimizes non-specific absorption of proteins [22]. When PEG polymers are crosslinked to form a gel, the materials mimic aspects of the native ECM in elasticity, diffusion and interstitial flow [139]. Additionally, PEG can be formed using physiologically mild conditions for 3D encapsulation of cells, as well

as be formed in tissues *in situ* through photopolymerization [140]. Therefore, PEG-based materials are widely used for cell matrix mimicry, carriers for delivering proteins, drugs and cells, and for tissue replacement scaffolds and other applications.

PEG can be polymerized to form hydrogels through different means, such as free radical chain polymerization (Figure 1.4B) and thiol-ene based Micheal-type addition [141, 142]. A commonly used method is to functionalize PEG with acrylate groups at the ends to generate PEG diacrylate (PEGDA, Figure 1.4A) and subsequently react via free radical chain polymerization as shown in Figure 1.4B. In this reaction, radicals can be generated through photo-initiation, thermal initiation, or a redox pair of initiators, e.g. TEMED and ammonium persulfate. After initiating radicals are generated, they propagate with carbon-carbon double bonds in PEGDA and propagate to form a growing kinetic chain. The chain growth of the PEG network is terminated when two propagating radicals react. As shown in Figure 1.4B, the resulting PEG hydrogel structures consist of polyacrylate chains crosslinked by PEG polymers [143]. This polymerization method is utilized in this thesis for manufacturing hydrogels of varying elasticity for cell culture.

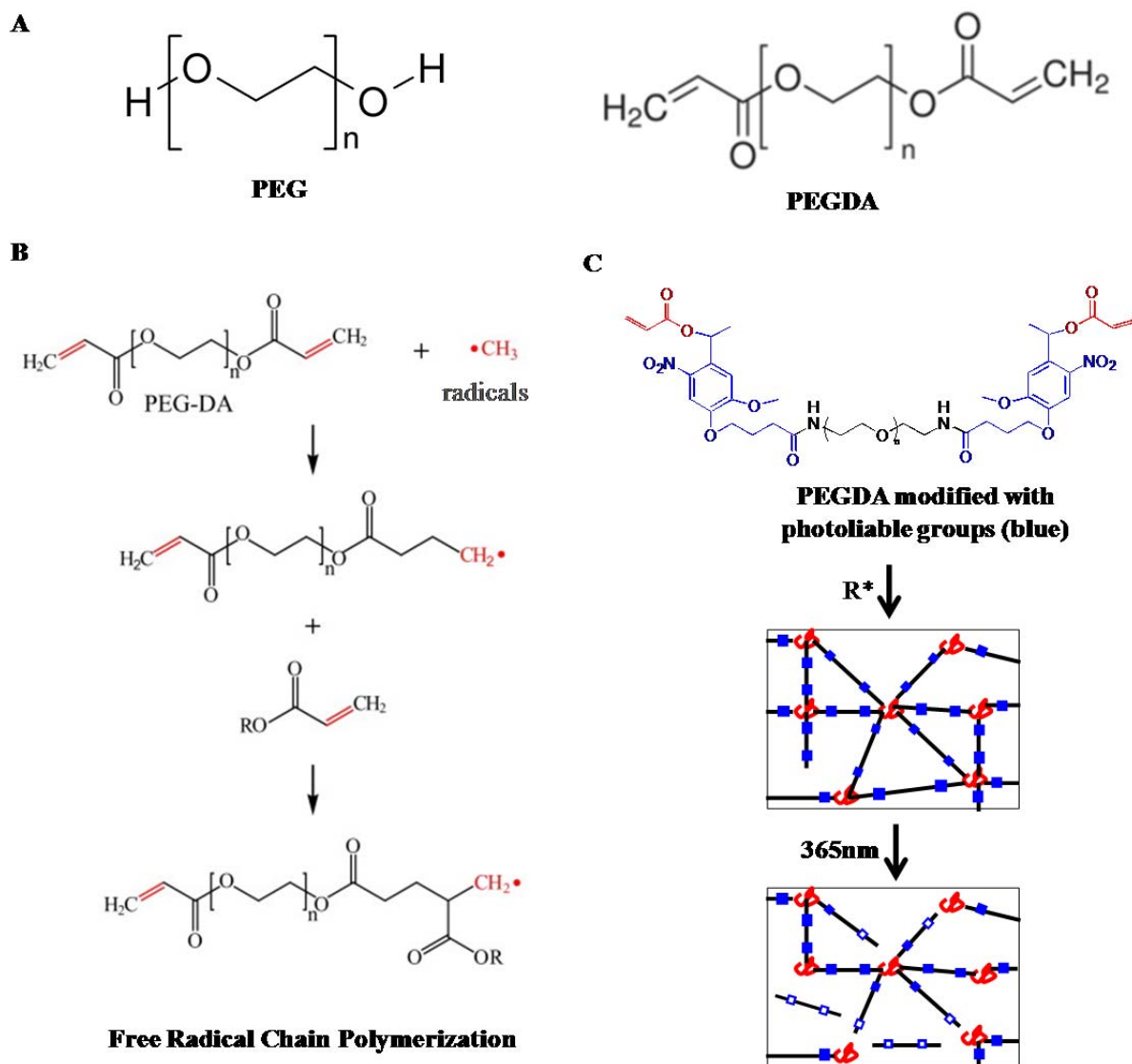


Figure 1.4 Formation of Photodegradable Hydrogels. (A) Chemical structures of PEG and PEGDA. (B) Schematic of free radical chain polymerization based on PEGDA [143]. (C) Structure of a novel photoliable crosslinker synthesized from PEGDA [144] and the cartoon of photodegradation of the hydrogels synthesized from this crosslinker (images modified from Dr. April Kloxin's).

Synthetic PEG hydrogels can be modified with different biochemical and biophysical cues for studying their specific interactions with cells and for providing an *in vivo*-like matrix environment. Modifying polymer surfaces with whole proteins (e.g. collagen, fibronectin and

laminin) has been shown to promote cell adhesion and functions, but faces various challenges, including protein denaturation, orientation of presentation, and protein isolation [145]. As an alternative, recent efforts have focused on presenting effective motifs or peptides in the whole proteins in PEG gels. For example, the Arginine-Glycine-Aspartate (RGD) peptide derived from the ECM protein fibronectin is widely used and incorporated into hydrogels to promote cell adhesion and differentiation in both 2D and 3D [145-149]. Additionally, various MMP-degradable peptides are crosslinked in PEG hydrogels so that cells can degrade the matrix locally, acquire their native morphology and migrate [139, 150, 151]. As mentioned previously, the Young's modulus (E) of the substrate is critical for many cellular functions. The E of PEG hydrogels is determined by the crosslinking density of the monomers based on the monomer concentration, the molecular weight of PEG, or its initial structure (e.g., linear versus star). For example, increasing the weight percentage of PEGDA (molecular weight 2000, or 2K) from 10% to 30% raised shear modulus, which is proportional to E , from ~46MPa to ~297MPa. However, changing the PEGDA molecular weight from 2K to 8K at 10% monomer concentration reduced the shear modulus from ~46MPa to ~39MPa [152].

Beyond controlling initial properties of hydrogels, there is also interest in strategies that allow tailoring of the material properties with time. The native ECM environment is far from static, so it is critical to consider the design of dynamic synthetic scaffolds, and several excellent reviews have presented versatile methods to reversibly present different biochemical cues [22, 23, 153] and to change mechanical properties of the hydrogels [154]. Specifically in this thesis, a photo-responsive hydrogel system developed by Kloxin *et al.* [26] is utilized. In this system, PEGDA is modified with two photoliable nitrobenzyl ether groups at both ends as shown in blue

in Figure 1.4C [26], and these macromolecules can form a hydrogel via redox initiated free radical chain polymerization. Then, upon light irradiation (365nm or 740nm two photon), the gel network can be degraded due to photo-cleavage of the nitrobenzyl ether groups (Figure 1.4C). Utilizing these hydrogels, the differentiation, apoptosis and proliferation of VICs is studied in a dynamic and physiologically relevant environment (Chapters III and IV).

PEG hydrogels have served as useful cell matrix mimicry for a variety of cell types, such as stem cells, chondrocytes and fibroblasts, in both 2D and 3D culture. Huebsch and Mooney *et al.* showed that MSC populations have the potential to differentiate into multiple lineages in 3D PEG hydrogels modified with RGD peptides, predominantly differentiating into adipocytes in hydrogels with $E \sim 2.5\text{kDa}$ and becoming osteogenic in 11-30kDa gels [155]. PEG hydrogels with muscle-mimicking stiffness (E , $\sim 10\text{kDa}$) have facilitated the stemness of muscle satellite cells [25] and hold promises in constructing a niche for these progenitors *in vitro* [156]. The Anseth and the Bryant groups have developed PEG hydrogels for encapsulating chondrocytes and enhancing their production of aggrecan and collagen type II to regenerate cartilage [157-160]. PEG hydrogels have also been optimized for culturing fibroblasts from various tissues and studying their migration [161, 162], differentiation [106, 163] and proliferation [164].

1.5 Summary of the Thesis

The overall goal of this thesis is to understand and mimic the cell-matrix interaction in the aortic valves and to explore the mechanisms of matrix elasticity, TGF- β 1 and cell-cell adhesion in regulating the pathogenic phenotype of VICs which contributes to the progression of CAS (Figure 1.5). Towards this goal, I have characterized the primary VIC population isolated

from porcine aortic valves by flow cytometry in Chapter II and shown that this is a relatively homogeneous population of fibroblasts with small fractions of cells expressing stem cell markers. Chapter III describes soft PEG hydrogels as a tissue-mimicking substrate for culturing VICs, compared with plastic plates. These hydrogels have E around 7kPa and preserve the inactivated fibroblast phenotype of VICs via a stiffness-regulated PI3K/AKT pathway. Further in Chapter IV, I have shown that if the hydrogels are softened from ~ 32 kPa (disease-mimicking modulus) to ~ 7 kPa (normal tissue-like modulus), this redirects the activated valvular myofibroblasts and lung myofibroblasts into a less proliferative fibroblast fate. However, mature myofibroblasts are not detected on soft substrates even in the presence of TGF- $\beta 1$. In Chapter V, genome-wide transcriptional changes associated with the myofibroblastic differentiation induced by TGF- $\beta 1$ were examined by microarrays. Interestingly, TGF- $\beta 1$ up-regulates cell-cell adhesion molecules, including OB-cadherin and N-cadherin, to inhibit the myofibroblastic differentiation. The last Chapter discusses conclusions and future avenues for designing proper scaffolds in culturing VICs and other fibroblasts *in vitro* and for studying not just individual chemical, physical or biological cues, but their interplay in regulating cellular functions.

Regulators of VIC Differentiation into Pathogenic Myofibroblast Phenotype

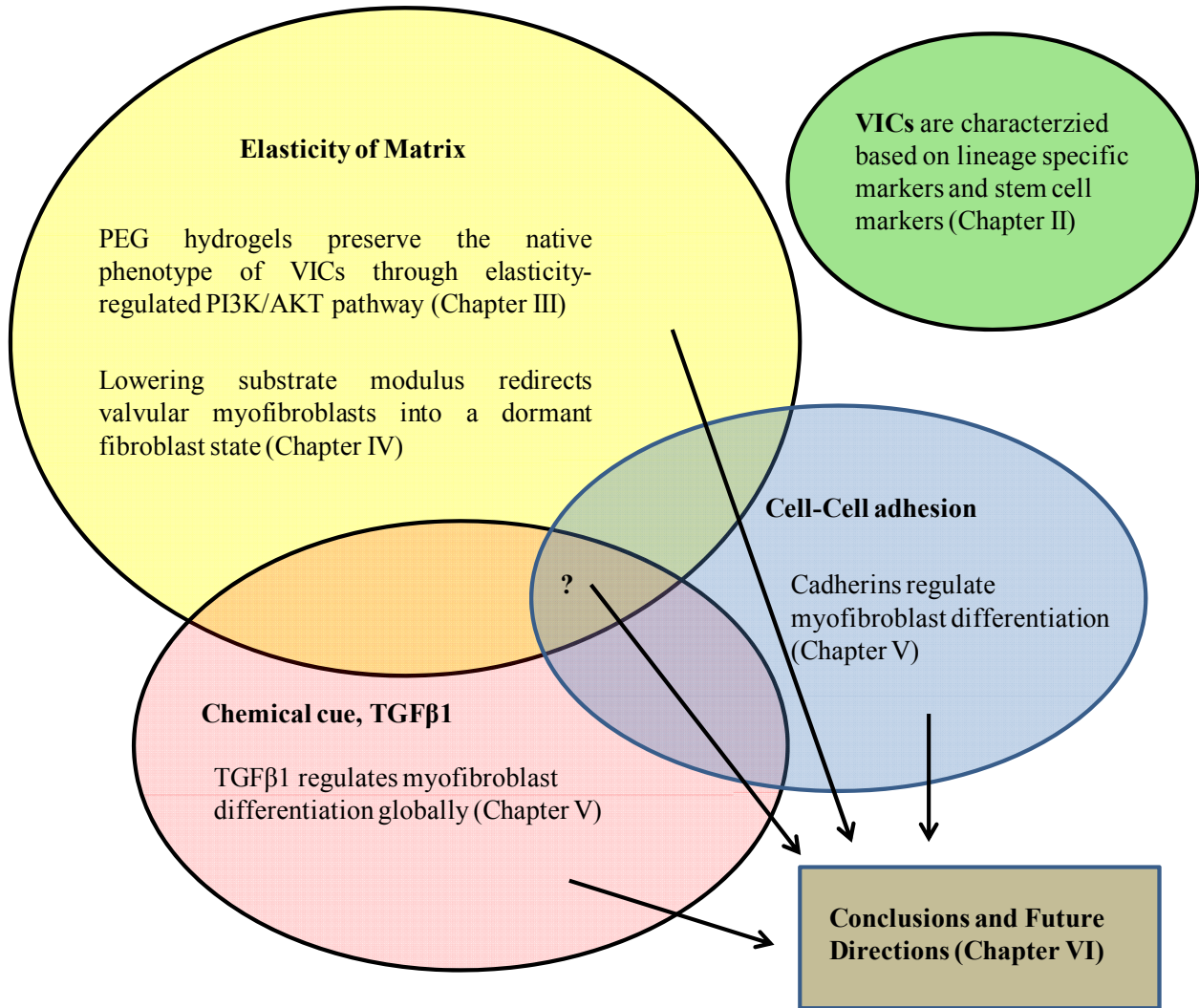


Figure 1.5 Thesis Outline.

CHAPTER II

CHARACTERIZATION OF PORCINE AORTIC VALVULAR INTERSTITIAL CELLS

2.1 Introduction

Cardiac valves open and close over 100,000 times a day ensuring directional flow of blood in the heart [2]. The cyclic movement and mechanical stress require that the tissue has the capacity to repair any damage that may occur during normal function. This remodeling has been suggested to be largely mediated by the main cell population in the valve, named valvular interstitial cells (VICs), since these cells have reversible and dynamic phenotypes and build the matrix structure from prenatal to postnatal valves [11, 13, 165]. VICs are somewhat heterogeneous but are largely fibroblasts, which play critical functions in both normal and diseased valves. VICs secrete not only the extracellular matrix components (e.g., collagen, fibronectin, etc.) of cardiac valves, but also the matrix remodeling enzymes, such as matrix metalloproteases (MMPs) that maintain valve homeostasis [78, 103]. However, in myxomatous valves, a portion of the VICs are activated to smooth muscle-like cells, or myofibroblasts, and produce higher level of MMPs that degrade the matrix [55]. In valve calcification, some VICs undergo differentiation into osteoblast-like cells, which actively mediate calcification inside the valves [46]. Collectively, this suggests that the cellular fates and functions of VICs play critical roles that determine the healthy or diseased state of heart valves.

Despite the important functions of VICs, it is not completely clear what the cellular composition of valves is and how different subpopulations of VICs regulate tissue functions. The

Magdi group found that human VICs from healthy valves express the fibroblast markers, fibroblast surface antigen (FSA) and vimentin, but only a small fraction of VICs express the human MSC marker, CD105, or the smooth muscle cell markers, desmin and smooth muscle myosin, based on immunocytochemistry [73, 78]. Bovine VICs have been shown to express integrin $\beta 1$ and type A nonmuscle myosin, but not the hematopoietic marker CD45 nor the endothelial/epithelial marker von Willebrand Factor (vWF) [71]. Additionally, c-Kit⁺ progenitor cells have been observed in human VICs [166], and bone marrow derived stem cells have been found to home to human and mouse cardiac valves and differentiate into fibroblast-like cells [167, 168]. As Liu *et al.* reviewed, VICs are a mixed population of different cell types, composed primarily of fibroblasts and a small percentage of myofibroblasts, smooth muscle cells and progenitor cells [12]. These cells regulate valvular functions coordinately.

However, most of the abovementioned studies have focused on characterizing protein markers of different subpopulations in VICs without doing functional studies. On the other hand, both porcine and bovine VICs have been shown to give rise to clones with different morphologies that maintain different levels of osteogenic potential [49, 71]. Yet, no protein marker(s) was identified to distinguish and purposely isolate the different VIC clones. There is a missing link between characterizing subpopulations based on protein markers and studying functions of those specific subpopulations from VICs. In this study, I aim to fill in the missing link by first characterizing cell surface markers of porcine VICs via flow cytometry and then sorting specific subpopulations of VICs based on those markers to study cellular functions. A collective list of cell surface protein markers, including CD45, CD31, CD105, Thy-1, ABCG2, NG2, OB-CDH and SSEA4, were used to quantify percentage of different subpopulations in

porcine VICs. This method not only enables us to quantitate VIC subpopulations, but also make it possible to reproducibly isolate desired subpopulations for studying their functions and contributions to valvular homeostasis and diseases.

2.2 Materials and Methods

2.2.1 Cell Isolation and Culture

Fresh porcine hearts were obtained from Hormel Foods Corporation (Austin, MN, USA) within 24 hour of sacrifice. Primary VICs were harvested from porcine aortic or pulmonary valve leaflets based on a sequential collagenase digestion as described previously [169]. Specifically, the aortic or the pulmonary valves were excised from the pig hearts and put into wash buffer comprised of Earle's Balanced Salt solution (Sigma, Cat# E2888), 50U/ml penicillin, 50µg/ml streptomycin, and 0.5µg/ml fungizone. After the wash, the leaflets were incubated with a Collagenase Type II solution at 250U/ml (Worthington Biochemical Corporation, Cat# LS004176, prepared in the wash buffer) for 30min at 37°C. The samples were then vortexed at a maximum speed for 30 seconds to remove endothelial cells. The leaflets were subjected to a second round of digestion with the Collagenase Type II solution for 1 hour and vortexed for 2 minutes to collect VICs. The isolated VICs were sorted and grown in growth media made from advanced DMEM/F12 (1:1) (Life technologies, Cat# 12634010) or Medium 199 (Life technologies, Cat# 11150067) with 15% Fetal Bovine Serum (FBS), 50U/ml penicillin, 50µg/ml streptomycin, and 0.5µg/ml fungizone. Media was refreshed every 2-3 days.

2.2.2 Flow Cytometry

Freshly isolated aortic or pulmonary VICs were strained through 100µm sieves twice and washed with cold PBS once. The cells were subsequently stained with selected primary

antibodies for 1 hour at 4°C. These antibodies were designed against ABCG2 (R&D systems, Cat# FAB995P), CD31 (Genway, Cat# 20-783-73927), CD45 (BD pharmigen, Cat# 560274), CD105 (R&D systems, Cat# FAB10971A), Thy1 (abcam, Cat# ab11155), OB-CDH (clone 15F7, a generous gift from Dr. Micheal Brenner group at the Brigham and Women's Hospital) and SSEA4 (R&D systems, Cat# FAB1435P). The samples were washed once with cold PBS after staining. For the CD31 antibody, samples were incubated with the secondary antibody goat-anti-mouse Alexa 488 (Life technologies, Cat# A-11001) for 1 hour at 4°C and washed once with cold PBS. DAPI was added to all samples at 0.1ng/ul to exclude the dead cells during flow cytometry. Percent of cells expressing these cell surface markers was quantified on a CyAN ADP flow cytometer (Dako). Cells were subsequently sorted based on positive or negative staining for ABCG2, gated with low DAPI staining (live cells).

2.2.3 Osteogenic and Adipogenic Differentiation

Sorted cells were expanded in growth media for a few weeks before re-seeding at an appropriate density for differentiation protocols. As a control, cells were cultured in control medium (High glucose DMEM (Life technologies, Cat# 11965-092) supplemented with 10% FBS, 50U/ml penicillin, 50µg/ml streptomycin, and 0.5µg/ml fungizone). For osteogenic differentiation, cells were treated with osteogenic medium (derived from the control medium supplemented with 100 nM Dexamethasone (Sigma, Cat# D1756), 50 µM ascorbic acid 2-phosphate (Sigma, Cat# 49752), and 20 mM β-glycerophosphate (Sigma, Cat# G9891)) for 15 days. For adipogenic differentiation, cells were treated with the adipogenic medium (derived from the control medium supplemented with 0.5mM 3-isobutyl-1-methylxanthine (IBMX, Sigma,

Cat# I5879), 1 μ M Dexamethasone and 5ug/ml insulin) for up to 16 days. Media was changed every 2-3 days.

2.2.4 Calcium Deposition Assay

Calcium deposition was assayed using a Calcium Reagent Set (Pointe Scientific, Inc), as described previously [170, 171]. Briefly, the matrix deposited by the cells cultured in osteogenic media was solubilized with 0.6N HCl overnight at 4°C. The supernatant was collected and diluted appropriately before mixing with the calcium reagent solution at 1:1. Absorbance was measured at 560nm. The relative calcium deposition was calculated by normalizing the blanked absorbance of the specified conditions to that of the ABCG2⁻ cells under the osteogenic condition at day 8.

2.2.5 Oil Red O Staining

Samples were fixed with 10% formalin at a neutral pH for ~40min. Oil Red O working solution was prepared fresh by mixing 3 parts of the Oil Red O stock solution (0.3 wt% of Oil Red O in isopropanol) and 2 parts of deionized (DI) water and filtering through a 0.2 μ m filter. After 2 washes with DI water, samples were incubated with 60% isopropanol for 5 min and subsequently incubated with the Oil Red O working solution for 5min. After washing with the tap water, cell nuclei were stained with hematoxylin 2.

2.3 Results and Discussion

2.3.1 Aortic and Pulmonary VICs Express very Low or None of the Lineage-specific Cell Surface Markers, But Small Percentages Express Stem Cell Markers

VICs were isolated from porcine aortic and pulmonary valves by collagenase digestion, which leaves the cell surface antigens/proteins intact. After isolation, the expression of

lineage-related cell surface markers, including CD45 (hematopoietic marker), CD31 (endothelial marker), CD105 (hMSC marker) and Thy1 (T cell or stem cell marker) was examined via flow cytometry. As shown in Figure 2.1, ~4% of aortic VICs express CD31, an endothelial cell marker, after subtracting the background. This small fraction of CD31⁺ cells could be due to contamination with valvular endothelial cells during VIC isolation. Aortic VICs do not express CD105, CD45 or Thy1 (Figure 2.1).

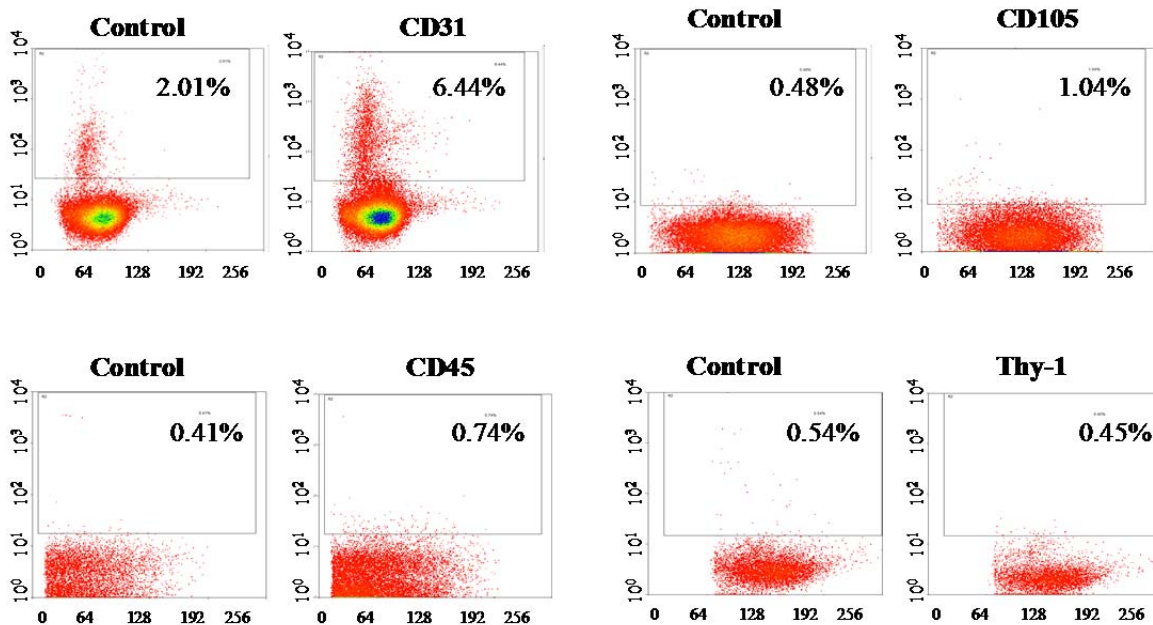


Figure 2.1 Aortic VICs Are Mostly Negative for CD31, CD105, CD45 and Thy-1. Freshly isolated porcine aortic VICs were stained with the antibodies for CD31, CD105, CD45 and Thy-1, and the corresponding control antibodies. Staining was quantified by flow cytometry, where the y-axis is the fluorescence intensity of the antibody staining and the x-axis is forward scattering. Rectangular boxes enclose the positively stained cells relative to background. VICs showed minimum CD31 staining (6.44%-2.01%=4.43%) and no staining for CD105, CD45 or Thy-1.

VICs isolated from aortic valves and pulmonary valves were compared and shown to have similar expression of the cell surface markers studied (Table 2.1). Besides the four protein

markers mentioned before, 3-6% of these cells express ABCG2, 5-6% express OB-cadherin (OB-CDH), and 7-9% of them express SSEA-4 (Table 2.1). SSEA-4 is a marker for embryonic stem cells [172] and may mark specific subpopulations in the valve. OB-CDH is a type of cadherin commonly expressed in mesenchymal cells and the expression of OB-CDH replaces that of N-cadherin during the myofibroblast activation in skin granulation tissue [120]. These OB-CDH⁺ VICs may be resident myofibroblasts in the valves, which regulate tissue remodeling. ABCG2 is a well established marker for somatic side population stem cells from a number of tissues [173, 174], and is therefore hypothesized to be resident progenitor cells in the valves.

Table 2.1 Aortic and Pulmonary VICs Express Similar Cell Surface Markers

Cell surface markers	Aortic VICs	Pulmonary VICs
CD105	-	-
CD45	-	-
Thy1	-	-
CD31	3.24±0.23%	n/a
ABCG2	3.57±0.94%	5.97±1.15%
OB-CDH	5.07±0.93%	5.66±1.46%
SSEA4	7.04±2.51%	8.66% *

Percent of VICs expressing specific cell surface markers was quantified by flow cytometry (2-5 independent experiments) and shown in the table. “-” means that cells stained negative for the marker. Data are presented as the average percentage ± standard error. “*” indicates that the experiment was done one time.

2.3.2 The Aortic ABCG2⁺ VICs Were Characterized for their Differentiation Potential *In Vitro*

The ABCG2⁺ VICs were isolated and characterized as a way to study the functions of VIC subpopulations. $3.57 \pm 0.94\%$ of VICs express ABCG2 (Figure 2.2A). Around 85% of the ABCG2⁺ VICs also express NG2 (Figure 2.2B). NG2 is a cell-surface proteoglycan, highly expressed by mural cells or pericytes, a type of progenitor cell closely associated with the microvascular tubes during development [175]. It is also expressed by the oligodendrocyte progenitors in the central nervous system [176]. The majority of the ABCG2⁺ VICs (>91%) do not express CD45 (Figure 2.2C). CD45 is expressed by most mature hematopoietic cells [177]. Our data suggest that these ABCG2⁺ cells could be pericyte-like progenitors, but because they are CD45⁻, they are not from the circulating blood lineage. This is consistent with the observation that the ABCG2⁺ cells in the interstitial of skeletal muscles also express NG2 [178].

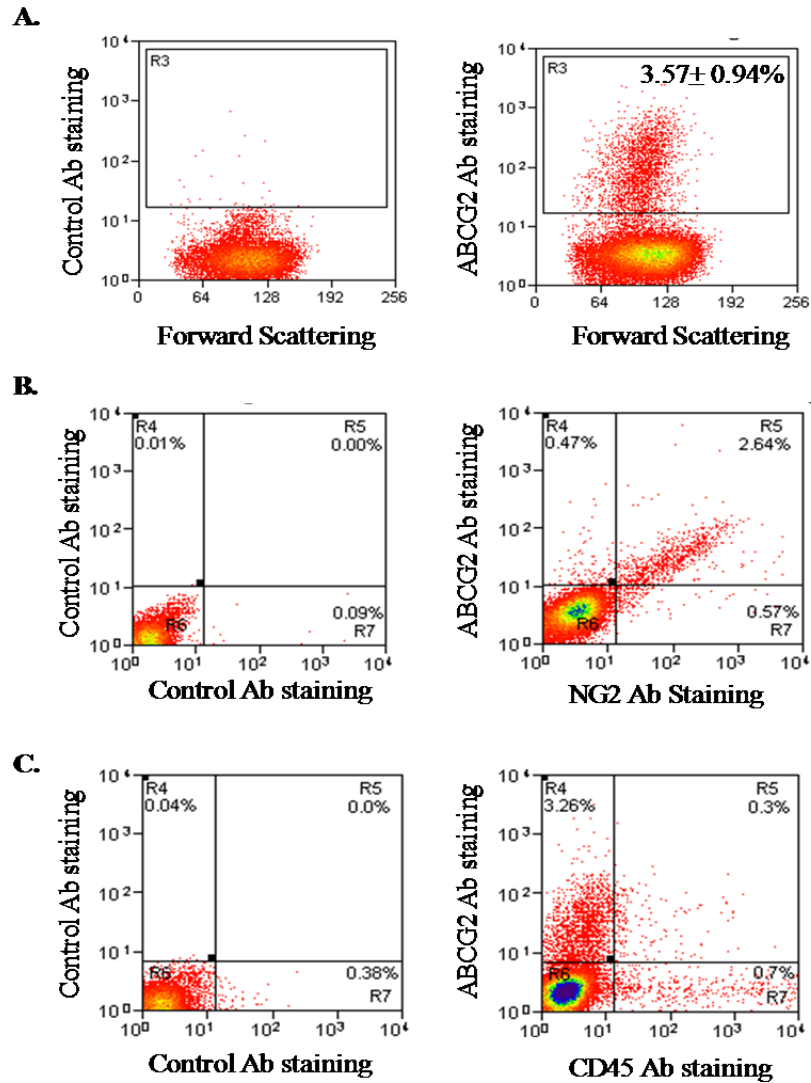


Figure 2.2 A Small Fraction of VICs Express Stem Cell Markers ABCG2 and NG2. Freshly isolated VICs were stained with the antibodies (Ab) against ABCG2, NG2, CD45 or the corresponding control antibodies before flow cytometry quantification. (A) $3.57 \pm 0.94\%$ of VICs express ABCG2. Around 85% of the ABCG2⁺ cells also express NG2 (B), however, only ~8% of the ABCG2⁺ cells express CD45 (C), indicating that most of these cells are not from the hematopoietic lineage.

When VICs were sorted and cultured on plastic plates, they mostly demonstrated fibroblast morphology (Figure 2.3). However, interestingly, some ABCG2⁺ VICs also demonstrated an endothelial cell-like morphology with tight cell-cell adhesion (Figure 2.3(i)). One group has shown that the endothelium of cardiac valves contains progenitors, which not only play a critical role for the initial cardiac cushion formation, but also maintain their differentiation potential in adult valves [179, 180]. As CD31 is a well-established marker for endothelial cells, the ABCG2⁺ VICs can be further characterized by CD31 expression to examine their relationship with the endothelium.

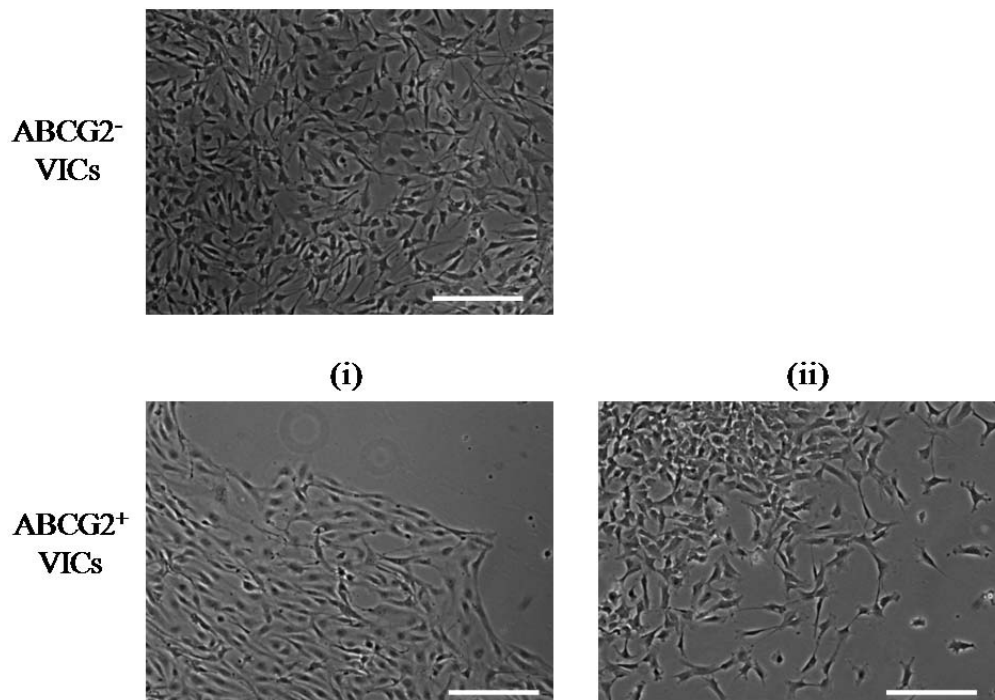


Figure 2.3 Morphology of the ABCG2⁺ VICs and the ABCG2⁻ VICs Grown on Tissue Culture Plates. Freshly isolated VICs were stained with an ABCG2 antibody linked with a fluorophore. Similar number of the ABCG2⁺ and the ABCG2⁻ cells were sorted by fluorescence activated cell sorting. When these cells were cultured on polystyrene plates, they both showed fibroblast morphology. However, the ABCG2⁺ cells had an additional phenotype where the cells formed tight cell-cell contacts (i). Scale bar: 100 μ m.

Despite markers consistent with other progenitor cell types, the ABCG2⁺ VICs did not show any differentiation advantages over the rest of the population in becoming osteoblasts or adipocytes (Figure 2.4). As shown in Figure 2.4A and quantified in Figure 2.4B, the ABCG2⁺ cells deposited more calcium mineralization on plastic plates than the ABCG2⁻ cells on day 8, but the difference was diminished over longer time scales, as on day 15 under osteogenic culture conditions. However, with adipogenic culture, neither the ABCG2⁺ nor the ABCG2⁻ cells were induced to become adipocyte-like cells, while bone marrow derived human mesenchymal stem cells differentiated into adipocyte-like cells with lipid droplets stained positive by Oil red O by day 15 (Figure 2.4C). It is possible that isolating the ABCG2⁺ VICs from their native niche and culturing them on plastic plate did not preserve their “stemness”, or that the differentiation protocols used for mesenchymal stem cells may not be optimal or appropriate for VIC progenitors. In the future, sorted ABCG2⁺ VICs could be introduced and cultured on soft hydrogels modified with extracellular matrix molecules, which would better mimic the stiffness and composition of the native leaflet, to enhance cell survival and maintain their native phenotypes [26, 109, 181].

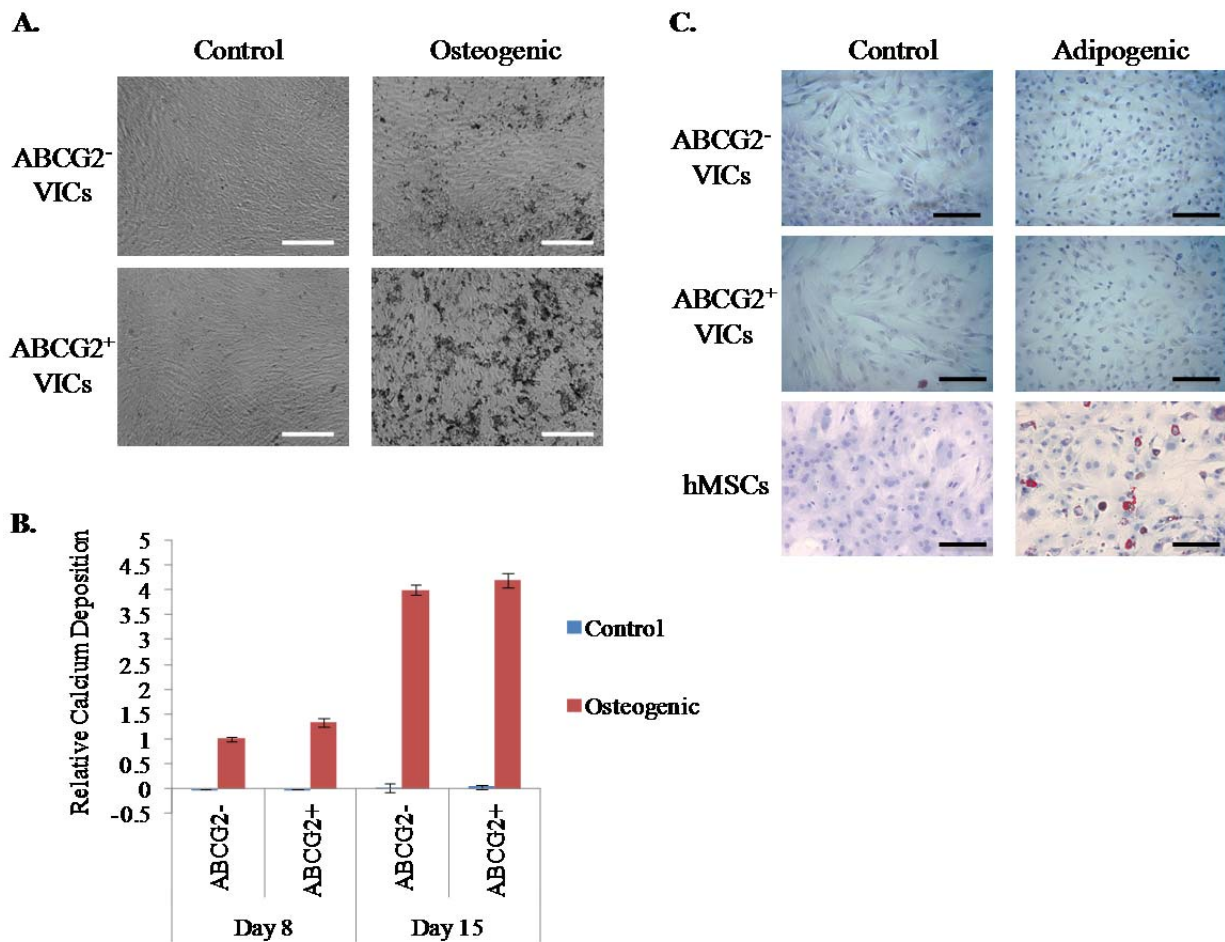


Figure 2.4 Both ABCG2⁺ VICs and ABCG2⁻ VICs Differentiate into Osteoblast-like Cells But Not Adipocytes. The sorted ABCG2⁺ or ABCG2⁻ cells were grown into confluency and re-plated in osteogenic or adipogenic media for up to 15 days. (A) Bright-field images of cells cultured in control condition or osteogenic condition were taken at day 8. The ABCG2⁺ cells had more mineralization spots than the ABCG2⁻ cells on the plates. (B) Compared with the ABCG2⁻ cells, the ABCG2⁺ cells produced a higher amount of calcium deposits at day 8, but a similar amount on day 15 when cultured in osteogenic media. (C) Cells were fixed and stained by Oil Red O after adipogenic stimulation for 15 days. Only hMSCs, but not VICs, showed red staining of lipid droplets inside cytoplasm, a characteristic marker of adipocytes. Scale bar: 100 μ m.

2.4 Conclusion

VICs, for a long time, have been defined based on the location of the cells within the valves. But, more and more studies contribute to our understanding of the cellular composition of VICs. I have characterized porcine VICs based on a number of lineage-associated cell surface makers, including CD31, CD105, CD45 and Thy-1, and some other markers either related to stem cell subpopulations (e.g., ABCG2, NG2, SSEA4), or associated with myofibroblast differentiation (e.g., OB-CDH). The results suggest that these cells are mostly negative for CD31, an endothelial cell marker, and negative for CD105, a marker for the mesenchymal stem cells. They are not from the hematopoietic lineage (CD45⁻) or from the T-cell lineage (Thy-1⁻). Additionally, small fractions of VICs express ABCG2, OB-CDH or SSEA4. These specific subpopulations can be sorted and studied for their functional properties (ABCG2⁺ VICs as a model), which should contribute to a better understanding as to how VICs, as a mixed population, maintain valvular homeostasis and participate in tissue repair and pathology.

CHAPTER III

POLY(ETHYLENE GLYCOL) HYDROGELS PRESERVE NATIVE PHENOTYPES OF VALVULAR INTERSTITIAL CELLS THROUGH AN ELASTICITY-REGULATED PI3K-AKT PATHWAY

3.1 Introduction

Every cell has its distinct niche. Fibroblasts reside in interstitial mesenchyme maintaining the balance and structure of its matrix scaffold; muscle satellite cells reside in between basal lamina and muscle fibers waiting to be activated by injure signals; hematopoetic stem cells circulate in bone marrow, replenishing blood cells continuously. In a basic sense, a niche is defined as the extracellular microenvironment surrounding progenitor cells; this niche can be comprised of extracellular matrix (ECM), soluble or tethered chemical factors and different cell types. The ECM plays an important role in maintaining the niche, as it is not just a passive scaffold, but rather presents a myriad of chemical and physical cues to instruct cell fate. These ECM changes can dramatically influence cellular functions. For example, when basal lamina is damaged, local muscle satellite will enter cell cycle, differentiate and fuse to regenerate damaged muscle tissue [182]. Additionally, in fibrogenic diseases, which are often associated with increased collagen deposition and elevated levels of matrix remodeling, resident fibroblasts acquire an activated myofibroblast phenotype with α -smooth muscle actin (α SMA) stress fibers [105]. The integrity and signaling of ECM are imperative for regulating normal cell functions and maintaining organism homeostasis; however, the processes can be complex and often

involve multiple pathways.

One such cellular matrix that is critical to tissue function is the aortic valve, which controls the unidirectional flow of blood during heart contractions. The aortic valve is composed of elastin-, proteoglycan- and collagen-rich layers of ECM [3] and supports survival and metabolism of valvular interstitial cells (VICs). VICs are the main fibroblast population in aortic valves that secrete ECM-related proteins for tissue development and homeostasis [12]. Normal valves maintain a bulk elastic modulus (E), which measures deformation of a material to external force, around 0.8-8 kPa [19]. As valve stenosis develops, which is characterized by fibrotic stiffening and nodule-like calcification, the tissue can become as stiff as bone (E , ~3-4 GPa). VICs have been shown to differentiate from quiescent fibroblasts in normal valves into pathogenic myofibroblasts and osteoblast-like cells in diseased valves [6]. In fact, valve matrix stiffening is often associated with the pathogenic phenotypes of VICs. Consistently *in vitro*, VICs are activated to myofibroblasts in response to a high substrate modulus ($E > 15$ kPa), but this phenotype can be reverted when the substrate modulus is reduced [106, 109]. Based on the evidence above, I hypothesize that the native quiescent VIC phenotype can be preserved when bio-scaffolds present appropriate physical cues and chemical cues, more closely mimicking valvular ECM.

Traditionally, primary cells once isolated from different tissues are cultured on polystyrene plates for studying their functions *in vitro*. While plastic plates have been very useful in supporting basic survival and proliferation of most cell types, they lack physiologically relevant elasticity for cell signaling. For example, muscle satellite cells lose their ability to self renew when cultured on stiff plastic plates, but maintain this stem cell property when cultured on

substrates with a muscle-like E around 10kPa [25]. To mimic the elasticity of human tissues, which have E ranging from ~ 0.1 kPa to a few GPa, synthetic poly(ethylene glycol)(PEG) based hydrogels have been developed [100, 154, 183]. PEG hydrogels are polymer networks with high equilibrium water content and minimal non-specific protein adsorption (i.e., fouling), mimicking several aspects of an endogenous tissue environment in terms of elasticity, diffusion and interstitial flow [139]. These gels can be fabricated with different elasticities, which relates to stiffness, by varying the macromer concentration or the molecular weight of PEG [143, 154]. In the present study, PEG diacrylate with a photolabile nitrobenzyl ether group [26] was utilized to synthesize culturing substrates for VICs with physiologically relevant E (from ~ 7 kPa to ~ 32 kPa), which spans the range of normal and diseased valves. Further, as the native ECM environment is far from static, it is advantageous to design dynamic synthetic scaffolds. The modulus of the photodegradable PEG hydrogels can be reduced by light irradiation *in situ* from 32 kPa to 7 kPa [26], enabling close monitoring of changes in intracellular signaling in response to modulus reduction.

Despite the important roles of elasticity in regulating the functions and differentiation of an array of cell types, including fibroblasts [104, 105, 110, 111], human MSCs [112] and myoblasts [113], there are still many questions about how the mechanical cue of elasticity gets translated into intracellular signaling. Dupont *et al.* showed that YAP and TAZ, two transcriptional factors, can serve as sensors to ECM stiffness in a Rho GTPase- and actomyosin cytoskeleton-dependent manner in MSCs and determine cell differentiation into osteoblasts on stiff substrates and into adipocytes on soft substrates [112]. As cells bind to their matrix via integrins, these transmembrane proteins are mechano-sensitive and elicit biochemical pathways

intracellularly, including FAK, ERK and JNK signaling [114]. Han and Schlunck have shown that soft substrata attenuated persistence of TGF β 1 signaling, which acted through Smad2/3, ERK and AKT in human trabecular meshwork cells [116]. Recently, Huang and Zhou *et al.* showed that lung fibroblasts initiated nuclear translocation of Megakaryoblastic leukemia factor-1 (MKL1) and RhoA/Rock activation on stiff substrata [117]. The PI3K/AKT pathway has been shown to be activated by the mechanical cue of cyclic strain in mesangial cells [118], but has not yet been shown to be regulated by substrate elasticity.

To understand VIC-matrix interactions, I set out to find a tissue-mimicking scaffold for culturing VICs and one that would more closely maintain their native phenotypes. I find that a soft PEG hydrogel is a promising candidate, as VICs cultured on these gels maintain the unactivated fibroblast phenotype, with lower mRNA level of myofibroblast differentiation genes, including α SMA, Col1A1 and CTGF, and lower α SMA protein expression, than those cultured on plastic plates. My data support that the *E* of the substrate is regulating pathogenic VIC differentiation. Further, VICs respond to reduction in *E* through the PI3K/AKT pathway, but not FAK or p38 MAPK. Blocking the PI3K/AKT activation significantly reduces myofibroblast differentiation on stiff gels and plastic plates. When constitutively active PI3K is over-expressed in these cells, they show more activation on plastic plates. These results point towards a molecular mechanism of how VICs respond to the elasticity of their microenvironment, which may be applicable to other fibroblasts. The therapeutic potential of the PI3K/AKT signaling in treating abnormally persistent myofibroblast activation warrants further exploration.

3.2 Materials and Methods

3.2.1 Cell Isolation

Primary VICs were harvested from porcine aortic valve leaflets based on a sequential collagenase digestion as previously described [169]. Briefly, leaflets were digested in a Collageneous Type II Solution (250U/ml, Worthington Cat# CLS-2) for 30min and vortexed briefly to remove endothelial cells. VICs were obtained after a second round of incubation in the Collageneous Type II solution for 1 hour and a vortex for 2min. The freshly isolated cells (P0) were seeded on day 0 at 90,000~100,000 cells/cm² on plastic plates or hydrogels, with basal medium (Medium 199, 50U/ml penicillin, 50µg/ml streptomycin, and 0.5µg/ml fungizone) supplemented with 1% fetal bovine serum (FBS). LY294002 (Cell Signaling Technology, Cat# 9901) or MK2206 (Selleck Chemicals, Cat# S1078) was treated on day 3 at 50-100µM or 3-5 µM respectively for 48 hours. For some experiments, VICs at early passages (1 to 2) were used. Valve cultures were based on culturing fresh valve leaflets, which were scraped gently by blades to remove endothelial cells, in the basal medium supplemented with 1% FBS for 5 days.

3.2.2 Porcine Genome Microarray

Total RNA was extracted using RNeasy Mini Kit (Qiagen, Cat# 74104) from P0 VICs or VICs cultured on plastic plates (Plated VICs). Plated VICs were grown up in basal medium supplemented with 15% FBS and subsequently cultured at 45,000 cells/cm² on plastic plates with the basal medium supplemented with 1% FBS for 2 days. All the RNA samples had 260/280 ratio ≥ 2.0 and RNA Integrity Number (RIN) ≥ 9.2 verified by RNA Bioanalyzer. Total RNA was amplified and labeled using Gene Chip 3' IVT Express Kit (Affymetrix, Cat# 901228) and hybridized to Porcine Genome Microarrays (Affymetrix, Cat# 900624). Three microarrays were

performed for each condition. Microarray data were analyzed using Spotfire (TIBCO) and DAVID Functional Annotation Bioinformatics analysis (<http://david.abcc.ncifcrf.gov/>).

3.2.3 Hydrogel Synthesis

Photodegradable poly(ethylene glycol) hydrogels (PD-PEG) were synthesized as previously described [26, 109]. Briefly, hydrogels were fabricated by copolymerizing the photodegradable crosslinker ($M_n \sim 4070$ g/mol, 8.2 wt%) [144] with PEG monoacrylate (PEGA, $M_n \sim 400$ g/mol, 6.8 wt%, Monomer-Polymer and Dajac Laboratories, Inc) and an acrylated adhesion peptide containing the RGDS sequence (5mM) via redox-initiated polymerization (with 0.2M Ammonium Persulfate and 0.1M Tetramethylethylenediamine (TEMED)). The peptide was synthesized as previously described [109]. The hydrogels were molded on coverglasses as thin films (0.25mm thick) with a surface area (A) of ~ 250 mm² and ~ 370 mm² respectively. The crosslinking density of the gels can be reduced by irradiation with a long wavelength (365nm), low intensity ultraviolet (UV) light (10mW/cm²) for 5 minutes. The initial Young's Modulus (E) of the material was measured at ~ 32 kPa (stiff gels), while E after 5 minutes of irradiation was reduced to ~ 7 kPa (soft gels) as verified by rheometry and atomic force microscopy [106].

3.2.4 Immunocytochemistry

Immunocytochemistry was performed according to standard methods developed for cells cultured on hydrogels [106, 109]. Briefly, samples were fixed with 4% paraformaldehyde, permeabilized in 0.1% TritonX100, and blocked with 1% bovine serum albumin (BSA) and 5% normal goat serum. Primary α SMA antibody (Abcam, Cat# ab7817) was diluted in the blocking solution at 1:100 and incubated with the samples overnight at 4°C. Following washes in PBS with 0.05% Tween 20 (PBST), samples were labeled with DAPI (1 μ g/ml) and goat-anti-mouse

Alexa Fluor 488 secondary antibody (Life technologies, Cat# A11017). A LSM 710 Laser Scanning Microscope (Carl Zeiss) was used to image the samples. Images were subsequently processed by Zen and ImageJ software. Myofibroblasts were defined as cells with α SMA staining organized into stress fibers, and the percentage of myofibroblasts was calculated based on (the number of myofibroblasts / total number of cells) x 100%. Six random fields of view were counted, calculated and averaged for each condition.

3.2.5 Quantitative Real-Time PCR (qRT-PCR)

qRT-PCR was performed for VICs as described in detail before [109]. Total RNA was collected from 2 hydrogels with A ~ 370 mm² based on a modified TRI Reagent extraction (Sigma, Cat# T9424). Briefly, 2 consecutive chloroform extractions were performed. cDNA was synthesized from total RNA with the superscript III reverse transcriptase (Life technologies, Cat# 18080-051) and random hexamer primers. SYBR Green-based qRT-PCR using gene specific primer sets (Table 3.1) was performed on an Applied Biosystems 7500 Real-Time PCR machine to determine gene expression.

Table 3.1 Gene Primer Sequences for qRT-PCR

Gene	Forward Primer Sequence	Reverse Primer Sequence
α SMA	GCAAACAGGAATACGATGAAG	AACACATAGGTAACGAGTCAGAGC
ACSS3	CTGACTTAGGCTGGGTTGTCG	CGGAAATAAGCACCAGCATCC
ADAMTS1	GTGATCCCAGTAGAAGCTGCTC	CATTGCTCGGCATCATCATG
CDC 20	CATTCGAATCTGGAACGTCTG	GAGACCAGAGAATGGAGCACA
CEBPD	GCAACCAAGAGATGCAGCA	TGCTTGAAGAATCGCCGCA
CHSY1	CGCCCAGAAATACCTGCAGA	CGACGTGTCTGAACCCTCACTAG
Col 1A1	GGGCAAGACAGTGATTGAATAC	GGATGGAGGGAGTTTACAGGAA
CPE	GAAAGTAGCTGTTCCCTATAGC	TCAGAAAATGACTCTAGCTCAAAA
CTGF	CTGGTCCAGACCACAGAGTGG	GCAGAAAGCGTTGTCATTGG
FN 1	GGCATTGATGAAGAACCCTTG	GCCTCCACTATGATGTTGTAGGTG
ID2	CGCTGACCACCCTAAATACG	GAGCGCTTTGCTGTCCTTG
ITGA5	CCAAAGGGAACCTCACCTACG	ACCTGTTCCCCTGAGAAGTTGTAG
MMP1	GGCATCCAGGCCATCTATG	CACTTGTGGGGTTTGTGGG
MYLIP	CTGTGCTGTGAGGGCGAGA	CACTCGCGACCTGCAAACG
NCDH	GTGGTATGGATGAAACGCCGG	CAGCTGGCTCAAGTCATAGTC
OB-CDH	GGGTCCCTGAGCTCCTTAGA	CGAGGTCCCAGTTCTGTAG
PDK4	CCACATTGGCAGCATTGAC	ACAGAGCATCTTGGAACACTCAA
PTGDS	CCAACTTCCAGGAGGACAAG	CCAGCGATTTGCACATGGAC
RASAL2	ACACGAGCTTTCGGCTTCC	GGCTCAGCAAGGATTCATGTG
S100A4	GAGCTAAAGGAGTTGCTGACC	CTGTCCAGGTTGCTCATCAG
SAT1	GGCATAGGATCAGAAATCCTG	GAAGTTGATAGATGGTTCATTCC
TIMP3	ATCCTGCTACTACCTGCCTTGC	GGATGCAGGCGTAGTGTTTG
TMPO	CTTCTACTCCTCTGCCAACA	GTGGTTCTCTTCTCAAGCTT
TUFT1	GGAGAAGATCCACCACTTGGA	GTGTCCTTTGACTGGATCACAG
USP14	GGTCTAGCTCTTCAGGCCAT	GCAAGATATCCTCTGGTGTCA
VIM	AGGAAGAGATGGCCCGTCA	CCTGCTCTCTTCTCCTTCCA

3.2.6 Western Blot

VICs were harvested from 2 hydrogels (A \sim 370 mm²) by trypsin and resuspended in the RIPA buffer (Upstate, Temecula, CA, Cat# 20-188) with protease inhibitor cocktail (EMD Milipore, Cat# 539134) and phosphatase inhibitors (Roche, Cat# 04906845001). Cell lysates were subsequently rotated at 4°C for 30 min and centrifuged at 12,000 RPM for 15min. Supernatant was saved for sodium dodecyl sulfate-polyacrylamide gel electrophoresis

(SDS-PAGE). The protein concentrations of the samples were measured by a microBCA kit (Thermo Scientific, Cat# 23235). 10-15µg of total protein for each sample was loaded into the 10% TGX mini gels (Bio-rad, Cat# 456-1033) and separated by electrophoresis for 1 hour at 200V. The proteins were subsequently transferred onto a nitrocellulose membrane using Trans Blot Semi-Dry transfer cell (Biorad) at 20V for 1 hour. The nitrocellulose membrane was blocked with TBST with 5% milk for 1 hour at room temperature (RT) and then incubated with primary antibodies overnight at 4°C. After washes with PBST (PBS with 0.05% Tween20), secondary antibodies conjugated with horseradish peroxidase (HRP) were applied for 1 hour at RT. Protein bands were visualized by applying a chemiluminescent substrate of HRP (Thermo Scientific, Cat# 34075) and exposing the membrane to x-ray films. Protein abundance was subsequently quantified by Image J. The following antibodies were used in this study: pFAK (Life technologies, Cat# 44-624G), FAK (Sant cruz biotechnology, Cat# sc-558), pAKT (Cell signaling technology, Cat# 4058S), AKT(Cell signaling technology, Cat# 9272), pp38 MAPK (Cell signaling technology, Cat# 4511), p38 MAPK (Cell signaling technology, Cat# 9212), GAPDH (Cell signaling technology, Cat# 2118) and αSMA (Abcam, Cat# ab7817). At least 3 biological replicates were screened by western blot for each condition.

3.2.7 Transfection

Freshly isolated VICs or VICs at passage 2 (P2) were transfected with pcDNA3 empty vector or pcDNA3 with myristoylated AKT based on protocol U23 on Lonza amaxa nucleofector. The pcDNA3 encoding myristoylated AKT was purchased from Addgene (Cat# 9008) and was described previously [184]. VICs were prepared in a single cell suspension at 2-3 million cells per 100ul of the buffer provided by the kit (Lonza, Cat# VPI-1002). After transfection, cells were

recovered in basal media with 15% FBS for 15min in the CO₂ incubator and seeded on plastic plates or soft hydrogels at desired seeding densities.

3.2.8 Adenovirus Production

Recombinant adenoviruses expressing GFP or p110-CAAX, a membrane-localized constitutively active subunit of PI3K, were amplified in 293 cells and purified based on banding in a CsCl buoyant density gradients. The p110-CAAX adenovirus was a generous gift from Dr. CS Chen (University of Pennsylvania). Virus concentration was determined as described [185]. VICs were infected with the adenoviruses at a multiplicity of infection (MOI) of 50, 100 and 150, all of which gave good infection efficiency based on the percentage of GFP expressing cells in the population.

3.2.9 Statistics

Data are presented as mean \pm standard error of the mean (SEM). SEM was calculated based on three biological replicates. Each biological replicate was based on an isolation of VICs from 60-90 pooled porcine aortic valves. A Student's *t test* was used to compare data sets with two conditions and the One-way ANOVA with Bonferroni's post test was used to compare data sets with more than two conditions. A *p* value less than 0.05 was considered statistically significant.

3.3 Results

3.3.1 Culture on Polystyrene Plates Changes the Whole-Genome Transcriptional Profile of VICs

I used porcine whole genome microarrays, to ask how plating freshly isolated VICs (P0 VICs) on tissue culture polystyrene (TCPS) changes mRNA expression (Figure 3.1A). In

Figure 3.1A, the heat map showed mRNA expression level for each probe detected in the microarrays after GC Robust Multi-array Average (GCRMA) normalization (green: low expression, red: high expression). Specifically, 2173 genes were up-regulated and 1926 genes were down-regulated in VICs cultured on plastic plates for only 24 hours, compared to P0 VICs, with fold change ≥ 2 and p value ≤ 0.01 (Figure 3.1B). These differentially regulated genes were further analyzed by DAVID Functional Annotation Bioinformatics tools. The most significantly up-regulated gene functions for plated VICs relative to P0 VICs related to cell cycle, cytoskeleton, and mitochondrion. In contrast, the most significantly down-regulated gene functions included cell adhesion, extracellular matrix, polysacharride binding, and acute inflammatory response (Figure 3.1C).

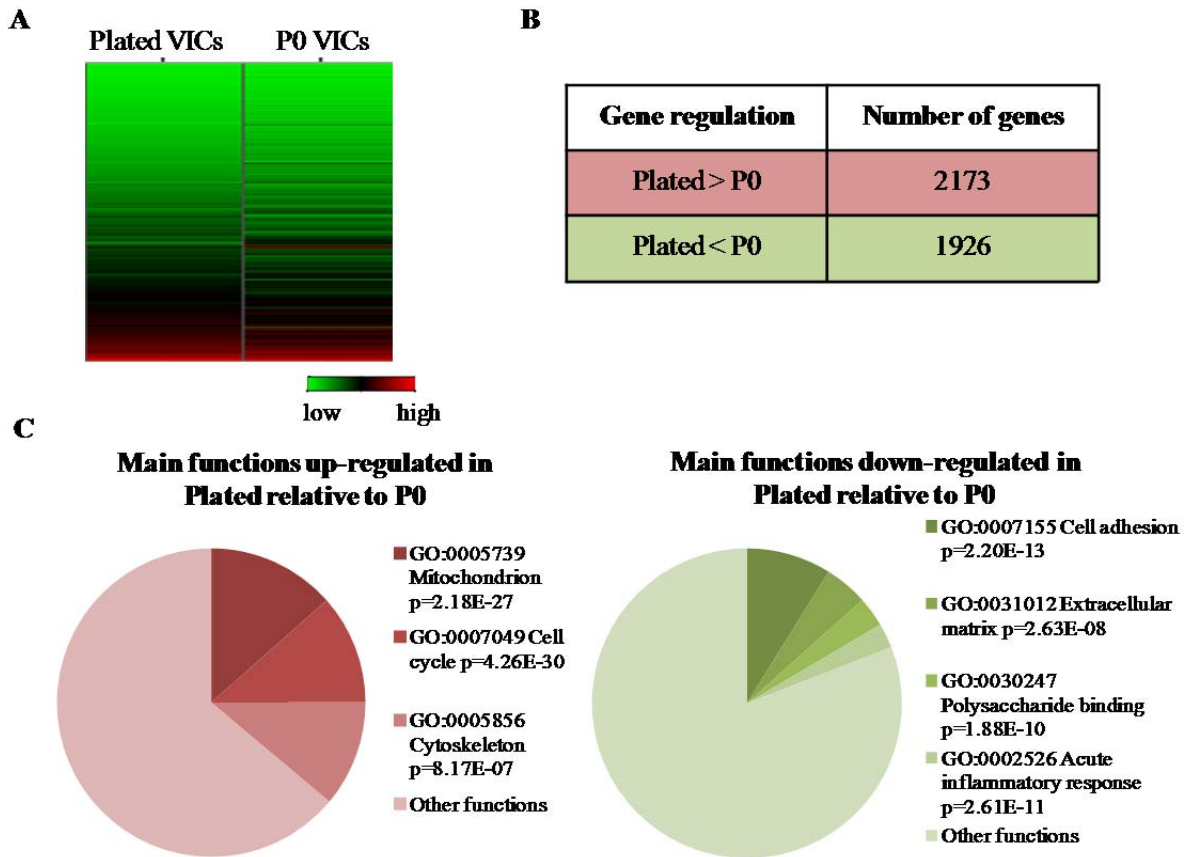


Figure 3.1 Culture on Plastic Plates Changes the Whole-Genome Transcriptional Profile of VICs Isolated from Porcine Aortic Valves. Transcriptional profiling (Affymetrix porcine genome microarray) was performed to examine the expression of over 20,000 genes in freshly isolated VICs (P0 VICs) and VICs cultured on plastic plates (Plated VICs). (A) Hierarchical clustering showed striking differences between the 2 conditions, indicating that plastic plates do not provide a physiologically relevant environment for preserving the native mRNA profile of these cells. (B) Based on statistical analysis, 2173 genes were significantly up-regulated (≥ 2 fold) and 1926 genes were significantly down-regulated (≥ 2 fold) in Plated VICs in comparison to P0 VICs, with $p < 0.01$. (C) DAVID functional annotation showed that genes related to mitochondrion, cell cycle, and cytoskeleton were significantly up-regulated, however, cellular functions, including cell adhesion, extracellular matrix, polysaccharide binding and acute inflammatory response were down-regulated in Plated VICs compared with P0. Percentage in the pie charts refers to the fraction of genes that fall into each functional category.

3.3.2 Microarray Data Are Validated Consistently by qRT-PCR

Genes were randomly selected from different functional categories for validation using qRT-PCR. S100A4, CDC20, TMPO, USP14 were significantly up-regulated, whereas, CPE,

PTGDS, SAT1, CEBPD were significantly down-regulated in plated VICs compared with P0 VICs (Figure 3.2). The fold change of each gene detected by qRT-PCR followed the magnitude of changes observed in the microarrays (table in Figure 3.2).

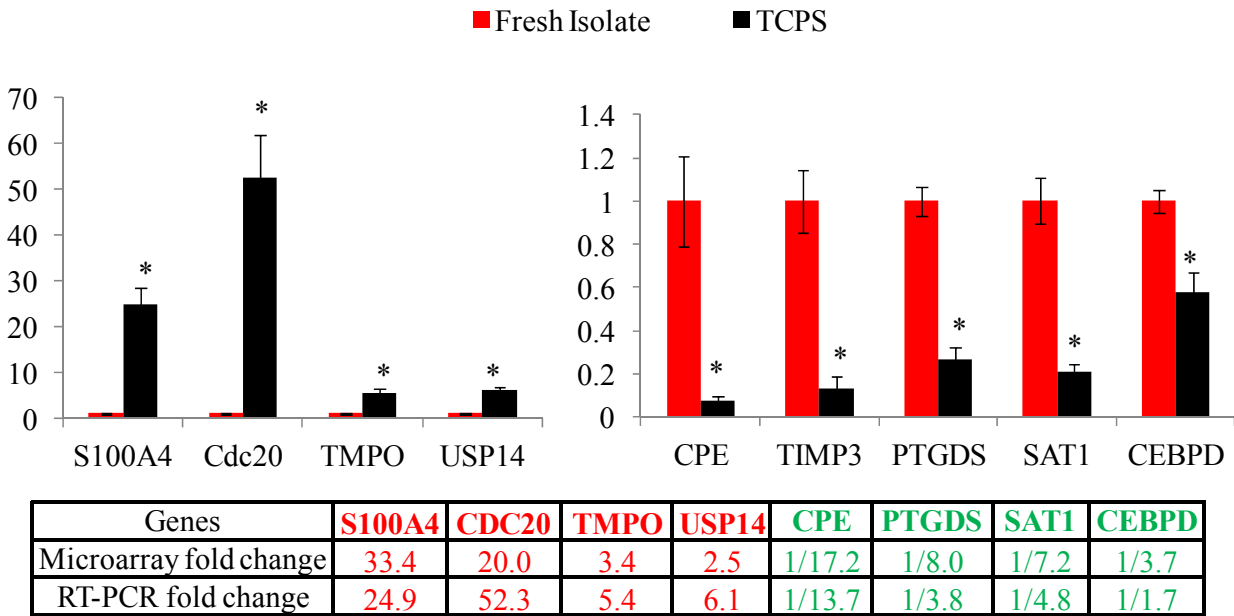


Figure 3.2 qRT-PCR Validation of Microarray. Four genes up- or down-regulated in VICs after culture on TCPS were measured by qRT-PCR. Expression levels of these genes were significantly different between P0 VICs and Plated VICs. * means $p < 0.05$. Error bars: standard error. As shown in the table, qRT-PCR-derived fold change of each gene (calculated based on Plated VICs/P0 VICs) was similar to that observed in the microarrays.

3.3.3 Soft PEG Hydrogels Preserve Native Phenotypes of VICs Better Than Plastic Plates

When VICs were cultured on soft PEG hydrogels or plastic plates, they maintained similar fibroblast morphology as observed in native VICs. However, at the gene expression level, VICs cultured on plastic plates had significantly higher expression of the fibrogenic promoting genes, including ~86 fold increase in α SMA, ~7 fold increase in CTGF and ~2 fold increase in Col1A1, than P0 VICs (Figure 3.3A). VICs cultured on soft gels or native valve matrix

maintained low expression of these genes, comparable to the level of P0 VICs (Figure 3.3A). TIMP2 and TIMP3 were highly expressed in P0 VICs and valve culture, but were significantly down-regulated with soft gels and plastic plates. At the protein level, freshly isolated VICs and VICs cultured on soft gels expressed much lower level of α SMA than those cultured on plastic plates (Figure 3.3B)

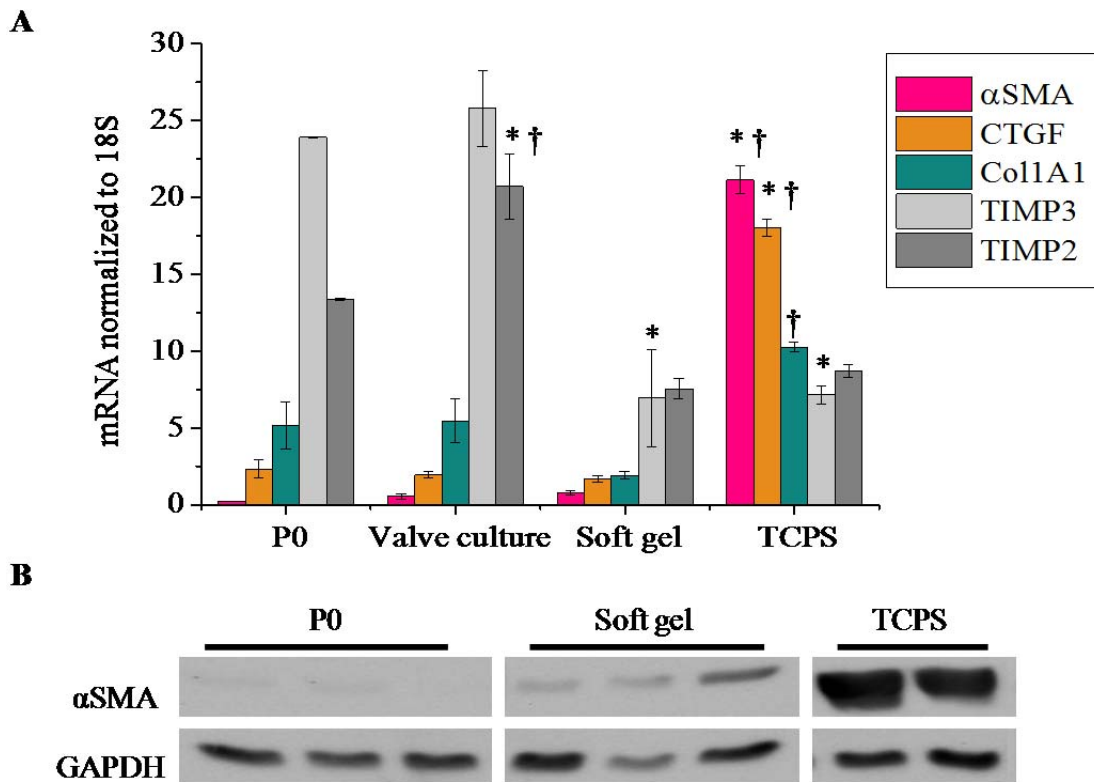


Figure 3.3 Soft PEG Hydrogels Preserve Native Phenotypes of VICs Better Than Plastic Plates. (A) Expression levels of multiple major fibrogenesis-associated genes were analyzed by qRT-PCR. α SMA, CTGF, and Col1A1 were significantly up-regulated when VICs were cultured on plastic plates, but were preserved at levels similar to native cells when cultured on soft hydrogels and in valve culture. TIMP3 and TIMP2 were expressed at high levels in P0 VICs and valve culture, but were inhibited for VICs cultured on both soft gels and plastic plates. * means significantly different from P0 with $p < 0.05$; † means significantly different from the soft gel condition with $p < 0.05$. (B) α SMA protein level was measured by western blot for VICs cultured on different substrates. VICs cultured on soft gels, like P0 VICs, express significantly less α SMA protein than those cultured on TCPS. All these data support that soft hydrogels preserve the native phenotype of VICs, while plastic plates promote the pathogenic myofibroblast phenotype.

3.3.4 Soft PEG Hydrogels Prevent Valvular Myofibroblast Activation through an Elasticity-regulated PI3K-AKT Pathway, But Not the FAK or the P38 MAPK Pathways

I hypothesize that substrate modulus, which relates to stiffness, contributes to VIC activation. Hydrogels with the same surface chemistry but tunable elasticity were synthesized to test this hypothesis. Stiff hydrogels ($E \sim 32\text{kPa}$) were fabricated and subsequently softened (final $E \sim 7\text{kPa}$) via exposure to collimated light ($\lambda = 365\text{nm}$; $I_0 = 10.0 \pm 0.5 \text{ mW/cm}^2$). As shown in Figure 3.4A, VICs cultured on plastic plates or stiff gels displayed a characteristic myofibroblast phenotype with αSMA stress fibers. However, cells residing in the valve or cultured on soft or stiff-to-soft gels had minimal αSMA staining and organization (Figure 3.4A). The activation levels of various phosphorylated signaling proteins were quantified by western blot (Figure 3.4B-D). pAKT/AKT, a readout of PI3K activation, showed significant up-regulation when these cells were cultured on stiff substrates (plastic plates and stiff gels), relative to P0 VICs (Figure 3.4B). However, when the Young's modulus of the culture substrates was reduced from $\sim 32\text{kPa}$ to $\sim 7\text{kPa}$ (stiff-to-soft gels), Akt phosphorylation was significantly reduced, which happened as early as 2 hours after softening and persisted at a low level 48 hours after modulus reduction (Figure 3.4B and 3.4E). Neither the pFAK/FAK nor the pp38 MAPK/p38 MAPK changed significantly when P0 VICs were cultured on materials with different mechanical properties (Figure 3.4C and 3.4D)..

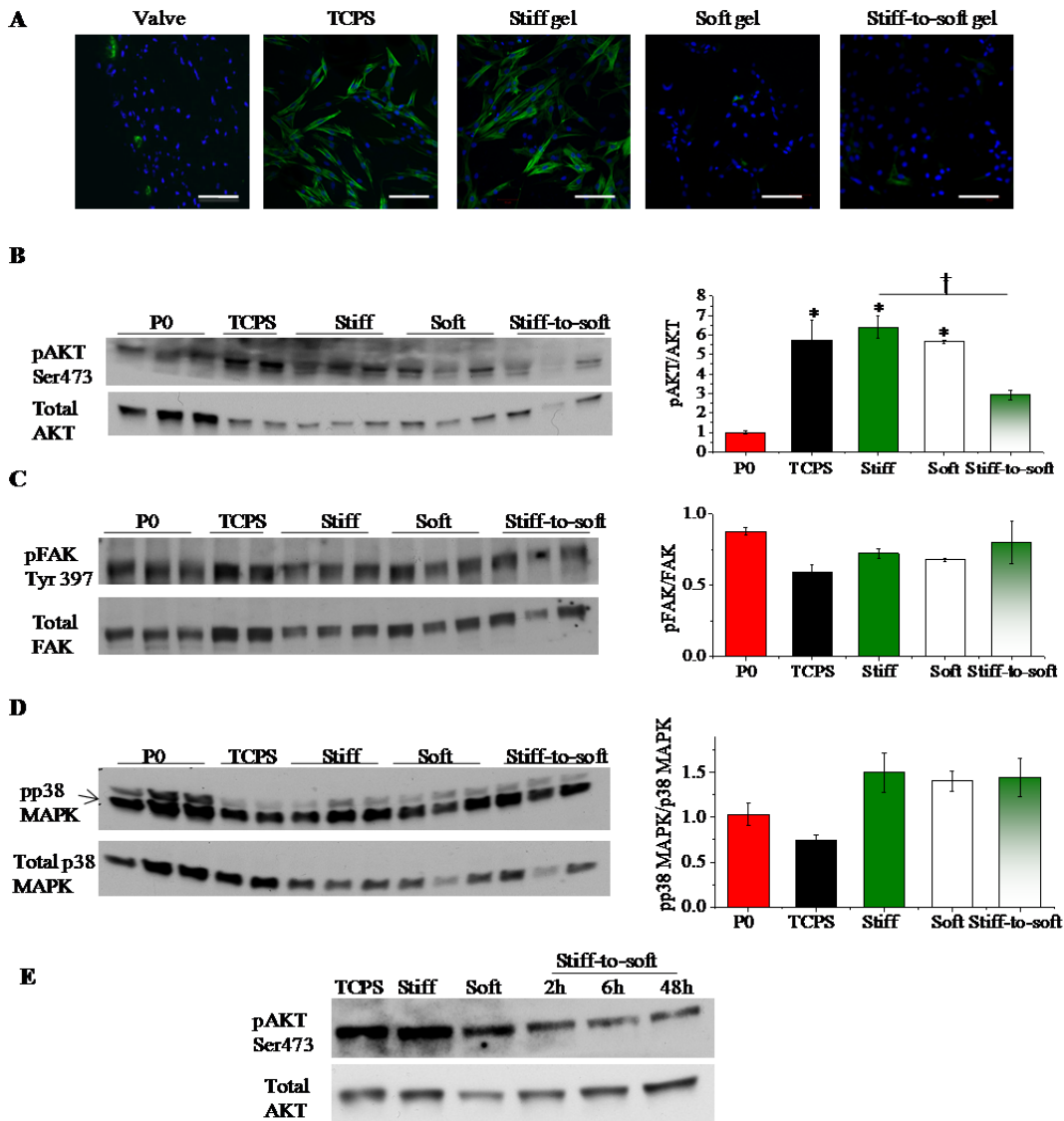


Figure 3.4 Soft PEG Hydrogels Prevent Myfibroblast Activation through an Elasticity-regulated PI3K-AKT Pathway, But Not the FAK or the P38 MAPK Pathways. (A) Representative staining of α SMA for VICs residing in native valve (Valve), cultured on plastic plate (Plate) and cultured on hydrogels with different elasticity (Stiff gel, Soft gel, Stiff-to-soft gel). VICs cultured on plastic plates and stiff gels showed an activated myfibroblast phenotype with striated α SMA stress fibers, but VICs in the native valve did not. Reducing substrate modulus inhibited myfibroblast differentiation in VICs on soft gels and stiff-to-soft gels. Green: α SMA; Blue: Nuclei. Activation of AKT, FAK and p38 MAPK was measured by western blot and quantified (B-E). As shown in (B), there was a significant reduction of pAKT/AKT in VICs cultured on stiff-to-soft gels compared to stiff gels. * means significantly different from P0 with $p < 0.05$. † means significantly different from the stiff condition with $p < 0.05$. Neither pFAK/FAK nor pp38 MAPK/p38 MAPK was changed significantly when VICs were cultured on different substrates (C and D). (E) shows the dynamic change of pAKT/AKT after 2, 6, and 48 hours of softening the gels. The reduction in pAKT/AKT was observed as early as 2 hours.

3.3.5 PI3K Inhibition Prevents Myofibroblast Differentiation on Stiff Substrates

Freshly isolated VICs were cultured on plastic plates or stiff gels and then treated with a small molecule inhibitor of PI3K, LY294002, for 2 days. Figure 3.5A shows that LY294002 can effectively reduce pAKT/AKT level, indicating reduced PI3K activity. With PI3K inhibition, VICs demonstrated decreased myofibroblastic differentiation on stiff substrates. First, α SMA protein level was significantly reduced in response to increasing concentrations of LY294002 (Figure 3.5A). Second, at the mRNA level, a number of myofibroblast activation genes, including α SMA, CTGF and Col1A1, were significantly down-regulated with LY294002 treatment (Figure 3.5B). Third, the percentage of myofibroblasts quantified based on α SMA stress fiber staining was significantly reduced with PI3K inhibition on both TCPS and stiff gels (Figure 3.5C). Specifically, percent of myofibroblasts was decreased significantly from $45.8 \pm 1.6\%$ to $4.2 \pm 0.3\%$ on TCPS in response to $100\mu\text{M}$ LY294002. Similarly on stiff gels, percent of myofibroblasts was decreased significantly from $34.0 \pm 3.8\%$ to $4.8 \pm 1.4\%$ with LY294002 treatment at $100\mu\text{M}$. As expected, higher percentage of myofibroblasts was observed on TCPS than on stiff gels for both the control condition (DMSO) and the LY294002 treatment at $50\mu\text{M}$.

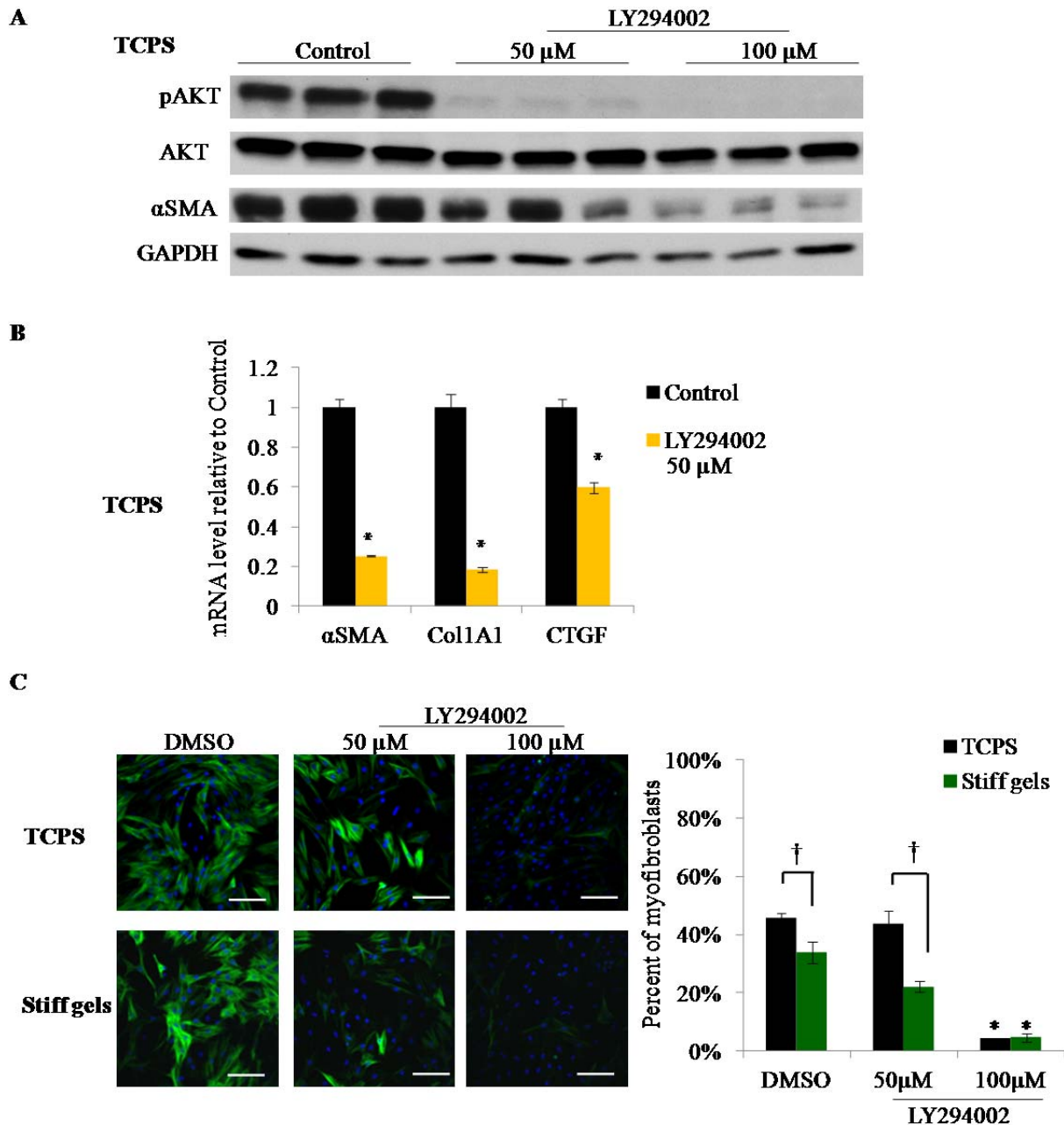


Figure 3.5 PI3K Inhibition Prevents Myofibroblast Differentiation on Stiff Substrates. (A) For VICs cultured on TCPS, treatment with LY294002, an inhibitor for PI3K, reduced the pAKT/AKT level and also α SMA protein expression in a dose-dependent manner. (B) Expression of fibrogenic genes, α SMA, Col1A1, and CTGF, was also inhibited with LY294002 treatment at 50 μ M. * indicates $p < 0.05$. (C) Immunostaining for α SMA showed consistent results that VICs cultured on stiff substrates, either TCPS or stiff gels, had reduced percentage of myofibroblasts with increasing concentration of LY294002 treatment. Green: α SMA, Blue: Nuclei. Scale bar: 100 μ m. Percent of myofibroblasts was quantified in the right panel. * means significantly different from the DMSO control with $p < 0.05$. † indicates $p < 0.05$.

3.3.6 Inhibition of AKT Partially Inhibits Myofibroblast Differentiation in VICs Cultured on TCPS

When cells were treated with an AKT inhibitor, MK2206, there was no change in α SMA protein levels even though this inhibitor was effective at inhibiting pAKT/AKT level (Figure 3.6A). MK2206 treatment at 5 μ M blocked formation of α SMA stress fibers in VICs cultured on TCPS, but not for those cultured on stiff gels (Figure 3.6B). The immunostaining data in Figure 3.6B is quantified in Figure 3.6C. Percent of myofibroblasts was $56.1 \pm 3.0\%$ in the control condition, but was decreased to $23.7 \pm 3.5\%$ at 3 μ M of MK2206 treatment and was further decreased to $1.7 \pm 0.05\%$ at 5 μ M of MK2206 treatment. However, for VICs cultured on stiff gels, percent of myofibroblasts was not changed significantly by AKT inhibition ($34.0 \pm 3.8\%$ for the DMSO condition, $28.8 \pm 10.5\%$ and $28.1 \pm 4.5\%$ for MK2206 treatment at 3 μ M and 5 μ M respectively).

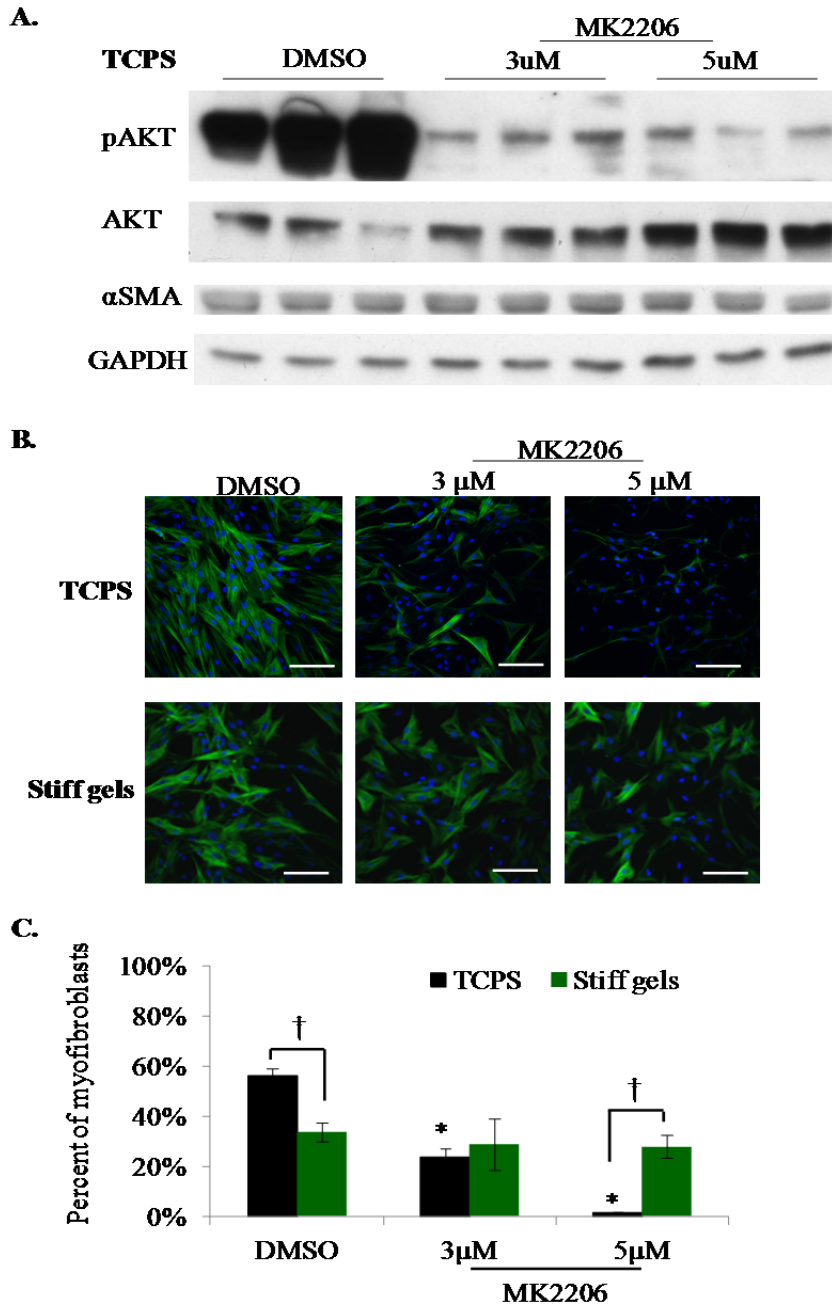


Figure 3.6 Inhibition of AKT Partially Inhibits Myofibroblast Differentiation in VICs Cultured on TCPS. (A) MK2206, a specific inhibitor for AKT, was used at 3 and 5 μ M to treat VICs on TCPS. The pAKT/AKT level was confirmed to be inhibited by MK2206 at both dosages. α SMA protein level was unchanged by the MK2206 treatment. (B) MK2206 inhibited α SMA stress fiber formation in VICs cultured on TCPS, but not so efficiently for those cultured on stiff gels. Green: α SMA, Blue: Nuclei. Scale bar: 100 μ m. (C) Quantification of percent of myofibroblasts for VICs treated with MK2206. MK2206 can significantly inhibit myofibroblast differentiation on TCPS, but not on stiff gels. * means significantly different from the DMSO control with $p < 0.05$. † indicates $p < 0.05$.

3.3.7 Constitutively Active PI3K Promotes Calcific Nodule Formation in VICs Cultured on TCPS

When VICs were infected with adenoviruses expressing constitutively active p110 α subunit of PI3K (caPI3K) or GFP, these cells were shown to have higher PI3K activation based on increased pAKT/AKT level in caPI3K condition than the GFP condition (Figure 3.7A). Meanwhile, VICs expressing caPI3K formed a significant larger number of nodules, which stained positive for calcium by alizarin red S (Figure 3.7B and C).

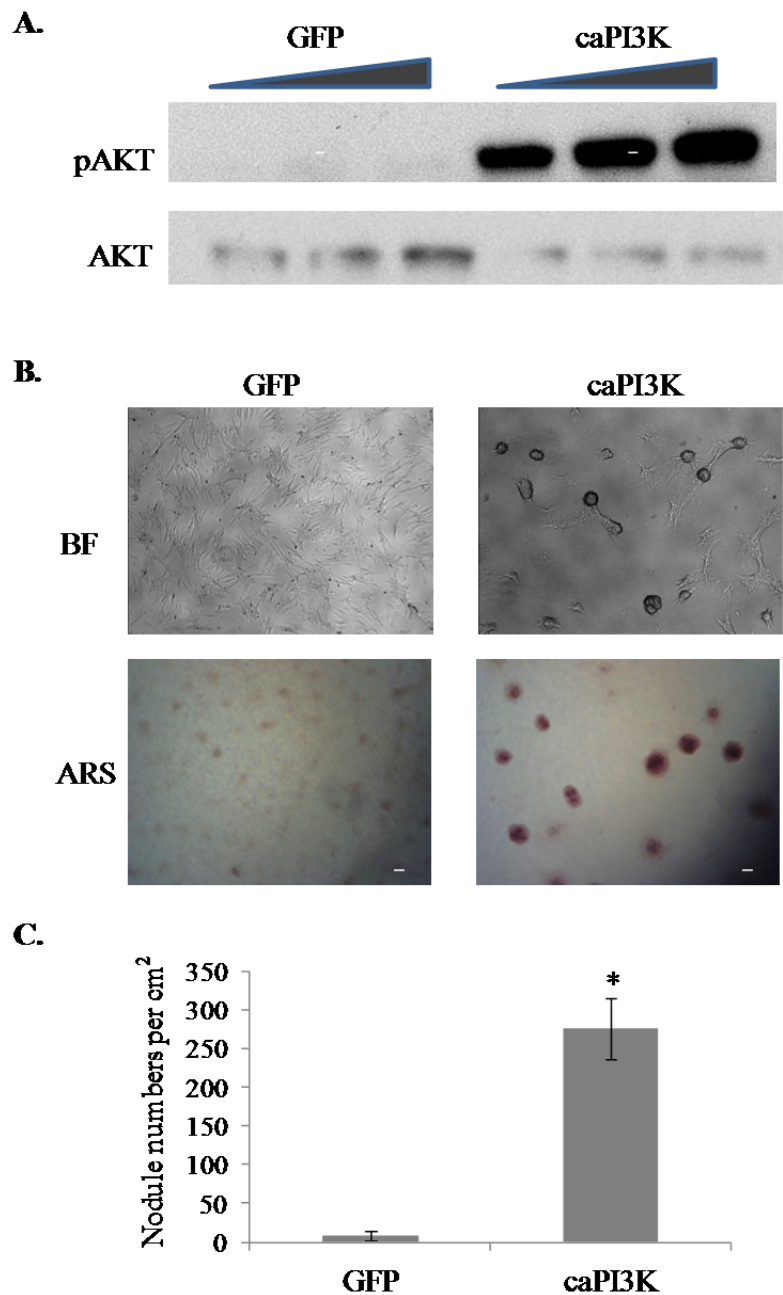


Figure 3.7 Constitutively active PI3K promotes calcific nodule formation in VICs cultured on TCPS. VICs were infected with adenoviruses which encode GFP (GFP) or constitutively active p110 α subunit of PI3K (caPI3K). (A) caPI3K was confirmed to increase PI3K signaling by increasing the pAKT/AKT level compared with the GFP condition. (B) Overexpression of caPI3K increased nodule formation of VICs, which stained positive for calcium by alizarin red S (ARS). Nodule number per area was quantified in (C).

3.4 Discussion

Studies on cellular niches have broadened our understanding of how various extracellular cues regulate cell functions at the molecular level [186]. However, many of these studies have been focused on niches for stem cells and how other cell types regulate stem cell functions through membrane-bound receptors [187]. In this study, I have begun to show that interstitial fibroblasts are highly responsive to their matrix niche, and elasticity of the matrix, as a physical cue, regulates the fibroblast-myofibroblast transition. I found that stiff tissue culture plastic plates ($E \sim 3\text{GPa}$) spontaneously activate the pathogenic myofibroblast phenotypes, including fibrogenic gene expression and αSMA stress fiber formation; whereas, soft hydrogels ($E \sim 7\text{kPa}$) inhibit these traits. Substrate modulus itself is implicated as a regulator of this process, as the myofibroblast phenotype can be de-activated when E is reduced from $\sim 32\text{kPa}$ to $\sim 7\text{kPa}$ (stiff-to-soft). In response to substrate modulus reduction, phosphoAKT, a downstream target of PI3K, is decreased at 2-hour and keeps on decreasing over a time course of 48 hours. Inhibition of PI3K with LY294002 prevents the myofibroblast differentiation on both stiff gels and plastic plates in a dose-dependent manner. Overexpression of constitutively active PI3K p110 α subunit can drive myofibroblast differentiation on TCPS. These data suggest a novel link between substrate modulus and intracellular biochemical signaling through the PI3K pathway and indicate that PI3K inhibition may prevent the vicious cycle of fibrosis, in which the stiffened tissue reinforces myofibroblast activation.

TCPS has been the traditional substrate for mammalian cell culture owing to its commercial availability, ease of use, and support for basic cell survival and function. However, the porcine genome microarray observations indicate that TCPS culture significantly alters the

whole genome transcriptional profile of primary porcine aortic VICs, as ~4000 genes were differentially regulated more than 2 fold ($p < 0.01$, Figure 3.1A and 3.1B). The expression changes revealed increased gene functions related to mitochondria, cell cycle, and cytoskeletal organization, as well as decreased gene functions associated with cell adhesion, polysaccharide binding, and extracellular matrix remodeling. Some of these functions, such as cell cycle, cytoskeletal organization, and extracellular matrix remodeling, are tightly associated with pathogenic myofibroblast activation and can negatively affect cell-mediated tissue homeostasis. The microarray data were validated by analyzing a select set of 8 genes that were up- or down-regulated in the microarray via qRT-PCR. Each of the 8 genes showed similar fold changes to those observed in the microarray based on qRT-PCR (Figure 3.2), validating the fidelity of the microarray data. Besides VICs, TCPS has also been found to alter the native properties of cardiac fibroblasts [62], mammary epithelial cells [188], certain cancer cells [189] and muscle satellite cells [25]. Admittedly, our microarray results reflect the gene expression changes also induced by the culturing media with its low amount of FBS (1%). However, the measurement of gene expression in VICs cultured in the same media, but on soft gels, suggests that a lot of the changes are due to substrate stiffness (Figure 3.3A). In addition, native valve tissues are immersed in blood with comparable amounts of proteins as FBS, but these scaffolds can still maintain the un-activated fibroblast phenotype of VICs (Figure 3.3A), suggesting that the scaffold itself is reserving positive signals for maintaining healthy VICs. This motivates us to explore whether a different synthetic material, other than polystyrene, can serve as a better substrate for culturing VICs without activating the pathogenic myofibroblastic phenotype.

PEG hydrogels are promising materials for this purpose as they are non-fouling, with

tunable elasticity, and can be modified to support cell adhesion [21]. Further, PEG hydrogels are chemically versatile and can be employed to create gels with elasticity, mass transport properties, and dynamics that mimic aspects of the native ECM [20-23, 154]. Figure 3.3 demonstrates that soft PEG hydrogels ($E \sim 7\text{kPa}$) preserve some aspects of the native phenotypes of VICs much better than TCPS. Specifically, VICs cultured on soft gels maintain low mRNA expression of the fibrogenic genes (αSMA , CTGF, and Col1A1) and the relative expression pattern of naïve VICs (Figure 3.3A). These cells also express αSMA protein at a low level (Figure 3.3B), closely mimicking P0 VICs. However, cells cultured on TCPS up-regulate αSMA expression significantly and change gene expression level and pattern for the 5 genes examined in Figure 3.3A. When cells are maintained in their native scaffold and cultured in the same media as the other conditions (valve culture), gene expression recapitulates that of P0 VICs better even than the soft gel condition. This indicates that the native scaffold may have an overriding effect beyond that of the media in controlling the fibroblast gene activation and that soft gels are not yet fully mimicking the native scaffold. Yet, these experiments highlight the importance of the cellular context on VIC phenotype and motivate the fabrication of hydrogel materials that better recapitulate the quiescent valve niche. For example, the design of PEG hydrogels can be improved by incorporating binding epitopes as presented in the native niche, including protein ligands, integrin binding sequences, and proteoglycans, or by encapsulating VICs in 3D culture. Nevertheless, these data reveal that soft PEG hydrogels can serve as a basic substrate for propagating unactivated VICs and may be applicable to quiescent fibroblasts from other tissues.

One prominent difference among the substrates used in these study, TCPS, PEG hydrogels, and native valve tissue, is the elasticity of the materials. Elasticity (E), or substrate

modulus, measures the degree of deformation of a material in response to an applied force and relates to the stiffness of the material. Plastic plates have $E \sim 3\text{GPa}$, whereas, normal aortic valves have a bulk E ranging from 0.8 to 8kPa [19] and PEG hydrogels used in this study possess a dynamic E which is tuned from $\sim 32\text{kPa}$ to $\sim 7\text{kPa}$. These PEG hydrogels have a modulus that more closely matches that of native valve tissues as compared to TCPS. Previous studies have shown that activated valvular myofibroblasts, which have been expanded on TCPS, can be de-activated to a less-proliferative phenotype by reducing substrate modulus from $\sim 32\text{kPa}$ to $\sim 7\text{kPa}$ [106, 109]. Fibroblasts isolated from lung and liver have also been found to be responsive to stiffness in a similar manner where high substrate modulus ($E > 15\text{kPa}$) promotes myofibroblast activation and low modulus inhibits activation [104, 105]. This study confirms that freshly isolated VICs, which are composed of $>90\%$ quiescent fibroblasts and have never been cultured on TCPS, respond to substrate modulus. Soft substrates with $E \sim 7\text{kPa}$ preserve their unactivated fibroblast phenotype, whereas, stiff substrates with $E \sim 32\text{kPa}$ activate myofibroblast characteristics (Figure 3.3A and 3.4A). I hypothesize that the tissue-mimicking elasticity of soft PEG hydrogels is one of the main reasons as to how these platforms better maintain the native phenotype of VICs than TCPS or stiff gels.

While the mechanoresponsive nature of fibroblasts from the valve, liver, and lung has been elucidated previously [19, 104, 105, 109], the manner by which these mechanical signals are integrated within the cell to direct cell phenotype is not well-understood. To define signaling pathways that regulate VIC differentiation in response to substrate modulus reduction, I monitored signaling pathways that have been suggested to be involved in myofibroblast activation over time by western blot. Phospho-AKT expression was significantly reduced with

decrease in substrate modulus and this was detectable as early as 2 hours after gel softening with light irradiation (Figure 3.4B). This suggests a potential direct link between the de-activation of AKT, which is a major downstream effector of PI3K, and reduced matrix modulus. Meanwhile, phosphorylation of FAK and p38 MAPK, which have been suggested to regulate myofibroblast activation [91, 190, 191], was not changed significantly with changes in *E*. To confirm the mechanoregulation of PI3K, VICs were treated with a small molecule inhibitor for PI3K, LY294002, and this prevented α SMA stress fiber formation and reduced both protein and mRNA expression of α SMA on stiff substrates (Figure 3.5). However, when an inhibitor of AKT, MK2206, was applied to VICs, it only replicated a part of the effects of LY294002 in the inhibition of α SMA stress fiber formation, but not in the reduction of α SMA protein expression (Figure 3.7). This indicates that AKT may not be the only downstream effector of PI3K involved in this regulation. Interestingly, MK2206 prevented α SMA stress fiber formation in VICs cultured on TCPS, but not on stiff gels (Figure 3.7B), suggesting that differences between the two substrates have rendered VICs more “addicted” to AKT activity/metabolism for myofibroblast activation on TCPS. It would be interesting to test the efficacy of LY294002 and MK2206 on myofibroblast inhibition in other types of fibroblasts and examine whether the AKT addiction is cell type-dependent or substrate-dependent. In fact, Conte *et al.* have shown that LY294002 can also inhibit myofibroblast differentiation of human lung fibroblasts [192]. This difference also suggests that PEG hydrogels, with appropriate moduli, may provide a more reliable platform for *in vitro* drug screening as they preserve native properties of VICs better than plastic plates.

PI3K is a phospholipid kinase, which specifically phosphorylates the 3-OH group of

the inositol ring and generates secondary messengers, such as phosphatidylinositol (3,4,5)-trisphosphate (PIP3) that is bound to the inner plasma membrane [193]. Downstream effector proteins then bind to PIP3 through the pleckstrin-homology (PH) domain and activate signaling events regulating actin polymerization, cell growth, cell cycle, apoptosis, among other functions [194]. PI3K can be directly activated by tyrosine kinase receptors, G protein-coupled receptors, and Ras [195]. Interestingly, the PI3K pathway has been shown to be mechanosensitive in muscle tissues. Elevated AKT phosphorylation has been observed in rat skeletal muscles in response to exercise or passive stretch [196] and in mice diaphragm in response to tissue stretch and aging [197]. In addition, cardiac-specific overexpression of active AKT has been shown to enhance myocardial contractility [198]. My study shows that PI3K is mechano-responsive in fibroblasts to elasticity changes of culture substrates. When softening the gel from ~32kPa to ~7kPa, there was reduced PI3K activity measured by pAKT/AKT, indicating that PI3K can respond bi-directionally to, either reduced mechanical force in response to substrate modulus reduction or increased mechanical load during muscle stretch and contraction.

Downstream signaling of PI3K subsequently regulates cellular mechanics through interaction with small GTPase, such as Rac and Rho. Reif *et al.* have shown that activation of PI3K promotes Rac- and Rho-dependent stress fiber formation, focal adhesion development and membrane ruffling in Swiss 3T3 cells [199]. Consistently, I observed that reducing PI3K/AKT activity, by substrate modulus reduction or LY294002, inhibited stress fiber organization and myofibroblast activation. In addition, it has been shown that calcific nodule formation of VICs is mediated by myofibroblast contraction and is dependent on α SMA expression [77]. In our study, overexpressing constitutively active PI3K promoted myofibroblast-mediated nodule formation in

VICs (Figure 3.7). In summary, the PI3K pathway can serve as a mechano-sensing mechanism for transmitting external biomechanical cues, including elasticity, stretch, or contraction, to intracellular cytoskeleton remodeling and phenotype regulation.

During normal wound healing of mesenchymal tissues, the fibroblast-to-myofibroblast transition is an essential process, as myofibroblasts contract and secrete ECM proteins to repair the tissue. Towards the end of healing, apoptosis of myofibroblasts has been observed to put a brake on the active tissue remodeling [67, 200]. When activated cells fail to undergo apoptosis, chronic fibrosis can occur. Therefore, temporal regulation of myofibroblast apoptosis and survival is crucial in determining healthy and diseased tissue regeneration. PI3K/AKT signaling antagonizes apoptosis and promotes cell survival and proliferation. This is largely mediated by the effector protein AKT. AKT has been shown to inhibit apoptosis by directly phosphorylating BAD, which prevents it from binding to and blocking the pro-survival factor Bcl-2 [201, 202]. In addition, AKT can also phosphorylate the Forkhead transcription factors, and redirect them from nuclear to cytoplasm to prevent transcriptional up-regulation of pro-apoptotic genes [203, 204]. Two independent reports have shown that AKT activation confers apoptosis-resistant phenotype to myofibroblasts [92, 205]. In fibrotic tissues, elevated AKT activity in myofibroblasts, induced either by stiffened matrix or pro-inflammatory cytokines, could be an important cause for their persistent activation. Therefore, targeting PI3K/AKT pathway may accelerate the turnover of myofibroblasts through apoptosis. When VICs were treated with LY294002, there was reduced cell number over time, indicative of cell death. In the future, it is worthwhile to explore if there are small molecule inhibitors of PI3K which selectively kill myofibroblasts over fibroblasts at appropriate dosage. As fibroblasts cultured on soft substrates ($E \sim 4.7\text{kPa}$) have increased

apoptosis compared with those on stiff substrates ($E \sim 14\text{kPa}$) [107], it is possible that reduced PI3K/AKT activation on soft gels tilts the counter-balance of pro-survival and pro-apoptotic signaling towards apoptosis.

From a systematic perspective, myofibroblast differentiation is regulated by multiple environmental cues, including chemical factors, physical cues, and cell-cell contact. For VICs in their native niche, they are constantly probing their environment through cell surface receptors, integrins, and cadherins, and process a complex web of signaling pathways elicited by external cues. Previous studies have focused mostly on isolated cues. For example, it has been shown that chemical factors, including TGF β 1 and endothelin 1, activate PI3K/AKT to induce myofibroblast characteristics [93, 95, 206]. Meanwhile, mechanical stretch activates AKT in mesangial cells to promote collagen production [118]. Here, I show that substrate modulus-dependent PI3K activity regulates myofibroblast activation. In tumor cells, E-cadherin has been shown to suppress PI3K signaling through PTEN [207]. It is clear that chemical, mechanical, and cell-cell interactions can all regulate the PI3K/AKT pathway. However, it is unclear how these different types of cues crosstalk and systematically regulate cell fate. We have previously shown that TGF β 1 cannot activate myofibroblast stress fiber formation on soft gels [109]. This is also observed in hepatic stellate cells [104]. As PI3K/AKT is an important pathway for both TGF β 1 and stiffness induced myofibroblast activation, it is possible that failure to activate PI3K on soft gels renders TGF β 1 unable to initiate the complete differentiation of myofibroblasts. PI3K/AKT pathway could be a nodal point and a superior target as it mediates signaling downstream of multiple factors.

Different from a decade ago, tissue engineering and regenerative medicine are not something that is only taking place in a laboratory. In fact, it has been implemented to help

patients, either to rebuild a functional windpipe [208] or to regenerate a severely damaged thigh muscle based on extracellular matrix [209]. From these successful cases, we have learned that the scaffold does not need to completely recapitulate the native tissue structures and functionalities before implantation, but can be instructive, since cells and scaffolds are plastic and mutually responsive. However, important properties of these cell culture scaffolds have to be defined by basic cell biology research. For example, the elasticity of the materials should mimic that of the *in vivo* tissue and it may be even better if the elasticity is tunable to match the changing environment [26, 210]. In addition, different functional peptides, such as RGDS and MMP binding sequences, can be introduced to the blank PEG hydrogels to promote cell adhesion, spreading, and migration [139, 151]. Over the years, PEG hydrogels have been studied to incorporate different functional and dynamic modules to serve as a better surrogate scaffold for cell culture and tissue regeneration [20, 22, 23, 211]. Even though one can change intracellular signaling by chemical cues and transcriptional factors easily, it is still attractive to learn how matrix mechanical cues can be utilized to regulate cellular functions, including survival, apoptosis, and matrix synthesis, to understand basic cell biology and for clinical applications. Furthermore, this outside-in programming may reveal unique manners to intervene during disease progression.

CHAPTER IV

REDIRECTING VALVULAR MYOFIBROBLASTS INTO DORMANT FIBROBLASTS THROUGH LIGHT-MEDIATED REDUCTION IN SUBSTRATE MODULUS

Published in PLoS ONE 7(7): e39969. DOI:10.1371/journal.pone.0039969.

4.1 Introduction

The microenvironment of a cell regulates cellular functions dynamically [1,2,3]. In particular, substrate elasticity has recently been shown to direct cell functions, such as stem cell differentiation [4] and renewal [5], independent of soluble growth factors. Soft matrices that mimic the stiffness of brain with Young's modulus (E) around 0.1-1kPa promote neurogenic differentiation of human mesenchymal stem cells, while rigid matrices that mimic collagenous bone (E , 25-40kPa) promote osteogenesis [4]. Further, rigid plastic tissue culture plates have a non-physiological stiffness ($10,000\times$ that of soft tissue) and are known to affect cell phenotypes. For example, when fibroblasts are cultured on plastic plates, they spontaneously differentiate into myofibroblasts with fibrogenic properties [6,7,8]. In contrast, soft substrata derived from polyacrylamide- or poly(ethylene glycol)-based hydrogels with physiologically-relevant moduli ($E < 10\text{kPa}$) inhibit myofibroblast differentiation, better preserving the inactivated cellular phenotype [9,10,11]. From this perspective, hydrogels with a tissue-mimicking elastic modulus provide an important culture system to study and direct fibroblast functions in vitro.

When fibroblasts are transformed into myofibroblasts over long time periods *in vivo*, tissue fibrosis can develop [12,13]. Tissue fibrosis presents serious health problems affecting multiple organs, including skin [14], lung [15], liver [16], kidney [17] and heart [18]. Resident fibroblasts in these tissues have been shown to play critical roles in disease progression. Fibroblasts respond to both chemical cues and the physical stiffness of tissue to become myofibroblasts [18,19,20]. For example, transforming growth factor β 1 (TGF- β 1) is a potent profibrotic cytokine that activates fibroblasts from valve, skin or liver to become myofibroblasts [9,18,21]. Myofibroblasts, characterized by increased secretion of ECM proteins (e.g., collagen and fibronectin) and higher contractile function mediated through α -smooth muscle actin (α SMA) stress fibers, exacerbate fibrosis [20,22]. Strategies to reverse the myofibroblast phenotype into a native fibroblastic phenotype could be of significant therapeutic impact in abrogating tissue fibrosis.

Primary fibroblasts isolated from pig aortic valves serve as a model system to study how the pathogenic myofibroblast phenotype is regulated by microenvironment modulus [23,24,25]. These fibroblasts, valvular interstitial cells (VICs), are the main cell population residing in aortic valves [26]. In a healthy valve, VICs maintain a quiescent fibroblastic phenotype; however, in a sclerotic valve, VICs are activated to myofibroblasts, which secrete excessive ECM degradative enzymes (e.g., MMPs) and collagen, leading to deterioration of the original valve structure and tissue thickening [27,28,29]. Persistence of the myofibroblast phenotype leads to further valve stiffening, which eventually restricts blood flow from the left ventricle to the aorta. Increased rigidity of valvular tissue associated with aortic valve (AV) sclerosis is not only a result of collagen deposition by myofibroblasts, but can also promote

pathology by a positive feedback mechanism, leading to the accumulation of myofibroblasts and the continual production of ECM [30].

Microenvironment stiffness has been shown to regulate the fate of fibroblasts, including differentiation into myofibroblasts, apoptosis and proliferation. When valvular, hepatic or lung fibroblasts are cultured on low modulus substrata ($E \leq 10\text{kPa}$), they maintain an un-activated phenotype; however, when cultured on higher modulus substrata, they are activated to myofibroblasts [10,11,31,32]. However, reducing the elastic modulus of the substratum to a very low level ($E \leq 1\text{kPa}$) promotes apoptosis in various fibroblasts [11,33,34]. Moreover, NIH3T3 fibroblasts grown on compliant substrata ($E \sim 5\text{ kPa}$) show a decrease in proliferation, compared with cells cultured on stiff substrata ($E \sim 14\text{ kPa}$) [33]. Based on previous findings, I speculated that substrata with E lower than 10 kPa , but not too low to activate apoptosis, may provide healthy physical signals to maintain quiescent fibroblast phenotypes. Specifically in this study, I test the hypothesis that the valvular myofibroblasts will either undergo apoptosis or de-activate to a quiescent fibroblast state when the substrate modulus is reduced.

I utilized a photodegradable poly(ethylene glycol) (PD-PEG) hydrogel [35] to study the fate of VICs in response to substrate modulus reduction. With this unique photo-sensitive material, I can change E *in situ* while VICs are adhered to the gels from $\sim 32\text{kPa}$, mimicking collagenous bone (which has been detected in diseased valves [36]), to $\sim 7\text{kPa}$, mimicking healthy valve fibrosa [31]. I found that VICs switched their fate from activated myofibroblasts to fibroblasts with reduced proliferation when the substrate was changed from stiff to soft. This de-activation process was not associated with significant apoptosis, but was characterized by down-regulation of critical myofibroblast phenotypic markers, including loss of αSMA stress

fibers, significant reduction in the expression of myofibroblast gene signatures (α SMA and CTGF) and a significant decrease in proliferation. These results provide insight into the potential fate of valvular myofibroblasts *in vivo* after tissue repair. Further, I established that de-activated VICs still maintain the potential to activate the expression of myofibroblast genes in response to TGF- β 1 and to proliferate in response to growth stimuli, indicating a reversible fibroblast state of the cells and contributing to our understanding of how modulus regulates the myofibroblast-fibroblast transition. This could be useful in developing novel treatments for tissue fibrosis and could result in new approaches to direct cell fate and function for tissue engineering.

4.2 Materials and Methods

4.2.1 Hydrogel Synthesis

The photodegradable crosslinker (PD-PEG) was synthesized as previously described [35]. PD-PEG ($M_n \sim 4070$ g/mol, 8.2 wt%) was copolymerized with PEG monoacrylate (PEGA, $M_n \sim 400$ g/mol, 6.8 wt%, Monomer-Polymer and Dajac Laboratories, Inc) and an acrylated adhesion peptide sequence RGDS (5mM, described below) via redox-initiated free radical chain polymerization [37]. The hydrogels were synthesized as thin films (0.25 mm thick) covalently attached to methacrylated coverglass. Hydrogels with surface areas (A) of ~ 250 mm² and ~ 370 mm² were made on coverglass of 18 mm and 22 mm in diameter, respectively, to enable harvest of appropriate cell numbers for specific assays. To reduce the crosslinking density and modulus of the hydrogels, samples were irradiated with long wavelength, low intensity ultraviolet (UV) light for 5 minutes (365nm at 10mW/cm²). These conditions have been previously demonstrated to be cytocompatible [10]. Hydrogel moduli were verified with rheometry and atomic force microscopy as described previously [10], where moduli of hydrogels (0.25 mm thick) in

phosphate buffered saline (PBS) were measured as $E \sim 32$ kPa and ~ 7 kPa after 0 minute and 5 minutes of irradiation (365 nm at 10 mW/cm²), respectively.

4.2.2 Peptide Synthesis

An integrin-binding adhesion peptide was synthesized and incorporated within the cell culture platform to promote cell attachment based on established protocols [37,38] Briefly, OOGRGDSG (diethylene glycol-diethylene glycol-glycine-arginine-glycine- aspartic acid -serine-glycine) was made on a solid phase peptide synthesizer (Tribute, Protein Technologies, Inc.) with HBTU/HOBt amino acid activation and Fmoc chemistry [38]. After synthesis of the primary sequence, the N-terminus of the peptide was modified on resin with an acryloyl group by reaction with HATU-activated acrylic acid in the presence of diisopropylethylamine (4 molar excess of each relative to N-terminus amine) [39]. Complete reaction of the amine was verified using the Kaiser test [40], and the peptide was cleaved from resin (5 wt% phenol in 95% trifluoroacetic acid, 2.5% triisopropylsilane, and 2.5% DI water) stirring for 2 hours at room temperature. The cleavage solution was precipitated in and washed with ice cold ethyl ether (3x), dried under vacuum overnight, purified by high-performance liquid chromatography (HPLC), and characterized by matrix-assisted laser desorption/ionization mass (MALDI-MS) [37]. The peptide has a molecular weight of ~ 892 g/mol, consistent with its amino acid sequence.

4.2.3 VIC Cell Culture

Fresh porcine hearts were obtained from Hormel Foods Corporation (Austin, MN, USA) within 24 hours of sacrifice and aortic valve leaflets were excised. Primary VICs were harvested from porcine aortic valve leaflets based on a sequential collagenase digestion as previously described [41]. The isolated cells were cultured in growth medium (Medium 199, 15%

fetal bovine serum (FBS), 50U/ml penicillin, 50µg/ml streptomycin, and 0.5µg/ml fungizone) and expanded up to passage 3. Passage 3 VICs were seeded on hydrogels at 35,000 cells/cm² and were cultured in low serum medium (Medium 199, 1% FBS, 50U/ml penicillin, 50µg/ml streptomycin, and 0.5µg/ml fungizone) for up to 5 days. Treatment with fibroblast growth factor 2 (FGF2, Sigma Cat# F0291, 16ng/ml) in 15% FBS medium or TGF-β1 (R&D systems, Cat# 101-B1-001, 5ng/ml) in 1% FBS medium was applied on day 4 for 24 hours.

4.2.4 Isolation and Culture of Rat Pulmonary Fibroblasts

Rat pulmonary fibroblasts were a gift from Dr. Leslie Leinwand lab (University of Colorado Boulder). Briefly, they were isolated from 6-7 week old Lewis rats, as previously described [212, 213]. The cells were cultured in DMEM medium (containing 10% FBS, 50U/ml penicillin, 50µg/ml streptomycin, and 0.5µg/ml Fungizone) and seeded on PD-PEG gels at 35,000 cells/cm² at passage 5. The culture was then maintained in low serum DMEM medium (1% FBS, 50U/ml penicillin, 50µg/ml streptomycin, and 0.5µg/ml fungizone) for up to 5 days.

4.2.5 Immunocytochemistry

Hydrogels (A ~ 250 mm²) were fixed with 4% paraformaldehyde (overnight at 4°C), permeabilized in 0.1% TritonX100, and blocked with 5% bovine serum albumin (BSA). Mouse anti-αSMA antibody (Abcam, Cat# ab7817) or rabbit anti-vimentin antibody (Cell Signaling Technology, Cat#5741) was diluted at 1:100 in PBS with 1% BSA and incubated with the samples overnight at 4°C. Following washes in PBS with 0.05% Tween 20, samples were labeled with goat-anti-mouse Alexa Fluor 488 secondary antibody (Life technologies (Invitrogen), Cat# A-11001) or goat-anti-rabbit Alexa Fluor 488 secondary antibody (Life technologies (Invitrogen), Cat# A11070), along with DAPI to visualize nuclei. Samples were subsequently imaged on a

LSM 710 Laser Scanning Microscope with transmitted light detector for differential interference contrast (DIC) (Carl Zeiss) or inverted epi-fluorescent microscope (Nikon), each with a 20X magnification objective. Images of different fluorescence channels were compiled with Zen or Metamorph software and analyzed by ImageJ for total nuclei number (Analyze Particles function, NIH). Myofibroblasts were counted as cells with α SMA staining organized into fibrils, and the percentage of myofibroblasts was calculated as (number of myofibroblasts / total number of cells) x 100%. To quantify each sample, 6 random fields of view were imaged, counted, and averaged.

4.2.6 Annexin V Staining

VICs were washed in PBS and detached from hydrogels ($A \sim 370 \text{ mm}^2$) using TrypLE (Life technologies, Cat# A1285901). Following centrifugation, cell pellets were re-suspended in Annexin V-binding buffer (10mM HEPES, 140mM NaCl, 2.5mM CaCl_2 , pH 7.4) and incubated with Alexa Fluor 594-labeled Annexin V (Life technologies, Cat# A13203) for 15 minutes at room temperature. DAPI was applied at 0.5 $\mu\text{g}/\text{ml}$ to distinguish live and dead cell populations. Percent of Annexin V⁺ cells was quantified using a CyAn ADP flow cytometer (Beckman Coulter). Early apoptotic cells were identified as those with high fluorescent emission in the Alexa Fluor 594 channel and low emission in the DAPI channel. On average, over 10,000 events were collected per sample. As a positive control, VICs were treated for 18 hours with 25 μM camptothecin, an apoptosis-inducing reagent.

4.2.7 EdU Labeling

For quantifying basal level proliferation amongst different substrate moduli, VICs were switched to medium with 5% FBS after photodegradation on day 3 and were subsequently incubated with 10 μM EdU for 3 hours on day 5. For examining proliferative response to growth

stimuli after modulus-driven deactivation, VICs were treated with or without FGF2 (Sigma-Aldrich, Cat# F0291, 16 ng/ml) and 15% FBS on day 4 for 24 hours and then incubated with 10 μ M EdU for 1 hour on day 5. For each condition, cells from two PD-PEG gels of A \sim 370 mm² were harvested by trypsinization. For EdU staining, samples were fixed and permeabilized using the Fixation and Permeabilization kit (Life technologies, Cat# GAS003). Following washes in PBS with 1% BSA, the cells were incubated with Click-iT reaction cocktail prepared from the Click-iT EdU Alexa Fluor 488 kit (Life technologies, Cat# C10337) for 30 minutes at room temperature. DAPI was applied at 5 μ g/ml as a measure for DNA content. Samples were analyzed by a CyAn ADP flow cytometer (Beckman Coulter). Over 10,000 events were collected per sample. Proliferative cells were counted based on high fluorescence in the Alexa Fluor 488 channel.

4.2.8 Quantitative Real-Time PCR

For each condition, two PD-PEG gels (A \sim 370 mm²) with attached VICs were harvested and submerged in TRI Reagent (Sigma, Cat# T9424), rapidly frozen in liquid nitrogen, and stored at -80 °C until processing. Samples were homogenized with individual DNase and RNase free pestles. Total RNA was purified according to a modified version of the manufacturer's protocol for TRI Reagent. Briefly, after chloroform extraction and aqueous phase collection, a second chloroform extraction with equal volume of chloroform to aqueous phase was performed. cDNA was synthesized from total RNA with Superscript III reverse transcriptase (Life technologies, Cat# 18080-051) and random hexamer primers. Gene expression was determined by SYBR Green-based quantitative real-time PCR (qRT-PCR) using gene specific primer sets (Table 3.1) and an Applied Biosystems 7500 Real-Time PCR machine.

4.2.9 Statistics

Data are presented as mean \pm standard error of the mean (SEM). SEM was calculated based on three biological replicates. Each biological replicate was based on an isolation of VICs from 60-90 pooled porcine aortic valves. A Student's t-test was used to compare data sets and a p value less than 0.05 was considered statistically significant.

4.3 Results

We synthesized PD-PEG hydrogels as dynamic culture substrates for VICs [10] with Young's modulus (E) \sim 32kPa (stiff gels), $E \sim$ 7kPa (soft gels), and E changed from \sim 32kPa to \sim 7kpa (stiff-to-soft gels). A peptide containing the adhesive sequence RGDS was incorporated within the gel to facilitate cell adhesion [42]. VICs were cultured on PD-PEG gels in low serum (1% FBS) medium for up to 5 days (Figure 4.1), where the low serum culture limits cellular response (i.e., differentiation or proliferation) to growth factors in the serum [43]. At day 3, half of the stiff gels were irradiated with low intensity UV light to reduce the crosslinking density and modulus (stiff-to-soft gels in Figure 4.1). We then investigated the mechanisms of myofibroblast deactivation, examining apoptosis and reversion to quiescence as potential pathways (Figure 4.1). Specifically, Annexin V staining was used to examine early apoptosis events. Formation of α SMA stress fibers, expression of myofibroblast genes, and relative proliferation rate were quantified by immunocytochemistry, qRT-PCR and an EdU-based proliferation assay, respectively.

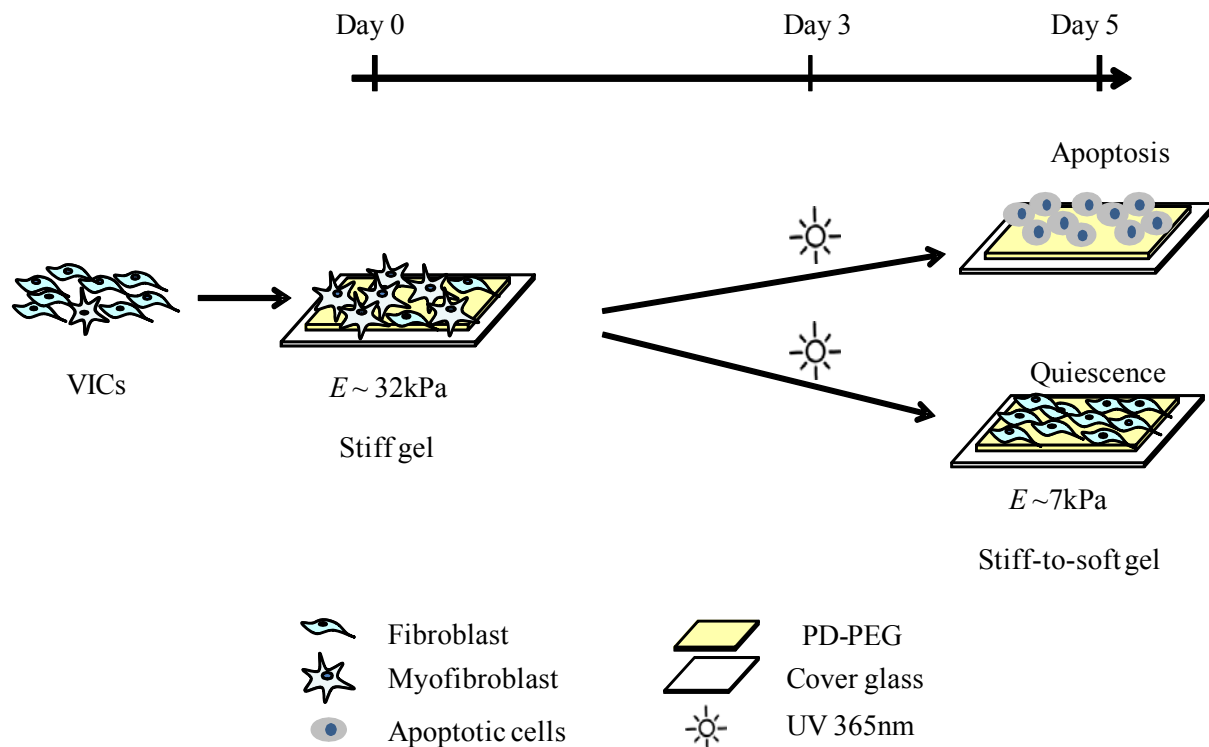


Figure 4.1 Cell Fate in Response to Substrate Modulus Reduction. VICs were seeded on PD-PEG gels on day 0. At day 3, a portion of the stiff gels was softened with light (365nm at $10\text{mW}/\text{cm}^2$). The fate of VICs on continuously stiff, continuously soft and stiff-to-soft gels was subsequently examined on day 3 and/or day 5 based on immunocytochemistry, apoptosis staining, proliferative assay and mRNA expression.

4.3.1 Primary Valvular Myofibroblasts Deactivate in Response to Substrate Modulus Reduction

The percent of activated myofibroblasts on different substrates was examined by αSMA immunocytochemistry (Figure 4.2). Figure 4.2A shows representative staining of VICs for αSMA on different gel conditions. Myofibroblasts are defined as cells with αSMA organized into stress fibers (Figure 4.2A, arrows). There were fewer myofibroblasts and lower αSMA

fluorescence intensity on soft and stiff-to-soft gels than on stiff gels (Figure 4.2A). Some VICs on softer substrates also showed diffuse α SMA staining in the cytoplasm (Figure 4.2A, star); however, these cells were not classified as myofibroblasts. The percentage of activated myofibroblasts was quantified (Figure 4.2B). Stiff gels activated $\sim 55\%$ of VICs to become myofibroblasts. In contrast, only $\sim 10\%$ myofibroblasts were observed when VICs were cultured on soft gels (Figure 4.2B). From day 3 to day 5, the fraction of myofibroblasts remained at a similar level for both the stiff and the soft gels (Figure 4.2B). When E was reduced from 32kPa to 7kPa (stiff-to-soft gels, Figure 4.2B), the percentage of myofibroblasts decreased from $56.7 \pm 5.2\%$ to $24.7 \pm 3.2\%$ over the course of 2 days. However, the total cell number was not changed significantly over time on any substrate (Figure 4.2C).

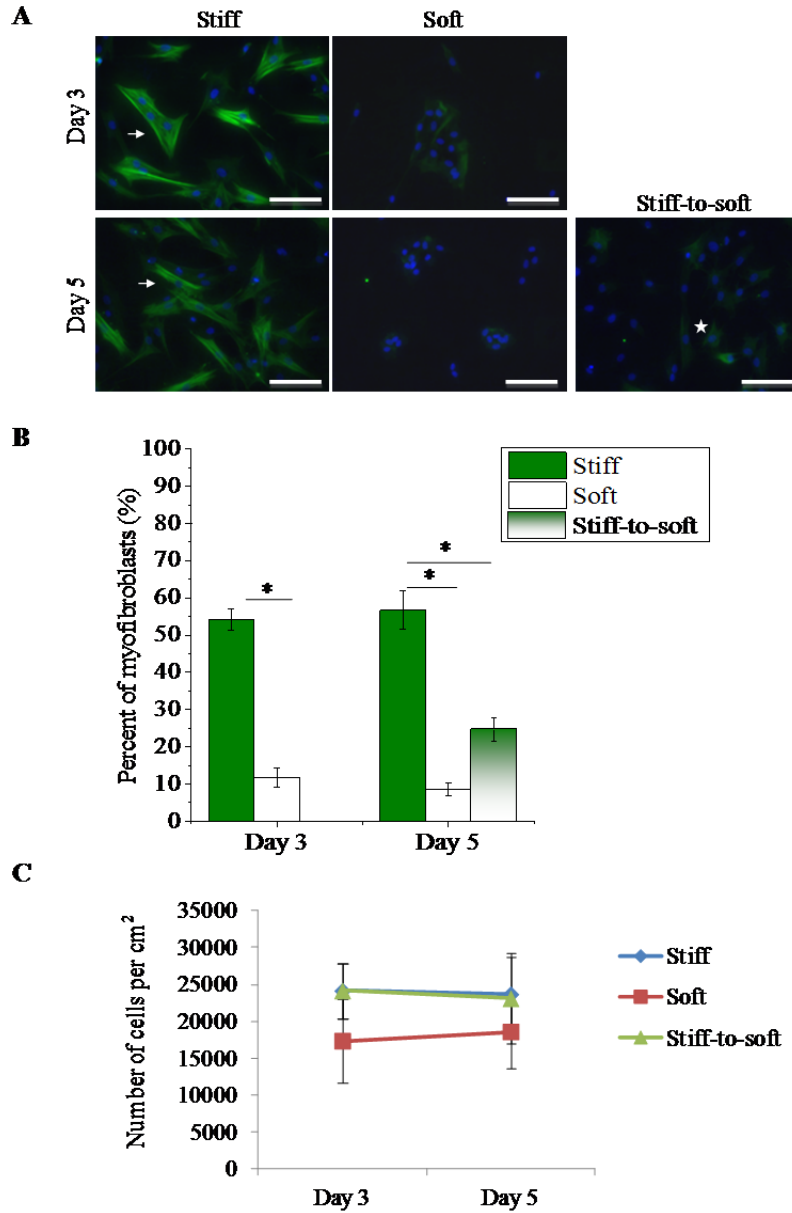


Figure 4.2 Reduced Myofibroblast Activation in Response to Lowering Substrate Modulus.

VICs cultured on stiff, soft or stiff-to-soft gels were fixed on day 3 and day 5, and stained for α SMA. (A) Representative staining of the myofibroblast phenotype for VICs cultured on substrates with different stiffnesses on day 3 and day 5. Green: α SMA. Blue: nuclei. Arrows: myofibroblasts characterized by organized α SMA⁺ stress fibers. Star: a cell stained with diffusive α SMA. Scale bar: 100 μ m. (B) Quantification of myofibroblast percentage on the substrates based on the staining in (A). The percentage of myofibroblasts on stiff-to-soft gels or soft gels was significantly lower than that on stiff gels. * indicates $p < 0.05$. (C) Quantification of the cell number (cells/cm²) on different substrates on both day 3 and day 5. There was no significant change in total cell number.

4.3.2 The Decrease in the Proportion of Valvular Myofibroblasts is Not Due to Apoptosis

To investigate apoptosis as a potential mechanism of the reduced proportion of myofibroblasts on stiff-to-soft gels, expression of the early apoptotic marker phosphatidylserine on the outer plasma membrane was examined. Annexin V, which binds phosphatidylserine, and DAPI staining coupled with flow cytometry was used to quantify the percentage of apoptotic cells. Live cells at an early stage of apoptosis stain positive for Annexin V and minimally for DAPI (Figure 4.3A, red box). Figure 4.3A shows a representative scatter plot of apoptosis staining for VICs cultured on stiff gels harvested on day 3. During 5 days of VIC culture, no significant change in cell number was observed (Figure 4.2C), and on average, minimal dead cells were detected across all culture conditions based on low DAPI staining (Figure 4.3A as an example). On day 3, similar percentages of apoptotic cells in VIC culture on stiff gels ($3.58 \pm 0.80\%$) and on soft gels ($4.41 \pm 0.09\%$) were detected. Interestingly on day 5, we observed a slight but significant increase in apoptosis on stiff-to-soft gels ($5.11 \pm 0.62\%$) as compared to stiff gels ($2.97 \pm 0.67\%$) (Figure 4.3C). However, the level of apoptosis was statistically the same between VICs on soft gels ($5.22 \pm 1.90\%$) and those on stiff-to-soft gels on day 5. As a positive control, VICs cultured on plastic plates were treated with camptothecin, an apoptosis-inducing reagent. The percentage of apoptotic cells increased from 3.72% to 32.10% (Figure 4.3C) with camptothecin treatment. Additionally, we examined the morphology of the Annexin V stained cells to confirm our observations. Cells that stained positive for Annexin V expressed a rounded morphology, whereas those that did not express Annexin V maintained a spindle-shaped morphology (Figure 4.3B).

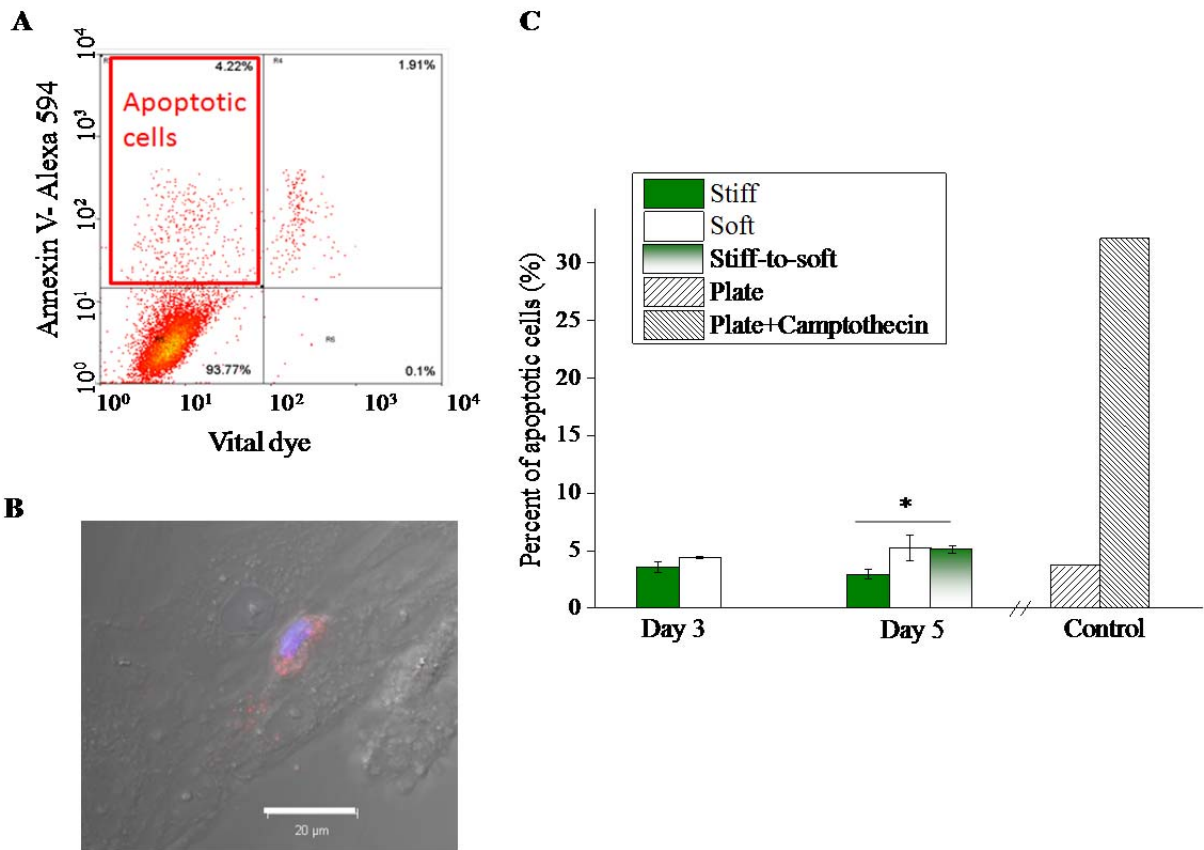


Figure 4.3 Decreased Number of Myfibroblasts on Stiff-to-soft Gels was not Due to Apoptosis. VICs cultured on different PD-PEG gels were stained with Annexin V linked with Alexa Fluor 594 and DAPI to detect apoptosis. (A) Scatter plot of Annexin V and DAPI staining for VICs cultured on stiff gels. Red box: apoptotic cells with high fluorescence in the Annexin V channel and low fluorescence in the DAPI channel. (B) A representative confocal image of a cell stained positively for Annexin V (red) overlaid with transmitted light DIC on stiff gels. Positively-stained cells were observed to exhibit a rounded morphology. Blue: Nucleus. Scale bar: 20 μ m. (C) Quantification of apoptosis based on flow cytometry as shown in (A). Low levels of apoptosis were detected for VICs cultured on either gels or plastic plates. VICs treated with camptothecin, an apoptosis-inducing reagent, showed a much higher level of apoptosis than any gel-based culture condition or plastic plate. * indicates $p < 0.05$.

4.3.3 Valvular Myofibroblasts Transform into a Less Proliferative Fibroblast Phenotype on Softer Substrates

We hypothesized that, when the Young's modulus of the microenvironment decreases, valvular myofibroblasts will revert to a quiescent fibroblast state. Expression of myofibroblast gene markers, including α SMA [20,44] and CTGF [45], and a fibroblast gene marker, vimentin [46], were measured by qRT-PCR at 6 hours after softening substrates on day 3. Figure 4.4A shows that VICs on stiff-to-soft gels expressed 49% less α SMA mRNA and 83% less CTGF mRNA than those cultured on stiff gels. VICs cultured continuously on a soft substrate expressed a similarly low level of α SMA and CTGF as those cultured on stiff-to-soft gels. However, the expression of vimentin mRNA was not changed significantly for cells cultured on any substrates (Figure 4.4A). Consistently, cells on gels with different moduli have the characteristic staining for vimentin, similar to those fibroblasts cultured on plastic plates (Figure 4.4D). Next, we examined the proliferative ability of VICs grown on PD-PEG gels by quantifying the incorporation of EdU, an analogue of thymidine, during DNA synthesis. One hour after irradiating stiff gels to soften them on day 3, VICs were treated with medium containing 5% FBS for all gel conditions. This was done to induce measurable proliferation with EdU treatment for 3 hours on day 5 followed by flow cytometry. As shown in Figure 4.4B, the percent of EdU+ cells on stiff-to-soft gels and soft gels was ~30% less than those cultured on stiff gels. When VICs were cultured on a plastic tissue culture plate and assayed for proliferation using the same experimental conditions, there were 2 fold more EdU+ cells on the plastic tissue culture plate than on the stiff gels (data not shown). I also observed that more cells stalled in the G2 or mitosis (M) phase of the cell cycle on soft or stiff-to-soft gels than on stiff gels (Figure 4.4C).

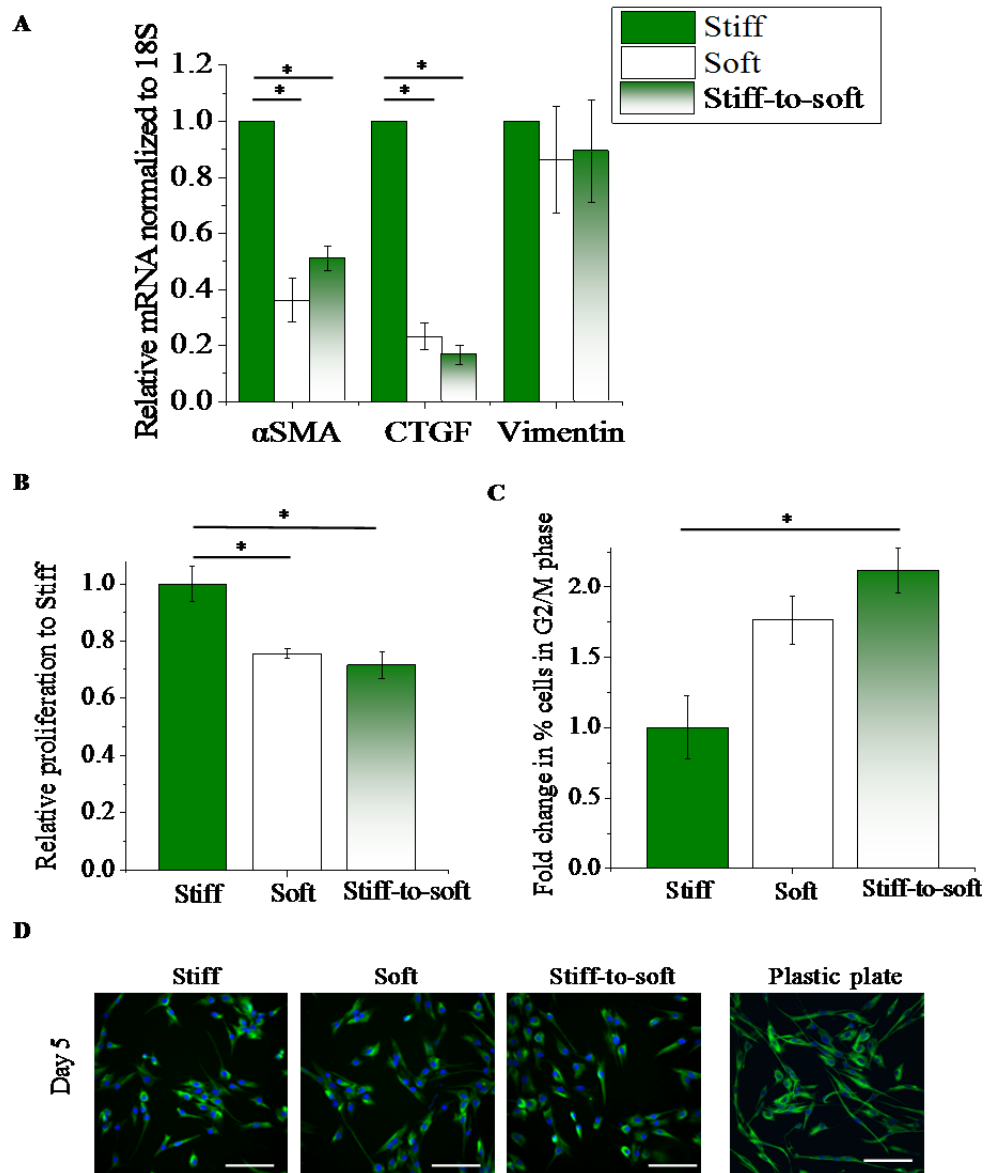


Figure 4.4 VICs Switch to a Less Activated and Less Proliferative Fibroblast Phenotype on Softer Substrates. (A) 6 hours after switching stiff gels to soft on day 3, VICs were collected for mRNA quantification based on qRT-PCR. Myofibroblast gene markers, α SMA and CTGF, were significantly down-regulated in soft and stiff-to-soft conditions compared with stiff. The fibroblast gene marker, vimentin, was expressed at a similar level on different substrates. (B) To measure proliferation, VICs cultured on stiff, soft or stiff-to-soft gels were chased with EdU for 3 hours on day 5. Relative proliferation was calculated based on normalizing the percent of EdU⁺ cells in each condition to that of the stiff condition. VICs were less proliferative on soft and stiff-to-soft gels than on stiff gels. (C) More cells reside in G2/M phase of the cell cycle on stiff-to-soft gels than those on stiff gels. (D) VICs cultured on plastic plates, stiff, soft or stiff-to-soft gels were fixed on day 5 and stained for vimentin. De-activated fibroblasts on stiff-to-soft gels maintain the mesenchymal fibroblast fate. Green: vimentin. Blue: nuclei. Scale bar: 100 μ m. * indicates $p < 0.05$.

4.3.4 Deactivated Fibroblasts on Stiff-to-soft Gels Maintain Responsiveness to a Proliferative Stimulus or TGF- β 1

To assess whether the de-activated fibroblast phenotype was reversible, the ability of the deactivated cells to proliferate and re-activate in response to chemical cues was examined. VICs cultured on stiff-to-soft gels were treated for 24 hours with (i) fibroblast growth factor-2 (FGF2) and 15% FBS to induce proliferation, or (ii) TGF- β 1 to induce myofibroblast differentiation. As shown in Figure 4.5A, deactivated VICs on stiff-to-soft gels responded to growth stimuli and exhibited increased proliferation by \sim 4 fold. These cells also up-regulated myofibroblast gene markers in response to TGF- β 1 (Figure 4.5B). CTGF mRNA expression was increased by 3.6 fold, and ECM genes, such as collagen 1A1 (Col1A1) and fibronectin 1 (FN1), were also significantly up-regulated, by 2.9 fold and 2.3 fold respectively, with TGF- β 1 treatment (Figure 4.5B). However, α SMA mRNA level was not significantly changed on stiff-to-soft gels with TGF- β 1 treatment. The number of mature myofibroblasts with α SMA stress fibers was not increased on either stiff-to-soft gels or soft gels in response to TGF- β 1 (Figure 4.5C).

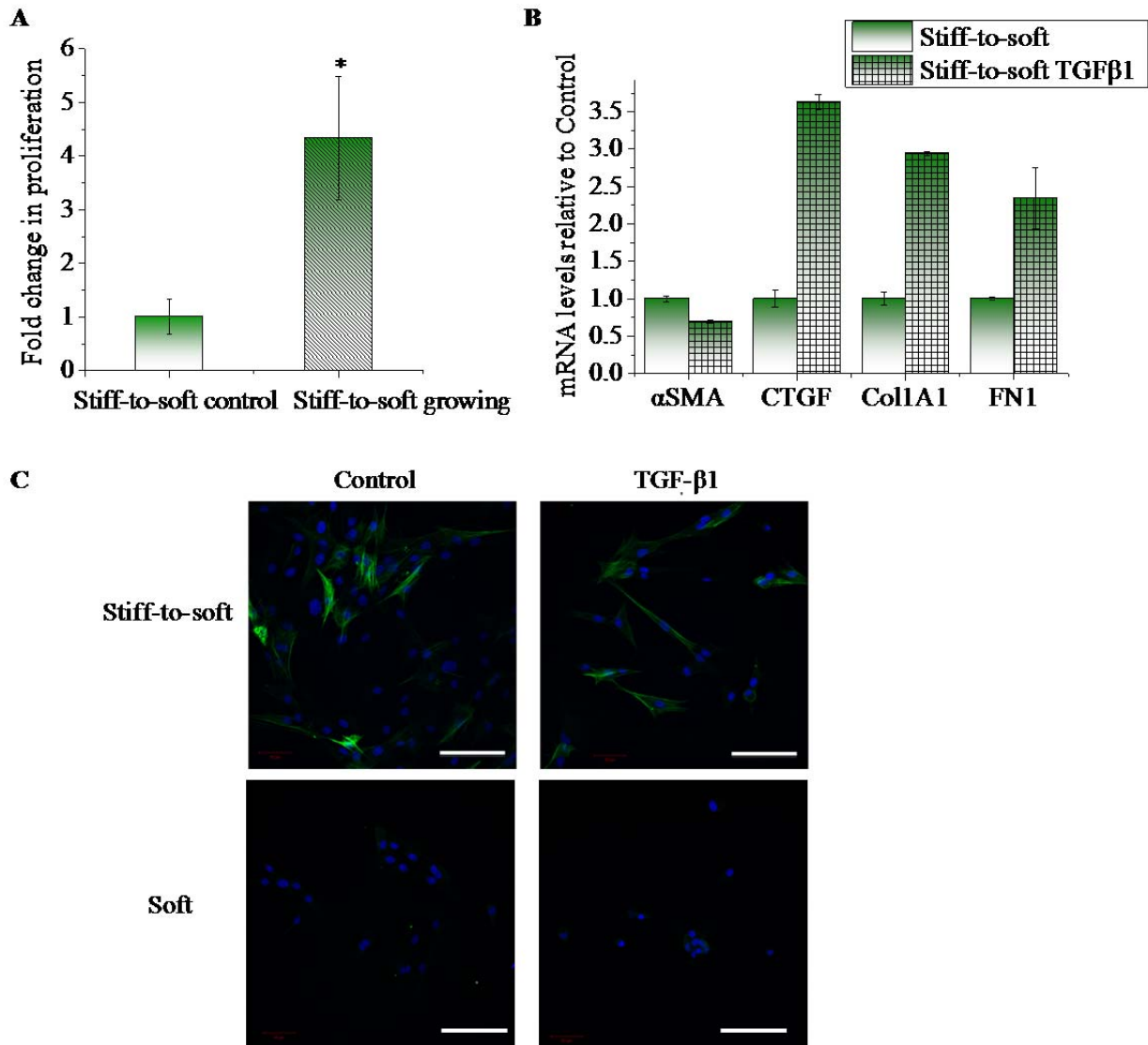


Figure 4.5 Deactivated VICs on Stiff-to-soft Gels Enter the Cell Cycle with Proliferative Stimulus and Activate the Myofibroblast Gene Program in Response to TGF-β1. VICs cultured on stiff-to-soft gels were treated with either proliferative media with 15% FBS and FGF2 or fibrogenic chemokine (TGF-β1) on day 4 for 24 hours. (A) Proliferation was measured by EdU chase for 1 hour on day 5. VICs treated with growth stimulus had ~4-fold more proliferating cells than those in control medium. (B) Myofibroblast gene markers, including CTGF, Col1A1 and FN1, were significantly up-regulated in deactivated VICs treated with TGF-β1. The mRNA level of αSMA was not changed significantly by TGF-β1 treatment. (C) Immunocytochemistry of αSMA showed similar levels of myofibroblasts for VICs cultured on stiff-to-soft gels treated with or without TGF-β1. This is also observed for VICs cultured on soft gels. Green: αSMA. Blue: nuclei. These results show that the de-activated fibroblasts have the potential to proliferate and to activate fibrogenic associated genes in response to chemical cues, but a stiffer substratum is likely required for αSMA stress fiber formation. Scale bar: 100μm. * indicates p<0.05.

4.3.5 Rat Pulmonary Myofibroblasts also De-Activate with Reduction in Substrate Modulus

To explore whether substrate modulus-mediated myofibroblast de-activation is a generalized mechanism, I examined the response of another cell type, rat pulmonary fibroblasts, to *in situ* modulus reduction using the PD-PEG gels. Rat lung fibroblasts were cultured on PD-PEG gels similarly to what was done for VICs (Figure 4.1). Rat pulmonary fibroblasts were activated to myofibroblasts on stiff gels and lost the myofibroblast phenotype upon modulus reduction (stiff-to-soft gels, Figure 4.6A). Based on the quantification in Figure 4.6B, ~85% of cells were activated to myofibroblasts on stiff gels, but only <5% of the cells were myofibroblasts on soft or stiff-to-soft gels.

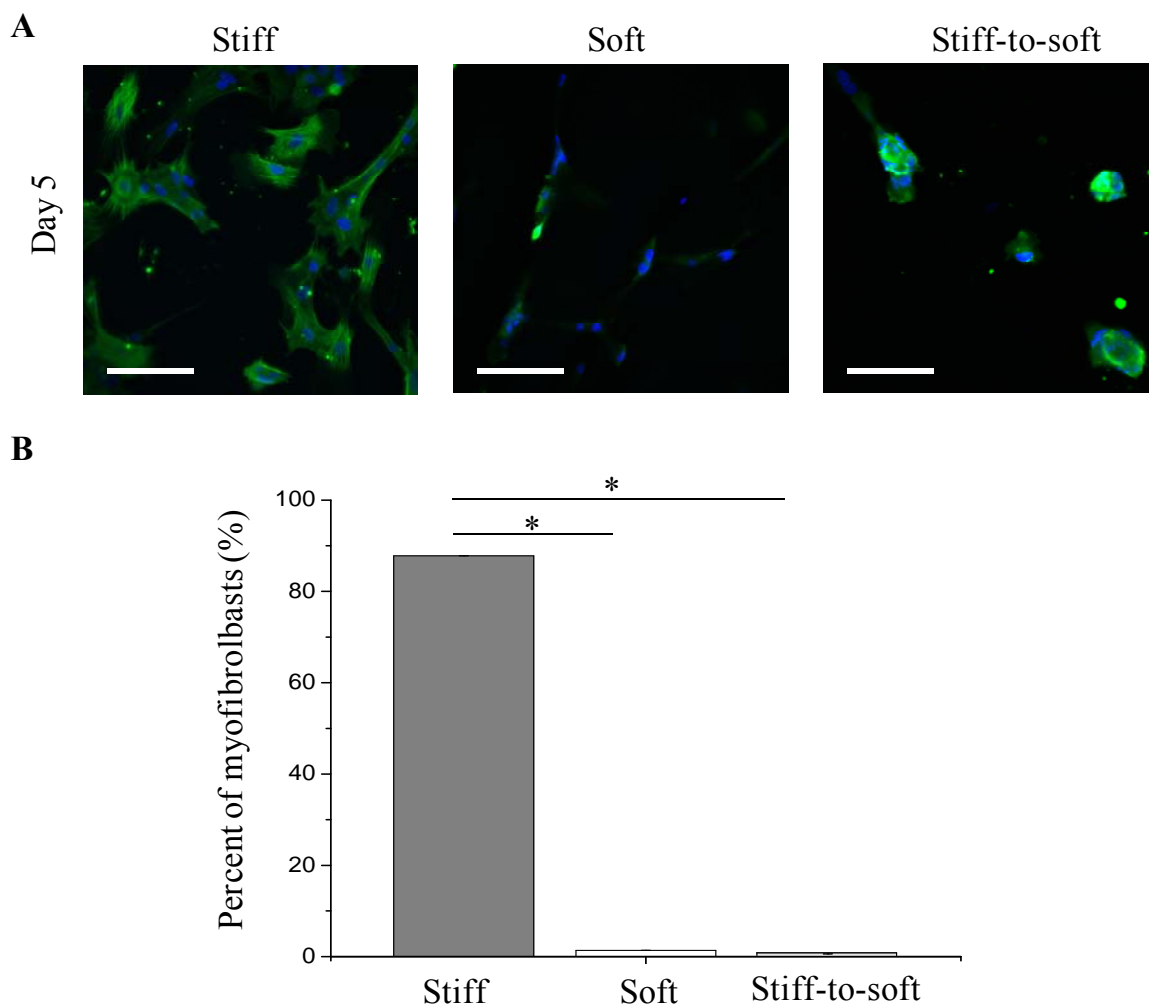


Figure 4.6 Rat Pulmonary Myofibroblasts De-Activated with Reduction in Substrate Modulus. Rat pulmonary myofibroblasts were stained with α SMA after culture on stiff, soft or stiff-to-soft gels until day 5. (A) Representative staining of α SMA to denote the myofibroblast phenotype. These cells lost α -SMA stress fibers on softer substrates. Green: α -SMA. Blue: nuclei. Scale bar: 100 μ m. (B) Quantification of the percent of myofibroblasts on the substrates based on staining in (A). The percentage of myofibroblasts on stiff-to-soft gels or soft gels was significantly lower than that on stiff gels. This is consistent with the observation on VICs in Figure 4.2, indicating a general role of substrate modulus in regulating the differentiation of myofibroblasts. * indicates $p < 0.05$

4.4 Discussion

Here, we have begun to explore how substrate modulus serves as a mechanical cue to regulate the fate of activated valvular myofibroblasts. Our studies revealed striking phenotypic

changes from activated myofibroblasts to less proliferative, quiescent-like fibroblasts when the culture substrate's elastic modulus was reduced from 32kPa to 7kPa. Apoptosis was minimally associated with this de-differentiation process. Within 6 hours of *in situ* substrate elasticity reduction, gene signatures of myofibroblasts (α SMA and CTGF) were down-regulated, while a fibroblast gene (vimentin) stayed at a similar level, confirming myofibroblast de-activation and suggesting potential signaling cascade mechanisms. Mechanically-reprogrammed VICs on stiff-to-soft gels were able to proliferate and re-initiate expression of myofibroblast genes in response to chemical cues. Considering the extensive health effects of tissue fibrosis, our study provides insight into possibly reducing fibrosis through preventing myofibroblastic activation and will assist with strategic *in vitro* tissue engineering to replace or re-organize severely fibrotic or calcified tissue.

Human tissues have stiffnesses ranging from ~ 0.1 kPa to ~ 20 GPa [4,47]. To recapitulate native stiffness *in vitro*, it is critical to culture cells on substrata with a physiologically relevant stiffness for understanding their functions. Previous studies indicated that normal valve fibrosa have a bulk elastic modulus from 0.8-8kPa [31]. When healthy valves become stenotic, osteoid, which is crosslinked collagen matrix as precursor to bone, has been detected in the valve [36]. While the stiffness of calcified valves has not been measured to our knowledge, Engler *et al.* have shown that osteoid matrix secreted by human mesenchymal stem cells has $E \sim 27 \pm 10$ kPa [4]. To mimic these microenvironments, we synthesized hydrogels with either a normal mesenchyme-like modulus (~ 7 kPa, soft gels) or a pathological osteoid-like modulus (~ 32 kPa, stiff gels) to probe the cell fate of VICs. Kloxin *et al.* previously demonstrated that valvular myofibroblast differentiation was promoted on stiff gels, but inhibited on soft gels

[10]. Similarly, fibroblasts isolated from different tissues, including lung [11] and liver [9], have been shown to activate with $E > 15\text{kPa}$ and maintain the αSMA negative fibroblast phenotype when the microenvironment had $E \leq 10\text{kPa}$. We observed consistent results for VICs cultured on either stiff or soft gels (Figure 4.2A). In addition, when we irradiated stiff gels with UV light to reduce the substrate modulus, valvular myofibroblasts were de-activated and lost previously formed αSMA stress fibers (Figure 4.2A). Similar behavior was observed for rat pulmonary fibroblasts (Figure 4.6), indicating a general role of substrate modulus in regulating the differentiation of myofibroblasts.

In these experiments, VICs were cultured on a 2-dimensional surface. While this is different from the 3-dimensional (3D) valve tissue in which the endogenous cells reside, a 2D culture approach has several advantages in understanding basic biological systems. 2D surfaces of functionalized biomaterials have served as unique tools for understanding how cells collectively migrate and how they differentiate in response to stiffness or shape [4,48,49]. Additionally, 2D culture enables one to readily monitor and image cells over time using real time microscopy tracking tools and to collect intracellular proteins or RNA more easily compared with 3D cultures. Currently, two types of scaffolds have been used for the 3D culture of VICs, enzymatically degradable synthetic gels [50] and natural matrices comprised of collagen [44] or hyaluronic acid [51]. Both of these materials have the complication that cells are changing their mechano-environment by degrading the matrix, so it becomes difficult to know the mechanical properties of the matrix in the pericellular region. In contrast, if VICs are encapsulated in non-degradable matrices with precisely defined mechanical properties, they remain in a rounded and un-natural morphology. Thus, it is difficult to de-couple the effect of modulus and cell

spreading on the cell fate within a 3D highly cross-linked matrix. For these reasons, our studies focus on isolating and understanding the effect of modulus on cell fate in 2D and believe that this knowledge will be helpful in better understanding VIC function in more complex, 3D matrices in future studies.

The fate of myofibroblasts after normal tissue repair has been an ongoing debate. In granulation and scar tissue, massive apoptosis has been observed [52]. Induction of apoptosis has been associated with matrix tension. For example, sudden release of collagen gels from their anchor causes programmed cell death in human dermal fibroblasts [53]. Additionally, compliant substrata with $E < 1\text{kPa}$ have been shown to induce significantly higher caspase 3 activity than stiff substrata in lung fibroblasts [11]. Consistently, we observed a small but significant increase of apoptosis on stiff-to-soft gels in comparison to stiff gels on day 5 (Figure 4.3C), indicating that some valvular myofibroblasts underwent apoptosis in response to reduction in modulus. However, this level of apoptosis on stiff-to-soft gels was similar to that observed for cells cultured on statically soft substrates. Additionally, the average level of apoptosis in VICs was $\sim 5\%$ on stiff-to-soft gels, which was too small to account for a nearly 35% decrease in the myofibroblast population. Therefore, most myofibroblasts did not undergo apoptosis in response to substrate modulus reduction. These findings within the context of the literature suggest that there may be different thresholds of substrate modulus for regulating myofibroblast activation and apoptosis. While $E \sim 7\text{kPa}$ is sufficient to de-activate valvular myofibroblasts without inducing significant apoptosis, I speculate that further reduction of E below or around 1kPa would induce most cells to undergo apoptosis. Additionally, softening the substrate did not select for specific populations of cells, as the cell number was not changed significantly from day 3 to

day 5 across all gel moduli (Figure 4.2C), and cells did not proliferate or undergo apoptosis significantly over time. There were slightly fewer cells attached on soft gels at day 1 than stiff gels, so we observed fewer cells on soft gels than on stiff gels from day 3 to day 5 (Figure 4.2C).

Since valvular myofibroblasts did not undergo significant programmed cell death, we hypothesized that these cells de-differentiated into a dormant, or quiescent-like, fibroblast state. Myofibroblasts are differentiated from fibroblasts through increased α SMA expression and its organization into stress fibers, which is regulated by mechanical stress [20,54]. When cells adhere to surfaces, traction forces are generated based on the resistance of the matrix to cellular adhesion and movement [54]. Cells on substrates with higher moduli have been shown to exert higher traction forces as measured by deformation of embedded fluorescent beads [55]. Mechanical strain generated on higher substrate moduli activate intracellular signaling potentially through p38 MAPK, Rho kinase and focal adhesion kinase to up-regulate transcription of α SMA and subsequent incorporation of α SMA into stress fibers [56,57]. Our results confirmed that α SMA stress fibers in VICs are dependent on substrate modulus. Based on Figure 4.2A, α SMA stress fibers in VICs were disassembled after 2 days of lowering substrate elasticity. Myofibroblast activation on substrates with varying moduli was independent of their time in culture (Figure 4.2B), indicating minimal influence from soluble factors in the medium. On stiff-to-soft gels, we observed a higher percentage of activated myofibroblasts (~25%) than that on soft gels (~10%). This indicates that not every myofibroblast can be efficiently de-activated by modulus reduction on stiff-to-soft gels.

Myofibroblasts not only differ from fibroblasts in the formation of α SMA stress fibers, but also have a distinct gene expression profile [58,59,60,61]. Through previous research, gene

signatures to distinguish myofibroblasts from fibroblasts have been revealed, such as α SMA and CTGF. α SMA is highly regulated at the transcriptional level with multiple serum response elements and CArG motifs in the promoter region of the gene [62]. CTGF expression is involved in the pathogenesis of fibrosis for various tissues and is tightly associated with the myofibroblast phenotype [45]. Both genes are more highly expressed by myofibroblasts than fibroblasts. As shown in Figure 4.4A, these myofibroblast genes, α SMA and CTGF, were significantly down-regulated with substrate modulus reduction, and the expression level of these genes was similar on stiff-to-soft gels compared with soft gels, suggesting reversion of activated VICs to a fibroblast-like phenotype. The reduction of these mRNAs was observed 6 hours after irradiating stiff gels to make them soft, indicating that cells change their molecular phenotype quickly in response to the mechanical cues. Uniquely, in comparison to substrates fabricated with discrete stiffness, changing substrate modulus *in situ* using PD-PEG gels enabled us to track dynamic transcriptional changes during myofibroblast de-activation and further reveal the molecular mechanisms regulating this process. As CTGF has been shown to be down-regulated through the YAP/TAZ pathway on soft substrata [63], it is possible that this signaling is involved in the early phase of myofibroblast deactivation on stiff-to-soft gels. Hinz *et al.* have discovered that latent TGF- β 1 from the ECM is activated by contraction of α SMA stress fibers in myofibroblasts [64]. Given that VICs rarely form α SMA stress fibers on soft or stiff-to-soft substrata, this result indicates a limited ability to activate TGF- β 1 from their microenvironment. This mechanism may act at a later phase to reinforce the un-activated fibroblast phenotype on stiff-to-soft gels.

Another functionally significant characteristic of myofibroblasts is their high rate of proliferation. Lung fibroblasts cultured on substrates with high modulus ($E \sim 100$ kPa) exhibited

increased myofibroblast activation and more proliferation [11]. In fibrotic lesions, a large number of myofibroblasts, generated through cell proliferation, exacerbates the inflammatory response and collagen deposition [65]. In contrast, VICs residing in healthy compliant valve matrices are mostly quiescent [26]. We found that the number of proliferating VICs was decreased by ~30% on stiff-to-soft gels in comparison to stiff gels. This result indicates that lowering substrate modulus inhibits cell cycle progression and directs cells to a more quiescent-like phenotype. In particular, a higher fraction of the cell population stalled in the G2 or mitosis (M) phase of the cell cycle on soft or stiff-to-soft gels than on stiff gels (Figure 4.4C), suggesting that mechanical tension conferred by substrate modulus is an important regulator for the G2/M phase of the cell cycle. From both Figure 4.4A and 4.4B, reducing substrate modulus not only down-regulated myofibroblast differentiation, but also controlled the proliferative response of these cells.

The myofibroblast phenotype has been suggested to be plastic, where myofibroblasts can be inhibited through different means including TGF- β 1 antagonist treatment [18] and low substrate modulus [10]. If the valvular myofibroblasts were reprogrammed to quiescent fibroblasts on stiff-to-soft gels, then these cells should maintain the fibroblast gene expression and the potential to proliferate and differentiate into myofibroblasts. Vimentin is an intermediate filament protein expressed in mesenchymal cells, including fibroblasts [66]. VICs expanded on plastic plates are all positive for vimentin staining (Figure 4.4D). This fibroblast property was preserved when substrate modulus was decreased. Based on Figure 4.4A and 4.4D, mRNA and protein expression of vimentin was present at a similar level in the de-activated cells on stiff-to-soft gels, compared with cells on either stiff or soft gels, indicating that the de-activated cells were still fibroblasts. Our results also suggest that these deactivated cells are in a reversible

state and respond to FGF2 and increased serum by entering the cell cycle and respond to TGF- β 1 by expressing myofibroblast gene markers (Figure 4.5A and 4.5B). Cell plasticity has become a blooming field of research with the paradigm-shifting discovery of reprogramming adult somatic fibroblasts into pluripotent stem cells by activating four transcription factors [67,68]. A culture substratum with appropriate elastic modulus and binding epitopes shows promise as a complementary approach to reprogram the cells into a developmental stage of interest and to dynamically dictate cell phenotype and fate in a non-invasive manner.

The timing and duration of matrix signaling events are emerging as important factors in myofibroblastic differentiation plasticity and ultimate cell fate. We observe myofibroblastic de-activation of VICs with substrate modulus changes at short culture times. In complementary studies, Balestrini *et al.* have observed that lung myofibroblasts “memorized” the stiff or soft substrates on which they were propagated for 3 weeks and stayed activated or un-activated even after they had been transferred to substrates with opposite stiffness [69]. By comparison, our cells have been cultured 7 days on stiff plastic plates before seeding on soft hydrogels for subsequent modulus tuning of 6 days in culture. Further, I observed similar levels of activation for freshly isolated VICs on stiff gels and stiff-to-soft gels as VICs at passage 3 (Figure 3.4A and Figure 4.2A). This indicates that our culture of VICs on plastic plates for about a week did not change the cellular response to substrate modulus. While there could be inherent differences between valvular fibroblasts and lung fibroblasts, our results and Balestrini *et al.* collectively indicate that as the myofibroblasts mature over time, there may be a time limit on their ability to revert back to fibroblasts.

Differentiation of myofibroblasts is regulated by multiple factors, including cell-cell

contact [6], adhesive epitopes [70], TGF- β 1 [18,21,71], and substrate elasticity [10,32]. However, cells *in vivo* encounter numerous signals and integrate different types and magnitudes of signals in choosing their fate. For example, cell-cell contact prevents TGF- β 1 from inducing epithelial-to-myofibroblast differentiation [72]. The ECM protein fibronectin with ED-A domain is required for TGF- β 1 mediated myofibroblast differentiation [73]. The Wells group has found that portal fibroblasts need both a stiff substrate and TGF- β 1 to become myofibroblasts [9]. Similarly, we observed that the myofibroblastic differentiation of VICs is regulated by both substrate stiffness and TGF- β 1. When VICs were cultured on stiff-to-soft substrata (E , from \sim 32kPa to \sim 7kPa), they can still activate fibrogenic genes (CTGF, FN1 and Col1A1) in response to TGF- β 1 (Fig 4.5B). However, these cells fail to develop α SMA stress fibers on the soft substrata even with TGF- β 1 treatment (Figure 4.5C). We speculate that a stiffer substrate is required for mature valvular myofibroblast formation and the de-activated VICs on stiff-to-soft gels were likely in a proto-myofibroblast state when treated with TGF- β 1 [20]. The PD-PEG gel system provides a powerful tool in studying cellular responses to competing signals *in vitro*, for example reduced substrate modulus while simultaneously increasing pro-fibrotic cytokines. This may provide insight into how microenvironment modulus in combination with other chemical or biological cues directs cell fate.

4.5 Conclusion

In summary, valvular myofibroblasts were reprogrammed to fibroblast-like cells when substrate modulus was reduced with light *in situ* from $E \sim$ 32kPa to $E \sim$ 7kPa. This de-differentiation process is characterized by low occurrences of apoptosis, dissolution of α SMA stress fibers, down-regulation of differentiation associated genes (α SMA and CTGF), and a

decline in cell proliferation. The de-activated fibroblasts on stiff-to-soft gels can be re-activated by FGF2 and serum to enter the cell cycle and by TGF- β 1 to express fibrogenic genes, such as CTGF, Col1A1 and FN1. Our data suggest that the fate of valvular myofibroblasts is regulated by substrate elasticity independent of soluble factors. This can potentially be applied to equivalent myofibroblasts from other tissues and presents a promising approach in tempering tissue fibrosis by de-differentiating activated myofibroblasts. Our study also provides an example of dynamically reprogramming differentiated cells through substrate modulus reduction and shapes the conception of designing user-defined 2-dimensional, or even 3-dimensional, platforms for controlling the developmental stage of cells.

CHAPTER V

TGF- β 1 UP-REGULATES OB-CADHERIN EXPRESSION TO INHIBIT VALVULAR MYOFIBROBLAST DIFFERENTIATION

5.1 Introduction

Cardiac valve diseases have arisen as a major health threat in western populations, especially for people over 65 years old or young adults with congenital valvular defects. Among various cardiac valve diseases, calcific aortic stenosis (CAS) is a predominant one. Statistics from the American Heart Association have shown that about 2-3% of people over 65 years old are affected by CAS and 1% of all live births have bicuspid valves, most of which eventually develop into CAS [10]. CAS is characterized by gradual stiffening and calcific nodule formation in aortic valves. Development of CAS has been associated with a number of risk factors, including old age, male sex, smoking, hypertension, and high serum lipid levels [6]. However, recent studies have started to reveal an important feature of the CAS pathology: this disease is not just a result of passive wear-and-tear of aortic leaflets, but an active process mediated by the resident cells, named valvular interstitial cells (VICs).

VICs are the main cell population in aortic valves that mediates valve homeostasis and disease progression. They are largely comprised of fibroblasts that maintain the potential to differentiate into pathogenic myofibroblasts or osteoblast-like cells [7, 49, 81]. VICs produce the major extracellular matrix (ECM) components of the valves, including collagen, fibronectin, elastin and proteoglycans, and secrete ECM remodeling enzymes, such as matrix

metalloproteases (MMPs) and tissue inhibitors of MMPs [12, 214]. During valve development, VICs have been shown to actively participate in tissue building and remodeling by secreting ECM-related proteins [13, 165]. Upon tissue damage, these cells are activated to a myofibroblast phenotype, which is characterized by increased deposition of collagen and increased contractility, mediated by α SMA⁺ stress fibers [55]. Myofibroblasts are important regulators of tissue repair in multiple mesenchymal tissues, such as skin, lung and liver [65, 215, 216]. However, if the myofibroblast phenotype persists, excessive collagen is deposited and ECM can be abnormally contracted, leading to tissue fibrosis and stiffening [66, 217]. Another pathogenic phenotype of VICs is the presence of osteoblast-like cells, which have been seen in stenotic leaflets from patients with CAS [46]. Benton *et al.* have shown that myofibroblast activation of VICs precedes the development of calcification-promoting cells, suggesting the importance of myofibroblasts in actively mediating valve diseases [77].

Many extracellular cues have been shown to regulate myofibroblast activation of VICs, including chemical factors, mechanical stress and cell-cell interaction. Despite the fact that a number of chemical cues can activate myofibroblasts, TGF- β 1 is one of the most common and potent chemokines to induce myofibroblast phenotypes in fibroblasts from different tissues [218]. It initiates phosphorylation and translocation of Smad2/3 into the nucleus, where they activate transcription of important myofibroblast genes, including α SMA, collagen 1A1 (Col1A1), and connective tissue growth factor (CTGF) to promote this differentiation [86-90]. Further, TGF- β 1 can also activate other signaling pathways, such as p38 MAPK and PI3K/AKT to regulate myofibroblast differentiation [91, 93]. Therefore, various biochemical signaling pathways initiated by TGF- β 1 coordinate in a systematic and temporal way to regulate myofibroblast

differentiation. In addition to TGF- β 1, mechanical cues, in the form of dynamic stretching or static elasticity, can modulate myofibroblast activation. It has been shown that substrates with high modulus promote myofibroblast activation, whereas, low modulus inhibits it [19, 104-106, 110]. For VICs cultured on soft substrates, even though TGF- β 1 can increase the expression of Coll1 and CTGF, it cannot promote myofibroblast maturation with respect to α SMA stress fiber formation, indicating complex interactions among different types of signals [109]. However, limited information is available for the role of cell-cell contact in myofibroblast differentiation.

Cadherins constitute a group of proteins mediating calcium-dependent cell-cell interaction, and they play vital roles in tissue formation and cell sorting during development [219]. Besides these major functions, cadherins are also involved in other important cellular functions, such as migration, proliferation and differentiation. N-cadherin has been shown to interact with FGF signaling to regulate the migration of breast cancer cells [220], or neurite outgrowth of neuronal cells [221]. VE-cadherin acts as a scaffold for the formation of a mechano-sensor to shear stress on the cell membrane of endothelial cells [114]. During skin myofibroblast differentiation, cells increase expression of OB-cadherin (OB-CDH), but decrease expression of N-cadherin (NCDH) [120]. Anti-OB-CDH peptides, but not anti-NCDH peptides, inhibit skin myofibroblast contraction [120]. A recent study has shown that OB-CDH knockout mice have reduced pulmonary fibrosis induced by bleomycin and OB-CDH promotes TGF- β 1 production in alveolar macrophages [94]. All of these results indicate that cadherins, especially OB-CDH, may be regulating the pathogenic myofibroblast phenotype.

As VICs in their native matrix constantly receive many different types of signals, it is important to understand systematically how cells process these signals to give the appropriate

phenotypic output. Further, TGF- β 1 is a pleiotropic factor and has cell type-specific and time-dependent effects, I decided to examine the gene expression program elicited by TGF- β 1 at early and late time points to understand its regulation of VICs in a systematic manner. Through microarrays, I found that TGF- β 1 induced distinct gene programs in VICs after 8 hours and 24 hours of treatment. Intriguingly, genes involved in cell adhesion were up-regulated by TGF- β 1 at a later time point (24 hours of treatment), with NCDH and OB-CDH increased by \sim 2 fold. When both cadherins were knocked down by siRNAs, there was an increase in VIC myofibroblast differentiation, which was inhibited by OB-CDH overexpression. This study suggests a novel mechanism as to how TGF- β 1 regulates myofibroblast differentiation through cadherins.

5.2 Materials and Methods

5.2.1 VIC Cell Culture

Fresh porcine hearts were obtained from Hormel Foods Corporation (Austin, MN, USA) within 24 hours of sacrifice and aortic valve leaflets were excised. Primary VICs were harvested from porcine aortic valve leaflets based on a sequential collagenase digestion as described in Chapter II materials and methods. The isolated cells were cultured in growth medium (Medium 199, 15% fetal bovine serum (FBS), 50U/ml penicillin, 50 μ g/ml streptomycin, and 0.5 μ g/ml fungizone) and expanded up to passage 3 (P3). P3 VICs were seeded directly or after transfection on plastic plates at 45,000 cells/cm² in low serum medium (Medium 199, 1% FBS, 50U/ml penicillin, 50 μ g/ml streptomycin, and 0.5 μ g/ml fungizone).

5.2.2 Porcine Genome Microarray

P2 VICs seeded on plastic plates were treated with or without TGF- β 1 (5ng/ml) for 8 hours and 24 hours. Cells from different conditions were cultured in low serum medium

supplemented with 1% FBS for 2 days. Total RNA was extracted using the RNeasy Mini Kit (Qiagen, Cat# 74104). All the RNA samples had 260/280 ratio ≥ 2.0 and RNA Integrity Number (RIN) ≥ 9.2 verified by RNA Bioanalyzer. Total RNA was amplified and labeled using Gene Chip 3' IVT Express Kit (Affymetrix, Cat# 901228) and hybridized to Porcine Genome Microarrays (Affymetrix, Cat# 900624). Three microarrays were performed for each condition. Microarray data were analyzed using Spotfire (TIBCO), DAVID Functional Annotation Bioinformatics analysis (<http://david.abcc.ncifcrf.gov/>) and Ingenuity Pathway Analysis (IPA, http://www.ingenuity.com/products/pathways_analysis.html).

5.2.3 Quantitative Real-Time PCR

For each condition, total RNA was isolated based on the RNeasy Mini Kit (Qiagen, Cat# 74104) or according to the manufacturer's protocol for TRI Reagent (Sigma, Cat# T9424). RNA concentration and integrity were measured and verified by Nanodrop 1000 (Thermo Scientific). cDNA was synthesized from total RNA with Superscript III reverse transcriptase (Life technologies, Cat# 18080-051) and random hexamer primers. Gene expression was determined by SYBR Green-based quantitative real-time PCR (qRT-PCR) using gene specific primer sets (shown in Table 3.1) and an Applied Biosystems 7500 Real-Time PCR machine.

5.2.4 Immunocytochemistry

VICs were fixed with 4% paraformaldehyde (15min at 25°C), permeabilized in 0.1% TritonX100, and blocked with 3% bovine serum albumin (BSA). Mouse anti- α SMA antibody (Abcam, Cat# ab7817) was diluted at 1:100 in PBS with 1% BSA and 5% normal goat serum and incubated with the samples overnight at 4°C. Following washes in PBS with 0.05% Tween 20 (PBST), samples were labeled with goat-anti-mouse Alexa Fluor 488 secondary antibody (Life

technologies, Cat# A-11001). Samples were mounted and subsequently imaged on a LSM 710 Laser Scanning Microscope (Carl Zeiss) with a 20X magnification objective. Images of different fluorescence channels were compiled with Zen or Metamorph software and analyzed by ImageJ for total nuclei number (Analyze Particles function, NIH). Myofibroblasts were counted as cells with α SMA staining organized into fibrils, and percentage of myofibroblasts was calculated as (number of myofibroblasts / total number of cells) x 100%. To quantify each sample, 6 random fields of view were imaged, counted, and averaged.

5.2.5 Western Blot

VICs were scraped into the RIPA buffer (Upstate, Temecula, CA, Cat# 20-188) with protease inhibitor cocktail (EMD Milipore, Cat# 539134) and phosphatase inhibitors (Roche, Cat# 04906845001). Cell lysates were subsequently rotated at 4°C for 30 min and centrifuged at 12,000 RPM for 15min. Supernatant was saved for sodium dodecyl sulfate-polyacrylamide gel electrophoresis (SDS-PAGE). Protein concentration of the samples was measured by a microBCA kit (Thermo Scientific, Cat# 23235). 10-20 μ g of total protein for each sample was loaded into the 10% TGX mini gels (Bio-rad, Cat# 456-1033) and separated by electrophoresis for 1 hour at 200V. The proteins were subsequently transferred onto a nitrocellulose membrane using tank transfer at 100V for 1 hour. The nitrocellulose membrane was blocked with PBST with 5% non-fat milk for 1 hour at room temperature (RT) and then incubated with primary antibodies overnight at 4°C. After washes with PBST, secondary antibodies conjugated with horseradish peroxidase (HRP) were applied for 1 hour at RT. Protein bands were visualized by applying a chemiluminescent substrate of HRP (Thermo Scientific, Cat# 34075) and exposing the membrane to X-ray films. Protein abundance was subsequently quantified by Image J. The

following antibodies were used in this study: GAPDH (Cell signaling technology, Cat# 2118), α SMA (Abcam, Cat# ab7817), phospho-Smad2 (Ser 465/467) (Cell signaling technology, Cat# 3101), Smad2/3 (Cell signaling technology, Cat# 3102), and OB-CDH (Clone 3H10, a generous gift from Dr. Micheal Brenner, Brigham and Women's Hospital). At least 3 biological replicates were screened by western blot for each condition.

5.2.6 Transfection

P3 VICs were transfected with either siRNAs or plasmids with the U23 protocol in amaxa nucleofector (Lonza). Briefly, cells were prepared in a single cell suspension at 2-3 million cells per 100ul of the transfection buffer provided by the kit (Lonza, Cat# VPI-1002). siRNA against CDH2 (sequence: CUGUGUCUGUCACAGUUAUUU) and siRNA against CDH11 (sequence: CAGACUUGGACUAUGACUAUU), both of which were customer-designed based on porcine mRNA sequences (Dharmacon), together with Non-targeting siRNA (Dharmacon, Cat# D-001210-02-20), were used at 2 μ M in the transfection buffer. pCEP4 empty vectors and pCEP4 vectors encoding full-length human CDH11 or mutated human CDH11 $\Delta\beta$ lacking the distal β -catenin binding site as described previously [222] (generous gifts from Dr. Micheal Brenner, Brigham and Women's Hospital), were used at 5 μ g per transfection. After transfection, cells were recovered in growth media with 15% FBS for 15min in the CO₂ incubator and cultured on plastic plates in low serum media (1% FBS) for 2 days.

5.2.7 Statistics

A Student's t-test was used to compare data sets with two conditions and the One-way ANOVA with Bonferroni's post test was used to compare data sets with more than two conditions. A *p* value less than 0.05 was considered statistically significant.

5.3 Results

5.3.1 TGF- β 1 Induces Common and Distinct Gene Expression Changes Globally in VICs after 8 and 24 Hours

Gene expression in VICs treated with TGF- β 1 over time was measured by porcine genome arrays. After GC Robust Multi-array Average (GCRMA) normalization, data were clustered based on hierarchical clustering as shown in Figure 5.1A. All the untreated control conditions clustered into one branch and segregated from the TGF- β 1 treated groups. However, TGF- β 1 treatments of 8 hours or 24 hours did not cluster together. Instead, each biological replicate with different duration of treatments clustered together. For the differentially regulated genes after 24 hours of TGF- β 1 treatment (fold change ≥ 1.5 , $p < 0.05$), DAVID functional annotation analysis showed that cell adhesion- and extracellular matrix-associated functions were significantly up-regulated, whereas oxidoreductase activity was significantly down-regulated (Figure 5.1B). Figure 5.1C shows the number of genes being differentially regulated at different time points of TGF- β 1 treatment with fold change ≥ 2 and $p < 0.01$. There were 35 genes significantly up-regulated by TGF- β 1 at 8 hours and 58 genes at 24 hours, with 21 overlapping genes. Forty four genes were significantly down-regulated by TGF- β 1 at 8 hours and 84 genes at 24 hours, with 20 genes in common.

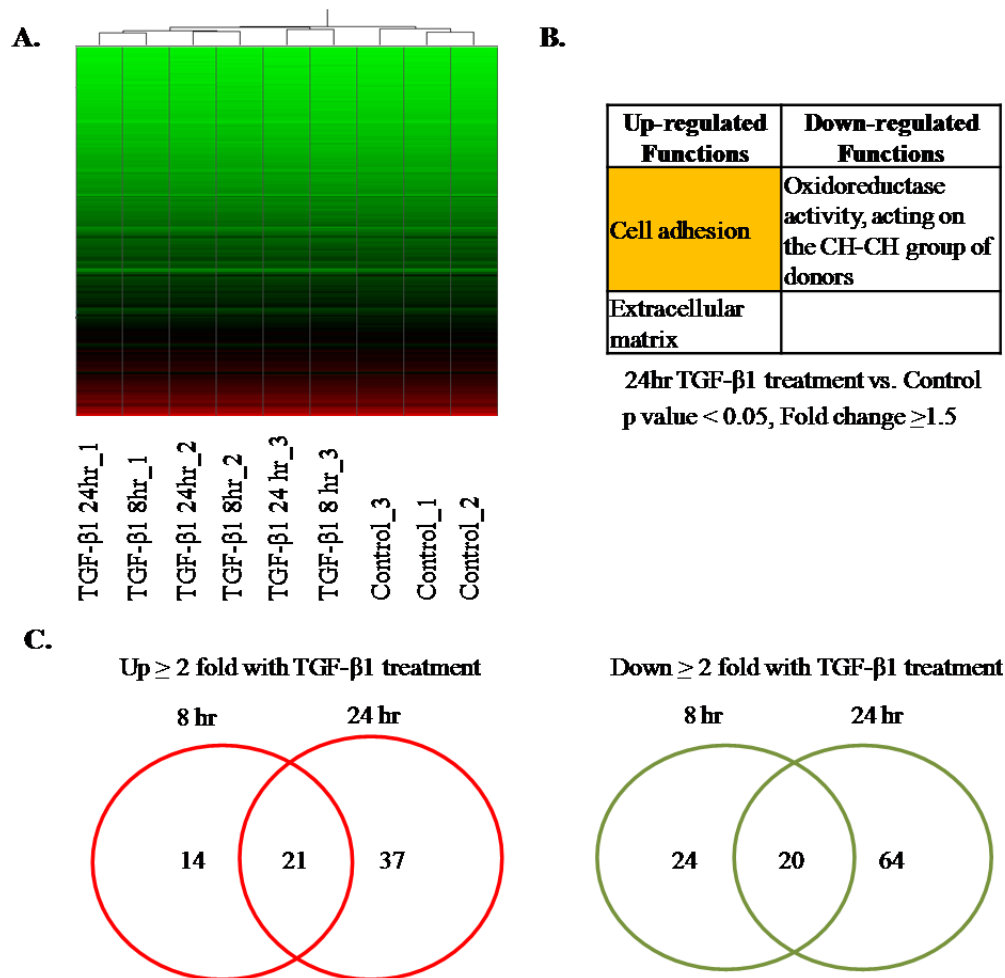


Figure 5.1 Global Gene Expression of Porcine VICs in Response to TGF-β 1 over Time. VICs cultured on plastic plates were treated with TGF-β1 at 5ng/ml for 8 hours and 24 hours. Total RNA from 3 biological replicates of each condition was collected for microarray analysis. (A) Hierarchical clustering of GCRMA-normalized microarray data showed that control conditions and TGF-β1 treated conditions segregated into 2 clusters. However, TGF-β1 treatment of the same biological replicate clustered together, rather than different time points of TGF-β1 treatment. (B) DAVID functional annotation analysis of genes differentially regulated by TGF-β1 at 24 hours (with fold change ≥ 1.5 and $p < 0.05$) showed that genes associated with cell adhesion and extracellular matrix were up-regulated by TGF-β1, whereas oxidoreductase activity was down-regulated. (C) Venn diagrams showing the number of genes that were differentially regulated by TGF-β1 treatment at different time points with fold change ≥ 2 and $p < 0.01$. 21 genes were up-regulated and 20 genes were down-regulated at both time points.

5.3.2 Microarray Data are Validated

Microarray data were consistently validated by qRT-PCR. Five genes up-regulated by

TGF- β 1 (TUFT1, RASAL2, FN1, CHSY1 and ITGA5) and 5 genes down-regulated by TGF- β 1 (PDK4, MYLIP, ADAMTS1, ACSS3 and ID2) were randomly selected and shown to have consistent regulation by TGF- β 1 over time via qRT-PCR (Figure 5.2).

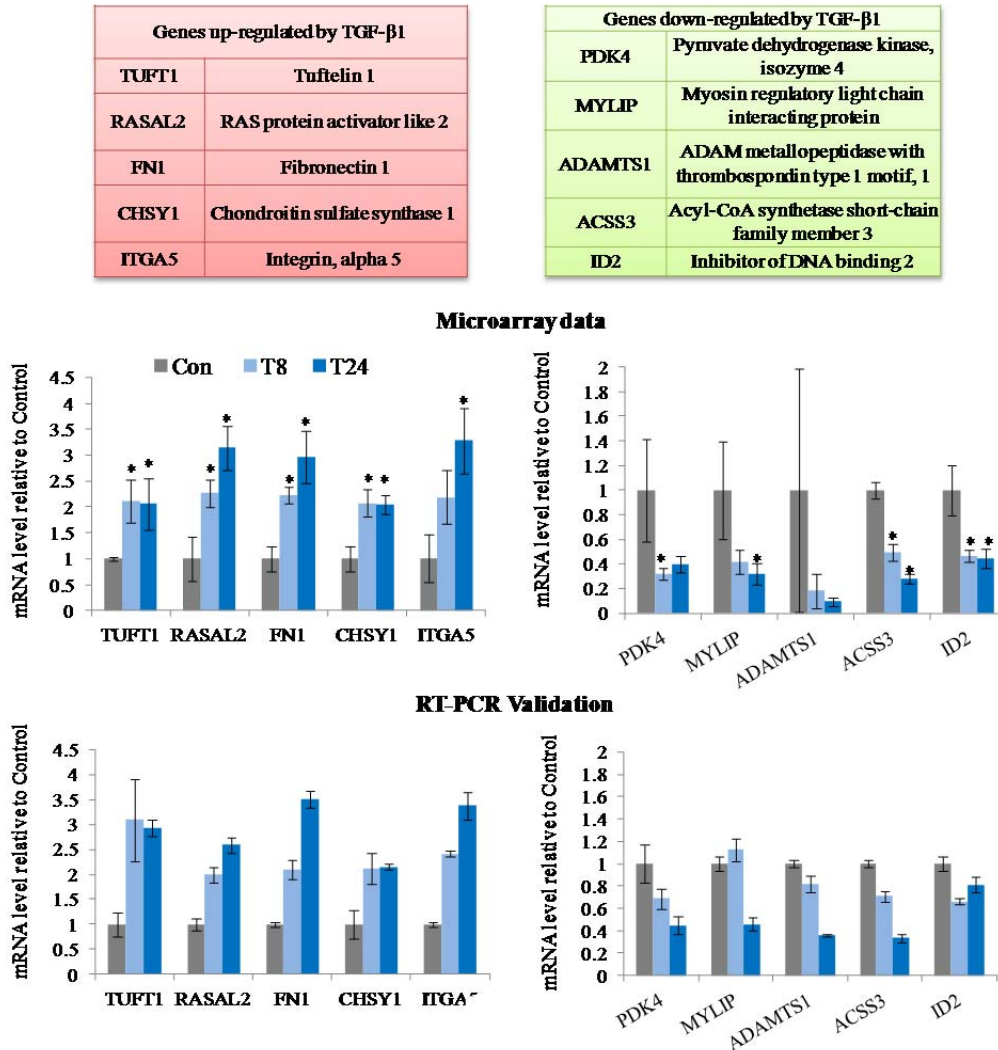


Figure 5.2 qRT-PCR Validation of Microarray. Five up-regulated (red table) and 5 down-regulated (green table) genes were randomly selected from the gene pools regulated at both time points of TGF- β 1 treatment. When qRT-PCR was performed, it showed that all 5 up-regulated genes had an expression pattern closely mimicking the microarray data. All 5 down-regulated genes showed reduced mRNA levels by TGF- β 1 treatment at 24 hours. Only MYLIP and ADAMTS1 did not show inhibition after 8 hours of treatment. Error bars for the microarray data are standard error, but error bars for the qRT-PCR validation are standard deviation. * indicates significantly different from the Con condition with $p < 0.05$. Con: untreated. T8: TGF- β 1 treatment for 8 hours. T24: TGF- β 1 treatment for 24 hours.

Additionally, some known TGF- β 1-responsive genes, including JunB, TGF- β 1, KLF10 and Smurf2, were increased in a time-dependent manner based on the microarray data (Figure 5.3).

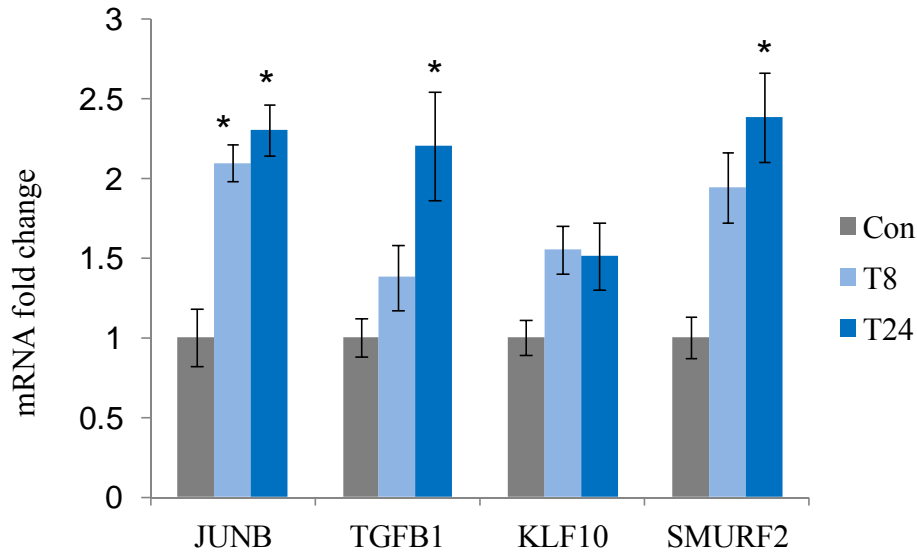


Figure 5.3 Expression Pattern of Known TGF- β 1-responsive Genes in the Microarrays. It has been shown that JUNB, TGFB1, KLF10 and SMURF2 have increased expression in response to TGF- β 1 treatment. Our microarray data were consistent with previous observations and showed that these genes were up-regulated by TGF- β 1 treatment at both 8 hours and 24 hours. * indicates significant difference relative to the Con condition with $p < 0.05$. Con: untreated. T8: TGF- β 1 treatment for 8 hours. T24: TGF- β 1 treatment for 24 hours.

5.3.3 Ingenuity Pathway Analyses Reveal Significantly Regulated Signaling Pathways

IPA analysis in Figure 5.4 showed that TGF- β 1 signaling was activated with the treatment as expected and also revealed that significant gene changes were associated with the TNF α pathway and the p53 pathway. These networks were built with lower than 0.01 chance of being random networks.

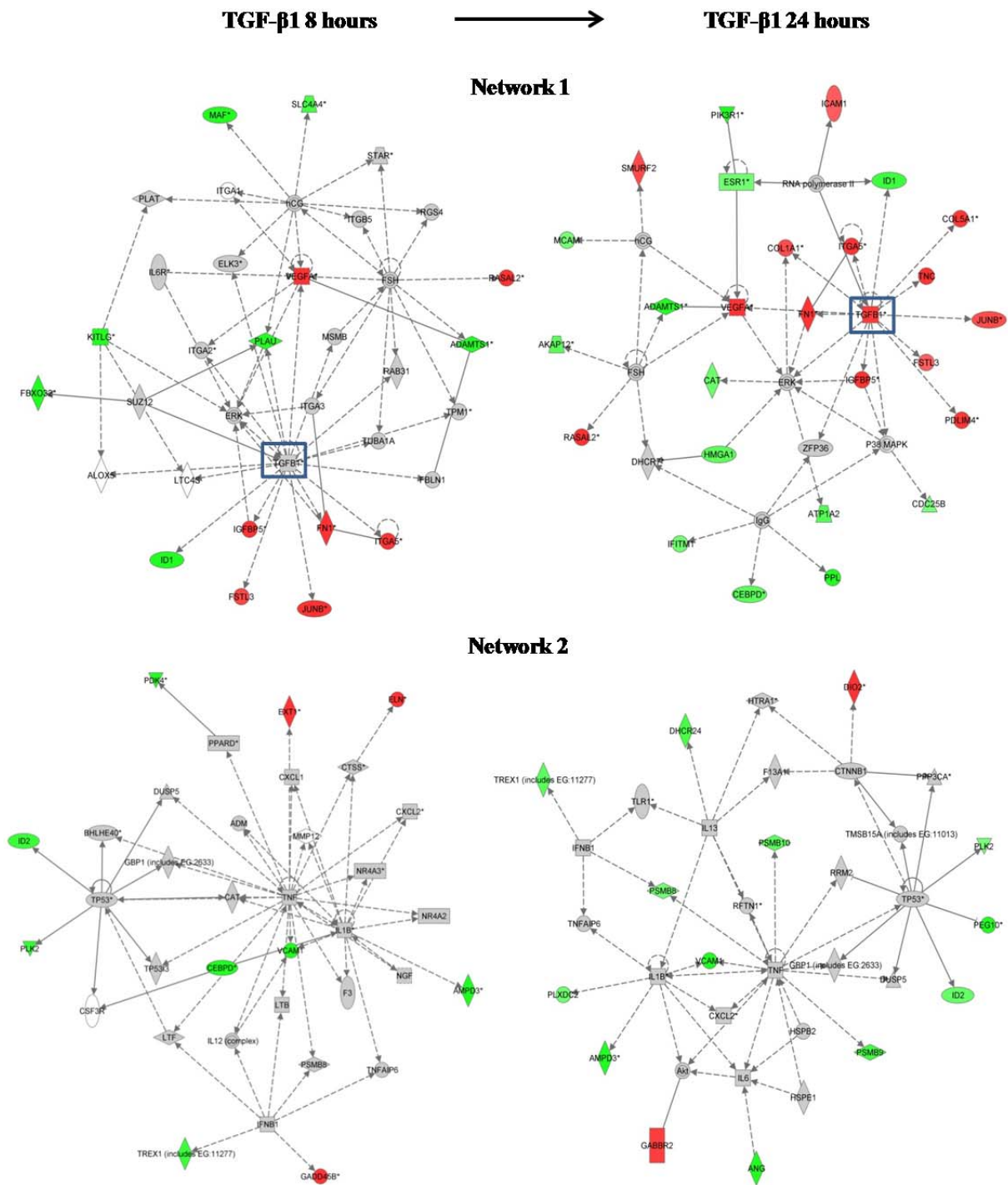


Figure 5.4 Ingenuity Pathway Analyses for Microarray Data. Genes differentially regulated by TGF- β 1 at 8 hours or 24 hours with fold change ≥ 2 fold and $p < 0.05$ were analyzed with the IPA software in order to find significantly activated signaling pathways. As expected, TGF- β 1 signaling was activated (Network 1). Other regulated pathways were related to TNF α and p53 (Network 2).

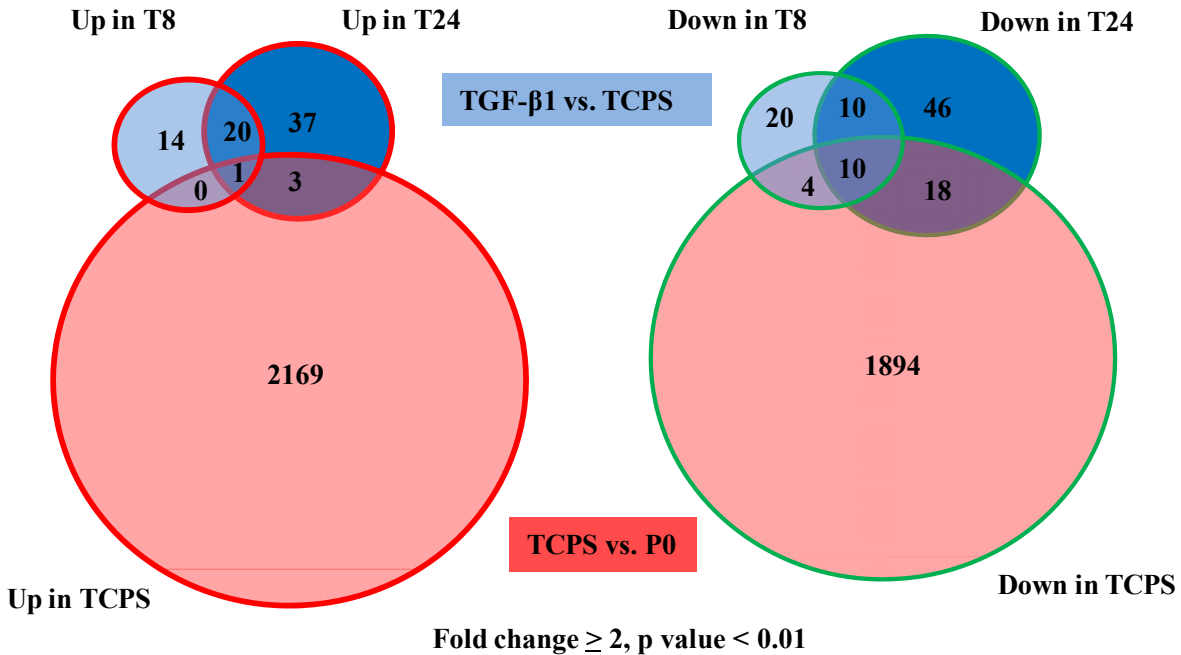


Figure 5.5 Numbers of Gene Probes Commonly and Distinctly Regulated by TGF- β 1 and TCPS. Based on the microarray data presented in Figure 3.1 and Figure 5.1 (which have been carried out in parallel), differentially regulated genes either induced by TGF- β 1 treatment or by the TCPS culture with the criteria of fold change ≥ 2 and $p < 0.01$ were compiled and compared. One gene probe was commonly up-regulated and 10 gene probes were commonly down-regulated by both time points of TGF- β 1 treatment and the TCPS culture. More genes were commonly regulated by 24h of TGF- β 1 treatment and the TCPS culture than those shared by 8h of TGF- β 1 treatment and the TCPS culture.

5.3.4 Numbers of Gene Probes Commonly and Distinctly Regulated by TGF- β 1 and TCPS

Combining the microarray data from Chapter III (Figure 3.1) and Chapter V (Figure 5.1), Venn diagrams were created to analyze genes that were commonly and distinctly regulated by TGF- β 1 or the TCPS culture. Only 1 gene, SLC40A1, was commonly up-regulated by both time points of TGF- β 1 treatment and the TCPS culture. However, 10 gene probes were commonly down-regulated by both time points of TGF- β 1 treatment and the TCPS culture. These gene probes correspond to the following genes: ADAMTS1, CEBPD, PDK4, MYLIP, ID2,

and ACSS3, among which there were 2 gene probes for CEBPD, PDK4 and ACSS3, and 1 gene probe unannotated)

5.3.5 TGF- β 1 Up-regulates the Expression of CDH2 (N-cadherin) and CDH11 (OB-cadherin) in VICs

From the microarrays, 4 types of cadherins, CDH2, CDH5, CDH11 and CDH13, were found to be abundantly expressed (Figure 5.6A). Among these, CDH2 (or NCDH) and CDH11 (or OB-CDH) were up-regulated by ~2 fold after 24 hours of TGF- β 1 treatment based on the microarrays (Figure 5.6B). Up-regulation of OB-CDH was validated by both qRT-PCR and western blot. With TGF- β 1 treatment for 24 hours, Col1, CTGF, Fibronectin 1 (FN1), Matrix metalloproteinase 1 (MMP1), and OB-CDH were all up-regulated by 3-7 fold (Figure 5.6C). At the protein level, TGF- β 1 induced phosphorylation of Smad2 and increased expression of OB-CDH relative to the internal control, GAPDH (Figure 5.6D).

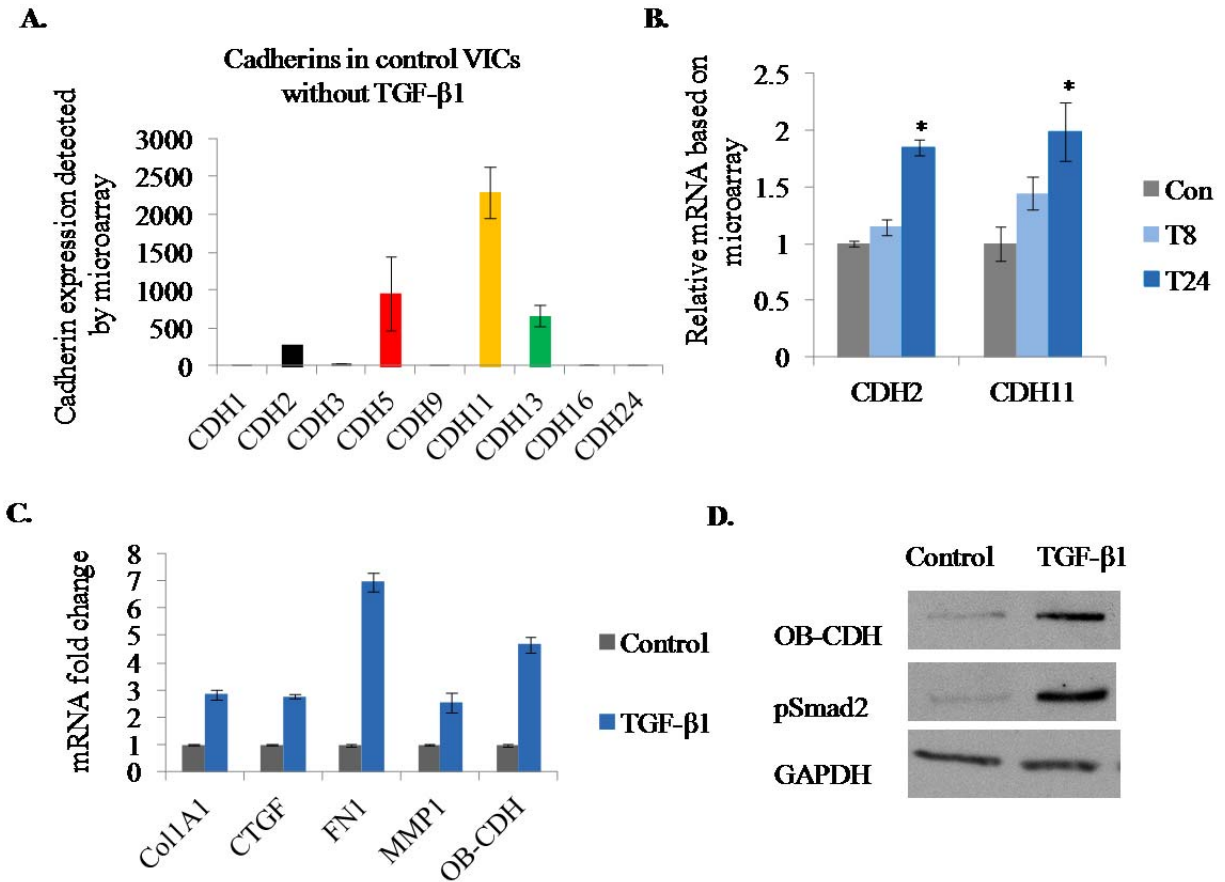


Figure 5.6 TGF- β 1 Up-regulates Expression of CDH2 (NCDH) and CDH11 (OB-CDH) in VICs. (A) Normalized expression value of different cadherins in VICs (no TGF- β 1) detected by microarrays. CDH2, 5, 11 and 13 were the most abundantly expressed cadherins in VICs. (B) Based on the microarrays, expression of CDH2 and CDH11 was up-regulated by \sim 2 fold after 24 hours of TGF- β 1 treatment. (C) TGF- β 1 treatment for 24 hours increased mRNA level of CDH11/OB-CDH and also up-regulated expression of the fibrogenic genes, including Coll1A1, CTGF, FN1 and MMP1. This is representative of at least 3 independent qRT-PCR experiments. Error bars are standard deviation. (D) At the protein level, TGF- β 1 treatment (24 hours), which activated pSmad2, also up-regulated OB-CDH protein expression. Representative data of at least 3 independent experiments.

5.3.6 Knocking Down both OB-CDH and NCDH Promotes Valvular Myofibroblast Differentiation

Two different siRNAs were designed against porcine OB-CDH (OB-siRNA) and NCDH (Ncdh-siRNA). VICs transfected with either OB-siRNA or Ncdh-siRNA were verified to have significant reduction of OB-CDH and NCDH at both the mRNA level (Figure 5.7A) and the protein level (Figure 5.7B), compared with those transfected with a non-targeting siRNA (NT-siRNA). Meanwhile, knocking down both OB-CDH and NCDH (CDHs-siRNA) in VICs increased expression of α SMA protein (Figure 5.7B). Further, cells treated with siRNAs against cadherins had reduced β -catenin staining, but had an increased percentage of myofibroblasts, marked by α SMA stress fibers, compared with those treated with NT-siRNA (Figure 5.7C).

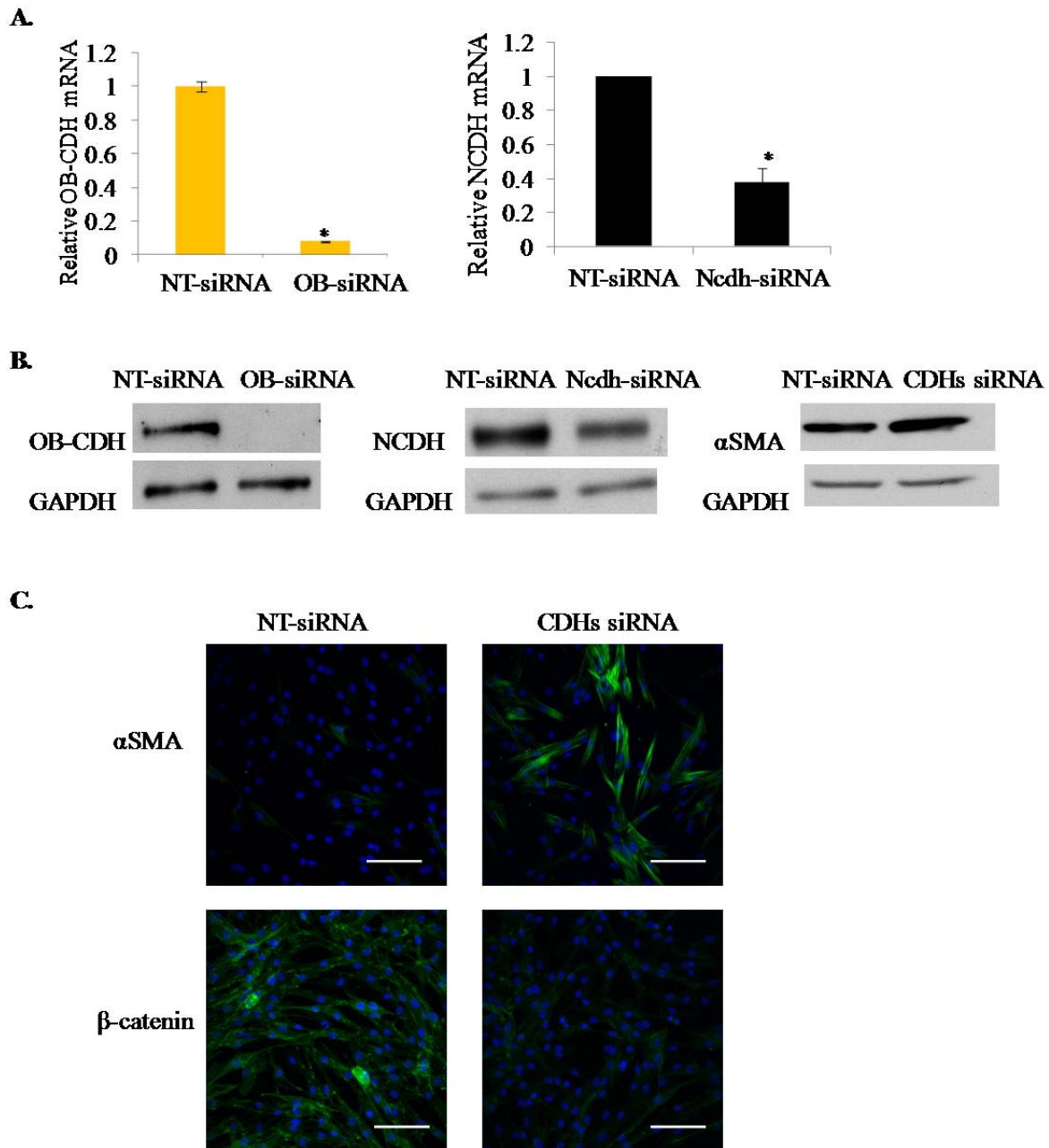


Figure 5.7 Knocking down both OB-CDH and NCDH Promotes Valvular Myfibroblast Differentiation. VICs were transfected with siRNAs against OB-CDH and NCDH and were examined at day 3 for myfibroblast activation. (A) Both OB-CDH and NCDH mRNA were effectively knocked down by siRNAs at day 3 based on qRT-PCR. * indicates $p < 0.05$. (B) Protein expression of OB-CDH and NCDH was also significantly reduced by siRNAs. Meanwhile, α SMA protein expression, a marker for myfibroblasts, was increased with siRNA treatment. (C) Consistently, myfibroblasts characterized by α SMA stress fibers were increased in CDHs siRNA-transfected cells compared with cells transfected with a non-targeting siRNA (NT-siRNA). Green: α SMA, Blue: nuclei. Scale bar: 100 μ m.

5.3.7 Overexpressing OB-CDH Inhibits Valvular Myofibroblast Differentiation

The effect of OB-CDH on valvular myofibroblast differentiation was examined by over-expressing OB-CDH. When OB-CDH was over-expressed, mRNA of OB-CDH was up-regulated by ~40 fold measured by qRT-PCR (Figure 5.8A). At the protein level, α SMA expression and Smad2 phosphorylation was inhibited by overexpressing full-length OB-CDH (CDH11 FL), but not by a mutated form of OB-CDH that lacks the β -catenin binding site (CDH11 $\Delta\beta$) (Figure 5.8B). Percentage of myofibroblasts in the population was reduced when over-expressing CDH11 FL, but not CDH11 $\Delta\beta$, based on immunocytochemistry (Figure 5.8C).

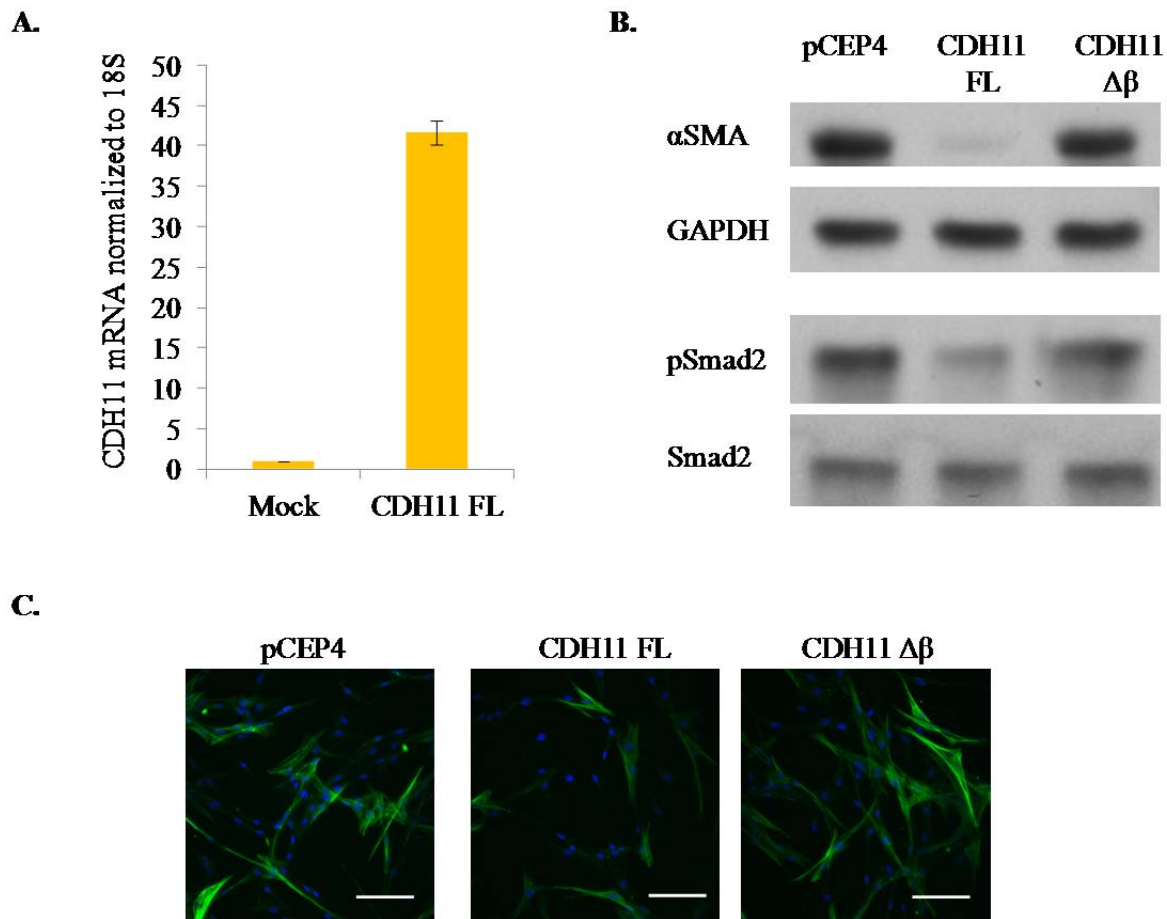


Figure 5.8 Overexpression of OB-CDH Inhibits Valvular Myofibroblast Differentiation. (A) VICs transfected with human full-length CDH11 (CDH11 FL) expressed ~40 fold higher mRNA level of the gene than the control as demonstrated by qRT-PCR. Representative data of at least 3 independent experiments. Error bars: standard deviation. (B) When full-length CDH11 was over-expressed, α SMA protein level and pSmad2/Smad2 were significantly decreased compared with the empty vector condition (pCEP4). However, this was not observed when a mutated form of CDH11 (CDH11 $\Delta\beta$) was over-expressed. (C) Based on immunostaining, myofibroblasts with α SMA stress fibers were inhibited by overexpressing CDH11 FL, but not CDH11 $\Delta\beta$. Green: α SMA, Blue: nuclei. Scale bar: 100 μ m.

5.4 Discussion

Myofibroblasts are like a double-edged sword. They are critical during wound healing to deposit more ECM and to contract the wound opening; however, if these cells are not

effectively turned over at the end of wound healing, their persistence can lead to tissue fibrosis in various organs [65, 216]. Understanding the regulation of the myofibroblast phenotype by chemokines can help reveal common molecular pathology of various fibrotic diseases. In this study, gene expression changes initiated by TGF- β 1, one of the most prevalent cytokines in fibrotic loci [84], were examined longitudinally by whole-genome microarrays. TGF- β 1 elicited some common and some distinct genes at 8-hour and 24-hour of treatment. These genes were involved in different cellular functions, and cell adhesion was up-regulated by TGF- β 1 at the later time point. Interestingly, both NCDH and OB-CDH were up-regulated by TGF- β 1. Knockdown and over-expression of OB-CDH directly demonstrated its inhibitory role in valvular myofibroblast differentiation. This study suggests that TGF- β 1 can initiate different early and late gene responses in VICs, and one of the late responses is to up-regulate cadherins to inhibit myofibroblast activation.

Microarrays with good experimental design and validation are powerful tools for detecting systematic changes in gene expression and revealing novel gene targets and signaling pathways for future exploration. In this study, I utilized porcine genome microarrays to examine mRNA changes in VICs treated with TGF- β 1 for 8 hours and 24 hours with 3 biological replicates for each condition. Ten out of 10 genes were validated positively by qRT-PCR (Figure 5.2). Hierarchical clustering in Figure 5.1A suggests that there are bigger differences among the biological replicates than between different duration of TGF- β 1 treatments. As I have utilized VICs isolated on different dates and from completely different pools of pig hearts, biological variance is expected. Based on these biological replicates with different background, filtering of genes that are responsive to TGF- β 1, but independent of cell source, is enhanced. Here, I showed

that shared sets of 21 genes and 20 genes were up- or down- regulated by TGF- β 1 at both time points, respectively. These genes probably play very important roles in the process of TGF- β 1-induced myofibroblast differentiation and are valuable targets to follow up for their functions (Figure 5.2). For example, TUFT1, or tuftlin, is a novel gene target of TGF- β 1 in fibroblasts where its functions are unknown. In addition, TGF- β 1 has induced more genes with significant expression changes at 24 hours than at 8 hours (Figure 5.1C). Utilizing ingenuity pathway analysis (IPA), I demonstrated that, as expected, TGF- β 1 signaling was activated and more downstream targets of TGF- β 1 were activated or inhibited with time (Figure 5.4). Interestingly, signaling changes associated with TNF α and p53 were also detected by IPA analysis (Figure 5.4), indicating that these pathways may be involved in the phenotypic changes of myofibroblasts induced by TGF- β 1.

TGF- β 1 is a well-established chemical factor involved in fibrosis [84]. However, it is a pleiotropic factor that can regulate a wide spectrum of cell types and has an impressive diversity of effects on cells depending on the context, dosage and duration [223]. This cytokine is found to be elevated at sites of fibrosis and can be secreted by recruited inflammatory cells and local fibroblasts/myofibroblasts [58, 79, 84, 224]. Canonical TGF- β 1 signaling activates phosphorylation and nuclear translocation of Smad2/3, which then binds to gene promoters with Smad-binding sequences in conjunction with other nuclear factors to regulate gene expression [84]. Smad3 knockout mice have reduced fibrosis in response to cutaneous injury [225] and reduced lung fibrosis with bleomycin treatment [226]. This supports the important role of TGF- β 1 in fibrosis pathology. *In vitro*, TGF- β 1 can induce myofibroblast differentiation in fibroblasts isolated from valve [81], skin [90], lung [87] and liver [82]. Previous studies have

shown that fibroblasts isolated from different organs in the human body have different gene expression profiles [68]. As TGF- β 1 treatment has been monitored by microarrays in human lung fibroblasts [227], corneal fibroblasts [228], etc., it would be interesting to find common and distinct gene regulation in these different fibroblasts, which may help understand the molecular pathology of fibrotic diseases in various tissues. Besides the canonical pathway via Smads, TGF- β 1 can also activate other signaling pathways, e.g. p38 MAPK and PI3K, and induce secondary effects through secreted proteins [91, 93, 229]. TGF- β 1 has been shown to induce the production of CTGF and Interleukin factors, which promote myofibroblast activation [89, 143, 230]. Based on our microarray analysis, TGF- β 1 up-regulates a number of extracellular proteins at 24 hours of treatment, including Col1A1, Col5A1, TNC (tenascin C), VEGF, IGFBP5 (insulin-like growth factor binding protein 5) and FSTL3 (follistatin-like 3), which serve as outside-in signaling to promote myofibroblast fate.

Interestingly, cell adhesion is among the most significantly up-regulated functions by TGF- β 1 at 24 hours. I hypothesize that genes associated with cell adhesion downstream of TGF- β 1 are regulating valvular myofibroblast differentiation. The term cell adhesion contains both cell-matrix interaction and cell-cell interaction. As cell-cell interaction is less studied than cell-matrix interaction in regulating myofibroblast differentiation, I decide to focus on the cell-cell adhesion. Based on the microarray probes, TGF- β 1 has up-regulated both NCDH and OB-CDH by at least 2 fold after 24 hours of treatment. Consistently, OB-CDH is up-regulated by TGF- β 1 in lung epithelial cells [94] and during skin myofibroblast activation [120]. Interestingly, when I knocked down both cadherins by siRNAs, there was enhanced myofibroblast differentiation in VICs characterized by increased α SMA protein level and increased stress fiber

organization (Figure 5.7B and 5.7C). When OB-CDH was over-expressed, it inhibited those phenotypes of valvular myofibroblasts and reduced Smad2 activation (Figure 5.8). These data suggest that OB-CDH plays an inhibitory role towards the actin stress fiber formation in myofibroblasts, possibly through blocking the canonical TGF- β 1/Smad2 signaling. Consistently, Li *et al.* have observed that OB-CDH overexpression inhibits actin filament formation in carcinoma cells [231]. Cadherins have been shown to interact with actin filaments intracellularly and can regulate Rho GTPase activities, which feed back to actin dynamics [232, 233]. For example, N-cadherin upregulates RhoA activity and inhibits Rac1 and Cdc42 in myoblasts [234]. So, it is possible that OB-CDH is regulating valvular myofibroblast phenotype through the small GTPases. In addition, cadherins bind to β -catenin, inhibiting its nuclear localization and gene regulation [235]. Yet, nuclear localization of β -catenin is necessary for valvular myofibroblast differentiation, including up-regulation of α SMA expression and stress fiber formation [19, 236]. It is hypothesized that knocking down cadherins redirects β -catenin into the nuclei, which then promotes myofibroblast gene expression. However, immunostaining of β -catenin in Figure 5.7C only shows overall reduction, but not re-distribution, of β -catenin in VICs treated with cadherin siRNAs compared with those treated with NT-siRNA.

The influence of cell-cell contact on myofibroblast differentiation is relevant for the progression of fibrosis. Fibroblasts are usually in closer contact with the surrounding matrix than with other cells, so there has been much focus on how cell-matrix interaction regulates fibrotic properties of the cells [237]. However, as fibrotic loci develop, resident fibroblasts and myofibroblasts proliferate and migrate towards the loci, increasing cell density and formation of adherent junctions through cadherins [238]. Cadherins regulate cell migration, survival,

apoptosis and differentiation, which are closely associated with fibrosis pathology. For example, cleavage of E-cadherin is an essential step for TGF- β 1-induced epithelial-to-mesenchymal transformation (EMT)-mediated fibrosis in both kidney [239] and liver [171]. Both OB-CDH and NCDH have been shown to promote migration and invasion of cancer cells [220, 240], and NCDH promotes myofibroblast migration into collagen gels in response to TGF- β 1 [216]. Recently, it has been shown that OB-CDH knockout mice have reduced fibrotic phenotypes in response to bleomycin-induced lung fibrosis [94] and are resistant to inflammatory arthritis [124]. This is different from what I have observed with VICs, that OB-CDH siRNA treatment promotes their myofibroblast differentiation. However, the development of fibrosis *in vivo* is mediated by multiple cell types and their complex interactions; it is possible that OB-CDH plays different roles in different types of cells and the outcome of tissue fibrosis depends on the additive effects of all the cells. OB-CDH engagement has been suggested to increase inflammatory cytokine production in alveolar macrophages [108] and MMPs production in synovial fibroblasts [122], which can exacerbate fibrosis. It would be worthwhile to examine the combinatorial roles of OB-CDH in myofibroblasts, macrophages, and endothelial cells, in an animal model of fibrosis.

5.5 Conclusion

TGF- β 1 is a potent chemical factor which helps wound healing by recruiting inflammatory cells and activating local fibroblasts, but it may also induce fibrotic phenotypes if the signaling pathways go awry. To understand the specific role of TGF- β 1 in inducing myofibroblast differentiation of VICs, I have examined whole-genome gene expression changes in response to TGF- β 1 at an early (8 hours) and a late (24 hours) time point. Based on the microarrays, there are distinct early and late gene expression programs activated by TGF- β 1.

Signaling pathway analysis shows that not only TGF- β 1 signaling is activated, but pathways related to TNF α and p53 are also activated, suggesting additional signaling cascades in mediating myofibroblast activation. Further, gene function analysis based on differentially regulated genes reveals cell-cell contact as a downstream target of TGF- β 1, and it is confirmed that both OB-CDH and NCDH have increased mRNA levels with TGF- β 1 treatment. Using gene knockdown and overexpression, I find that OB-CDH inhibits valvular myofibroblast differentiation. These results suggest that TGF- β 1 is up-regulating cadherins to modulate myofibroblast differentiation and functions. Novel targets of TGF- β 1 signaling discovered in microarrays warrant further study. It is also meaningful to construct a systematic map as to how TGF- β 1, which not only elicits its canonical Smad2/3 pathway, but also induces other genes (e.g., cadherins, collagens, TUFT1) and interacts with other signaling pathways (e.g., TNF α and p53) to coordinately regulate myofibroblast differentiation, survival and apoptosis, which are important parameters in determining tissue repair and fibrosis.

CHAPTER VI

CONCLUSIONS AND RECOMMENDATIONS

6.1 Summary

Aortic valves guide the directional flow of oxygenated blood from the left ventricle to the aorta and then to different tissues in the human body. They are an integral part of cardiac structure and function. If the normally compliant leaflets stiffen and calcify, the orifice of the valve opening becomes smaller and the leaflets cannot close completely, which negatively affects blood flow through the valves and may cause backflow. The structure of the valves is largely maintained by valvular interstitial cells (VICs), as they secrete ECM proteins and ECM remodeling enzymes. VICs are quiescent fibroblasts in normal valves, but have been shown to become activated to myofibroblasts and osteoblast-like cells in aortic sclerosis and stenosis. Persistence of myofibroblasts can lead to fibrosis and tissue stiffening with excessive collagen deposition and abnormal tissue contraction. As there have been few effective treatments for aortic stenosis besides valve replacement so far, understanding molecular mechanisms that regulate pathogenic VIC phenotypes, which are a major determinant of healthy vs. diseased valves, may facilitate new therapeutic design.

Cell fate is shaped by both intrinsic and extrinsic factors. The surrounding microenvironment of cells is defined as a niche. The physical, chemical and biological factors of the niche can direct cells with the same genetic background into different types during development. When we isolate primary cells, such as VICs, to study their functions, it is often

necessary to provide these cells with a nature-mimicking matrix to preserve their native properties. However, tissue culture polystyrene (TCPS) spontaneously promotes valvular myofibroblast activation when they are isolated from valves and cultured. In this thesis, poly(ethylene glycol) (PEG) based hydrogels were explored and shown to be a better substrate for culturing VICs without activating their pathogenic phenotypes. I have shown regulation of VICs by the physical cue of elasticity, the chemical factor of TGF- β 1, and the biological interactions through cadherins at the mechanistic level.

First, I characterized the heterogeneity of VICs based on lineage-specific cell surface markers by flow cytometry and found that these cells were relatively homogeneous with small fractions expressing stem cell markers (Chapter II). This validated our use of the total population of freshly isolated VICs since the majority of them are fibroblasts. To understand how matrix properties regulate VIC phenotypes, I compared culturing P0 VICs on TCPS and PEG hydrogels and found that these cells were more activated to myofibroblasts on TCPS (Chapter III). This activation was mediated through an elasticity-regulated PI3K/AKT pathway, which was inhibited with substrate modulus reduction in a time-dependent manner (Chapter III). In addition, reducing substrate modulus redirected activated valvular myofibroblasts into dormant fibroblasts with the potential to proliferate and to differentiate again and this process was not associated with significant apoptosis (Chapter IV). Finally, whole-genome gene expression of VICs in response to TGF- β 1, a potent cytokine that induces myofibroblast differentiation, was examined longitudinally with time (Chapter V). TGF- β 1 elicited different gene programs after 8 hours and 24 hours of treatment in VICs and specifically activated expression of OB-CDH as a downstream effector to regulate the cell fate of VICs (Chapter V). As outlined in Figure 1.5 of the

introduction (Chapter I), this thesis has examined the effects of different types of extracellular cues on valvular myofibroblast differentiation; meanwhile, the data point to interesting future directions to explore, not only how each individual cue works, but also how cells process all these signals in a quantitative and temporal manner to output a specific fate/phenotype.

6.2 Future Directions

6.2.1 As an Important Cellular Determinant of Valvular Diseases, What Are VICs Really?

Despite that the sorted ABCG2⁺ VICs did not show the anticipated stem cell properties (Chapter II), I think that the cellular composition of VICs and which subpopulation(s) contributes to valvular complications is worth further investigation. In Chapter II, VICs are characterized based on the expression of a number of cell surface markers by flow cytometry (Table 2.1 in Chapter II). A more comprehensive list of cell surface markers should be employed to describe VICs further. But, importantly, with these cell surface markers, different subpopulations of VICs can be isolated in a targeted way to help reveal different functions of the subpopulations *in vitro*. For example, ~5% of endogenous VICs express OB-CDH (Table 2.1 in Chapter II). Given the roles of this protein in valvular myofibroblast differentiation (Chapter V), it would be interesting to sort the OB-CDH⁺ and the OB-CDH⁻ VICs and examine their myofibroblast characteristics, including fibrogenic gene expression and α SMA stress fiber organization. Meanwhile, the culturing environment (e.g., substrate, media) should be optimized to preserve the native properties of the sorted cells. For example, sorted ABCG2⁺ VICs can be cultured on soft PEG hydrogels, instead of TCPS, for studying their functions. Complementary with the *in vitro* study, lineage-tracing analysis *in vivo* can serve as a powerful tool to examine

whether specific subpopulations of VICs contribute during the development of valve sclerosis and stenosis. Using lineage tracing, it has been shown that myofibroblasts are derived from ADAM12⁺ perivascular cells upon acute tissue injury in the muscle and dermis [241]. In addition, the ABCG2 expressing cells have been traced and shown to play a role during skeletal muscle regeneration [178]. It would be interesting to trace the fate of the ABCG2⁺ VICs during valve development and disease progression.

6.2.2 Multi-factorial Interactions of Extracellular Cues (Matrix Elasticity, TGFβ1, Cadherins, Binding Epitopes, etc.): the More the Merrier?

As mentioned throughout this thesis, cells reside in a complex microenvironment with physical, chemical and biological cues. It is important to understand the functions of individual cues in an isolated way since that is how we can elucidate their distinct functions. However, it is also critical to start looking at their interplay. In Chapter IV, I have shown that, when VICs were treated with TGF-β1 on soft substrates, there was activation of Col1, FN1 and CTGF at the mRNA level, but no formation of αSMA stress fibers in the cells. This indicates that matrix elasticity is necessary for the cytoskeleton change in myofibroblasts, independent of TGF-β1. However, the interaction between elasticity and TGF-β1 seems to be more complicated and interesting when I observed that VICs cultured on soft gels had higher fold change of the fibrogenic genes than those cultured on stiff gels in response to TGF-β1 (Figure 6.1). It would be worthwhile to look at the intersection of signaling between elasticity and TGF-β1. This line of inquiry could also be expanded to include the interaction of other forms of physical cues (e.g., mechanical stretching, fluid shear stress) and other chemical factors (e.g., TNFα, FGF2) in the cells. As elasticity has been shown to regulate the activity of the PI3K/AKT pathway (Chapter

III), it would be interesting to examine whether PI3K is the nodal point of regulation for different types of signals, or whether additional signaling pathways are involved.

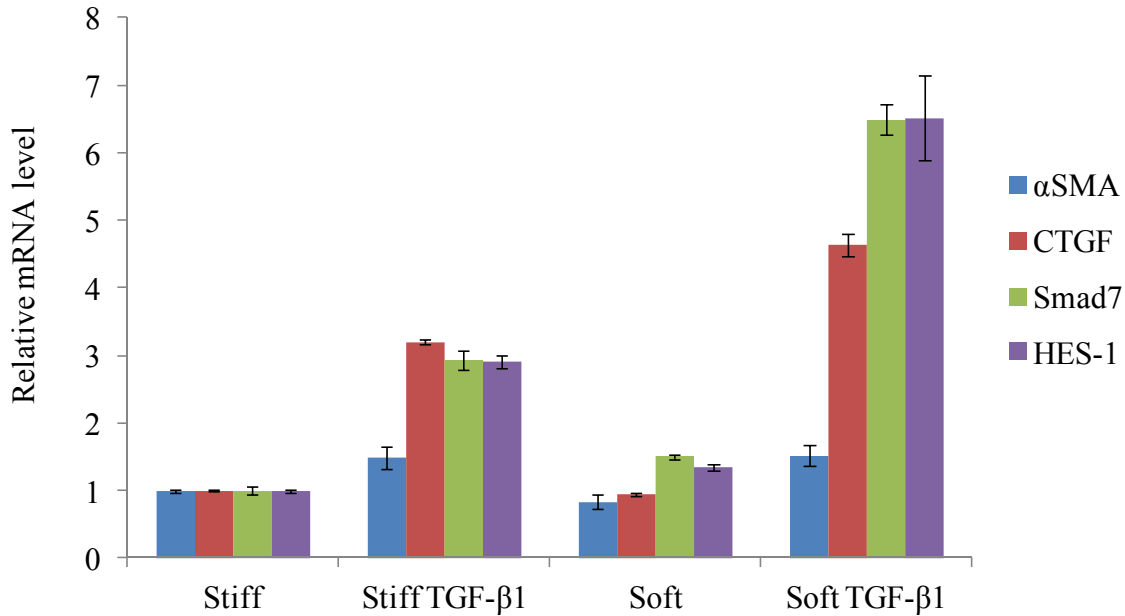


Figure 6.1 Gene Expression of VICs in Response to TGF- β 1 when Cultured on Stiff or Soft Hydrogels. P3 VICs cultured on stiff or soft gels were treated with TGF- β 1 at 5ng/ml for 40 hours and total RNA was collected on day 5 after seeding. TGF- β 1 responsive genes, including α SMA, CTGF, Smad7 and HES-1, were up-regulated with a higher fold change for VICs cultured on soft gels than those cultured on stiff gels. This experiment was carried out once. Error bars: standard deviation.

Cell-cell contacts also play important roles in regulating cellular functions. In Chapter V, I show that OB-CDH can negatively affect myofibroblast differentiation. It will be interesting to see if we can utilize this outside-in signaling to modulate VIC phenotypes. For example, the culture surfaces can be coated with a cadherin-Fc antibody, which contains the cadherin extracellular calcium-binding domains and a Fc fragment of the antibody, to mimic cadherin

engagement in between cells and regulate cellular functions. If this strategy works, the cadherin Fc antibodies or cadherin-derived peptides can be incorporated into the PEG hydrogels to direct cell fate or create a tissue-mimicking niche for the cells. In addition, I have observed that OB-CDH mRNA level is higher for VICs cultured on stiff-to-soft gels than on stiff gels (Figure 6.2). It is reasonable to hypothesize that cadherin is regulated by matrix elasticity and cell-matrix interaction, pointing to a new interesting direction related to how cell-matrix and cell-cell interactions crosstalk. Finally, cell-cell interactions are not just confined to VIC-to-VIC contacts. Valves are also enclosed by an endothelium, and it would be interesting to examine the interplay between the endothelial cells and the VICs.

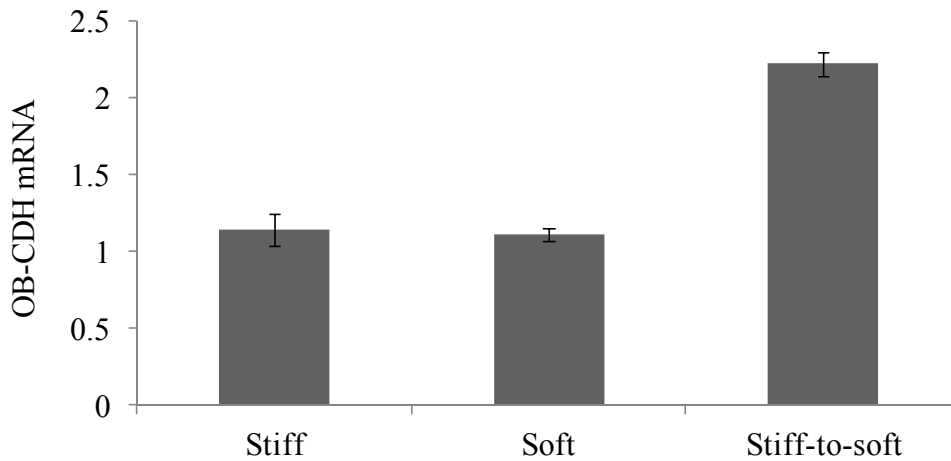


Figure 6.2 OB-CDH mRNA Levels for VICs Cultured on Different Substrates. VICs were cultured on stiff, soft or stiff-to-soft gels for 5 days before RNA isolation. mRNA level of OB-CDH was quantified by RT-PCR. There was a trend that OB-CDH was increased in VICs cultured on stiff-to-soft gels than those cultured on stiff or soft gels. Error bars: standard deviation.

Cells sense the physical properties of the matrix through binding to certain adhesive sequences in the matrix. Trappmann *et al.* have shown that cells sense the matrix based on how collagen is anchored to a surface [242]. This indicates that surface binding epitopes may modulate cellular response to substrate stiffness. Previous work in the lab has shown that different ECM proteins coated on TCPS regulate VIC phenotypes and ECM mimetic peptides can regulate myofibroblast activation and matrix production of VICs when cultured on different substrate stiffnesses [243, 244]. Utilizing the PEG hydrogel platform, further questions can be asked about how cells sense physical cues through binding epitopes on scaffolds and how the chemical sequences of matrices interact with physical elasticity in regulating cellular phenotypes.

6.2.3 The Microarrays: from the Finish Line to A New Starting Line

In Chapter III and Chapter V of this thesis, I have utilized porcine genome microarrays to examine the gene expression of P0 VICs before and after culturing on TCPS and P2 VICs in response to TGF- β 1 over time. These microarray data can be analyzed more deeply in the following aspects to reveal a systematic picture on the complex biological processes. First, IPA analysis has been employed for the microarrays in Chapter V and helped discover TNF α and p53 as novel pathways differentially regulated by TGF- β 1 treatment (Figure 5.4). Similar methods can be utilized to analyze the activated or inhibited signaling pathways between P0 and plated VICs in Chapter III. Second, myofibroblast differentiation from fibroblasts in other tissues, such as lung and cornea, has been studied by microarrays. It would be interesting to compare our microarray data with those data sets to extract common and distinct regulatory mechanisms for different fibroblasts. Last but not least, microarrays for VICs cultured on different elasticities or in a 3D hydrogel environment can be examined. As microRNAs are implicated in mediating

fibrosis progression [245], it will be complementary to use high throughput sequencing to look at microRNA expression changes with different elasticities. More bioinformatic analysis can be carried out to find the correlation between miRNA levels and mRNA expression based on microarrays. This approach should reveal more molecular mechanisms to investigate and validate through experiments and help improve our understanding of matrix elasticity-regulated myofibroblast differentiation systematically.

One last recommendation for the future is to prove that matrix physical cues do matter *in vivo*. Despite the finding that fibrotic regions of the lung have higher Young's modulus than the healthy regions [105], it is still not clear whether increasing stiffness in the microenvironment is a trigger for fibrosis *in vivo*. More experiments need to be performed to link the relevance of matrix elasticity to the pathology associated with tissue stiffening and fibrosis. The joy of doing science is about endless seeking. Hopefully, some readers of this thesis become interested in participating in research to understand how extracellular cues regulate VIC phenotypes, which may one day contribute to the understanding and the cure of valvular diseases.

BIBLIOGRAPHY

1. Balachandran, K., P. Sucusky, and A.P. Yoganathan, *Hemodynamics and Mechanobiology of Aortic Valve Inflammation and Calcification*. International Journal of Inflammation, 2011. **2011**: p. 15 pages.
2. Mohler III, E.R., *Mechanisms of aortic valve calcification*. The American Journal of Cardiology, 2004. **94**(11): p. 1396-1402.
3. Hinton, R. and K.E. Yutzey, *Heart valve structure and function in development and disease*. Annu Rev Physiol., 2011. **73**: p. 29-46.
4. Roberts, W.C. and J.M. Ko, *Frequency by Decades of Unicuspid, Bicuspid, and Tricuspid Aortic Valves in Adults Having Isolated Aortic Valve Replacement for Aortic Stenosis, With or Without Associated Aortic Regurgitation*. Circulation, 2005. **111**(7): p. 920-925.
5. McKellar, S.H., et al., *Novel NOTCH1 mutations in patients with bicuspid aortic valve disease and thoracic aortic aneurysms*. J Thorac Cardiovasc Surg, 2007. **134**(2): p. 290-296.
6. Rajamannan, N.M., et al., *Calcific Aortic Valve Disease: Not Simply a Degenerative Process*. Circulation, 2011. **124**(16): p. 1783-1791.
7. Mohler, E.R., et al., *Bone Formation and Inflammation in Cardiac Valves*. Circulation, 2001. **103**(11): p. 1522-1528.
8. Poggianti, E., et al., *Aortic valve sclerosis is associated with systemic endothelial dysfunction*. Journal of the American College of Cardiology, 2003. **41**(1): p. 136-141.
9. Otto, C.M., et al., *Association of Aortic-Valve Sclerosis with Cardiovascular Mortality and Morbidity in the Elderly*. New England Journal of Medicine, 1999. **341**(3): p. 142-147.
10. Roger, V.L., et al., *Heart Disease and Stroke Statistics-2011 Update: A Report from the American Heart Association*. Circulation, 2011. **123**(4): p. e18-e209.
11. Rabkin-Aikawa E, F.M., Aikawa M, Schoen FJ., *Dynamic and Reversible Changes of Interstitial Cell Phenotype During Remodeling of Cardiac Valves*. J Heart Valve Dis., 2004. **13**: p. 841-847.
12. Liu, A.C., V.R. Joag, and A.I. Gotlieb, *The Emerging Role of Valve Interstitial Cell*

- Phenotypes in Regulating Heart Valve Pathobiology*. Am J Pathol., 2007. **171**(5): p. 1407-1418.
13. Aikawa, E., et al., *Human Semilunar Cardiac Valve Remodeling by Activated Cells From Fetus to Adult*. Circulation, 2006. **113**(10): p. 1344-1352.
 14. Kaden, J.J., et al., *Inflammatory regulation of extracellular matrix remodeling in calcific aortic valve stenosis*. Cardiovasc Pathol. , 2005. **14**(2): p. 80-7.
 15. Edep, M.E., et al., *Matrix Metalloproteinase Expression in Nonrheumatic Aortic Stenosis*. Cardiovascular Pathology, 2000. **9**(5): p. 281-286.
 16. Pho, M., et al., *Cofilin is a marker of myofibroblast differentiation in cells from porcine aortic cardiac valves*. American Journal of Physiology - Heart and Circulatory Physiology, 2008. **294**(4): p. H1767-H1778.
 17. Yip, C.Y.Y., et al., *Calcification by Valve Interstitial Cells Is Regulated by the Stiffness of the Extracellular Matrix*. Arteriosclerosis, Thrombosis, and Vascular Biology, 2009. **29**(6): p. 936-942.
 18. Chen, J.-H. and C.A. Simmons, *Cell-Matrix Interactions in the Pathobiology of Calcific Aortic Valve Disease: Critical Roles for Matricellular, Matricrine, and Matrix Mechanics Cues*. Circulation Research, 2011. **108**(12): p. 1510-1524.
 19. Chen, J.-H., et al., *β -Catenin Mediates Mechanically Regulated, Transforming Growth Factor- β 1 induced Myofibroblast Differentiation of Aortic Valve Interstitial Cells*. Arteriosclerosis, Thrombosis, and Vascular Biology, 2011. **31**(3): p. 590-597.
 20. Drury, J.L. and D.J. Mooney, *Hydrogels for tissue engineering: scaffold design variables and applications*. Biomaterials, 2003. **24**(24): p. 4337-4351.
 21. Peppas, N.A., et al., *Hydrogels in Biology and Medicine: From Molecular Principles to Bionanotechnology*. Advanced Materials, 2006. **18**(11): p. 1345-1360.
 22. Zhu, J., *Bioactive modification of poly(ethylene glycol) hydrogels for tissue engineering*. Biomaterials, 2010. **31**(17): p. 4639-4656.
 23. Deforest, C.A. and K.S. Anseth, *Advances in bioactive hydrogels to probe and direct cell fate*. Annual review of chemical and biomolecular engineering, 2012. **3**(1): p. 421-444.
 24. Engler, A.J., et al., *Matrix Elasticity Directs Stem Cell Lineage Specification*. Cell, 2006. **126**(4): p. 677-689.

25. Gilbert, P.M., et al., *Substrate Elasticity Regulates Skeletal Muscle Stem Cell Self-Renewal in Culture*. Science, 2010. **329**(5995): p. 1078-1081.
26. Kloxin, A.M., et al., *Photodegradable Hydrogels for Dynamic Tuning of Physical and Chemical Properties*. Science, 2009. **324**(5923): p. 59-63.
27. Anderson, R.H., et al., *Development of the heart: (2) Septation of the atriums and ventricles*. Heart, 2003. **89**(8): p. 949-958.
28. Armstrong, E.J. and J. Bischoff, *Heart Valve Development: Endothelial Cell Signaling and Differentiation*. Circulation Research, 2004. **95**(5): p. 459-470.
29. Combs, M.D. and K.E. Yutzey, *Heart Valve Development: Regulatory Networks in Development and Disease*. Circulation Research, 2009. **105**(5): p. 408-421.
30. Ma, L., et al., *Bmp2 is essential for cardiac cushion epithelial-mesenchymal transition and myocardial patterning*. Development, 2005. **132**(24): p. 5601-5611.
31. Rivera-Feliciano, J. and C.J. Tabin, *Bmp2 instructs cardiac progenitors to form the heart-valve-inducing field*. Developmental Biology, 2006. **295**(2): p. 580-588.
32. Brown, C.B., et al., *Antibodies to the Type II TGFbeta Receptor Block Cell Activation and Migration during Atrioventricular Cushion Transformation in the Heart*. Developmental Biology, 1996. **174**(2): p. 248-257.
33. Timmerman, L.A., et al., *Notch promotes epithelial-mesenchymal transition during cardiac development and oncogenic transformation*. Genes & Development, 2004. **18**(1): p. 99-115.
34. Camenisch, T.D., et al., *Disruption of hyaluronan synthase-2 abrogates normal cardiac morphogenesis and hyaluronan-mediated transformation of epithelium to mesenchyme*. The Journal of Clinical Investigation, 2000. **106**(3): p. 349-360.
35. Henderson, D.J. and A.J. Copp, *Versican Expression Is Associated With Chamber Specification, Septation, and Valvulogenesis in the Developing Mouse Heart*. Circulation Research, 1998. **83**(5): p. 523-532.
36. Lincoln, J., C.M. Alfieri, and K.E. Yutzey, *BMP and FGF regulatory pathways control cell lineage diversification of heart valve precursor cells*. Developmental Biology, 2006. **292**(2): p. 290-302.
37. Abdelwahid, E., L.J. Pelliniemi, and E. Jokinen, *Cell death and differentiation in the development of the endocardial cushion of the embryonic heart*. Microscopy Research

- and Technique, 2002. **58**(5): p. 395-403.
38. Keyes, W.M. and E.J. Sanders, *Regulation of apoptosis in the endocardial cushions of the developing chick heart*. American Journal of Physiology - Cell Physiology, 2002. **282**(6): p. C1348-C1360.
 39. Martin, R.T. and T. Bartman, *Analysis of heart valve development in larval zebrafish*. Developmental Dynamics, 2009. **238**(7): p. 1796-1802.
 40. Sacks, M.S. and A.P. Yoganathan, *Heart valve function: a biomechanical perspective*. Philosophical Transactions of the Royal Society B: Biological Sciences, 2007. **362**(1484): p. 1369-1391.
 41. Yap, C., N. Saikrishnan, and A. Yoganathan, *Experimental measurement of dynamic fluid shear stress on the ventricular surface of the aortic valve leaflet*. Biomech Model Mechanobiol., 2012. **11**(1-2): p. 231-44.
 42. Yap, C.H., et al., *Dynamic deformation characteristics of porcine aortic valve leaflet under normal and hypertensive conditions*. American Journal of Physiology - Heart and Circulatory Physiology, 2010. **298**(2): p. H395-H405.
 43. Hara, H., Pedersen, W. R., Ladich, E., Mooney, M., Virmani, R., Nakamura, M., Feldman, T., Schwartz, R.S., *Percutaneous Balloon Aortic Valvuloplasty Revisited: Time for a Renaissance?* Circulation 2007. **115**(12): p. e334-338.
 44. Pohle, K., et al., *Progression of Aortic Valve Calcification: Association With Coronary Atherosclerosis and Cardiovascular Risk Factors*. Circulation, 2001. **104**(16): p. 1927-1932.
 45. Cowell, S.J., et al., *A Randomized Trial of Intensive Lipid-Lowering Therapy in Calcific Aortic Stenosis*. New England Journal of Medicine, 2005. **352**(23): p. 2389-2397.
 46. Rajamannan, N.M., et al., *Human Aortic Valve Calcification Is Associated With an Osteoblast Phenotype*. Circulation, 2003. **107**(17): p. 2181-2184.
 47. Miller, J.D., R.M. Weiss, and D.D. Heistad, *Calcific Aortic Valve Stenosis: Methods, Models, and Mechanisms*. Circulation Research, 2011. **108**(11): p. 1392-1412.
 48. Yu, Z., et al., *Tumor Necrosis Factor-alpha Accelerates the Calcification of Human Aortic Valve Interstitial Cells Obtained from Patients with Calcific Aortic Valve Stenosis via the BMP2-Dlx5 Pathway*. Journal of Pharmacology and Experimental Therapeutics, 2011. **337**(1): p. 16-23.

49. Chen, J.-H., et al., *Identification and Characterization of Aortic Valve Mesenchymal Progenitor Cells with Robust Osteogenic Calcification Potential*. The American Journal of Pathology, 2009. **174**(3): p. 1109-1119.
50. Miller, J.D., et al., *Evidence for Active Regulation of Pro-Osteogenic Signaling in Advanced Aortic Valve Disease*. Arteriosclerosis, Thrombosis, and Vascular Biology, 2010. **30**(12): p. 2482-2486.
51. Angel, P.M., et al., *Networked-based Characterization of Extracellular Matrix Proteins from Adult Mouse Pulmonary and Aortic Valves*. Journal of Proteome Research, 2011. **10**(2): p. 812-823.
52. Shah, D.N., S.M. Recktenwall-Work, and K.S. Anseth, *The effect of bioactive hydrogels on the secretion of extracellular matrix molecules by valvular interstitial cells*. Biomaterials, 2008. **29**(13): p. 2060-2072.
53. Soini, Y., et al., *Expression of MMP2, MMP9, MT1-MMP, TIMP1, and TIMP2 mRNA in valvular lesions of the heart*. The Journal of Pathology, 2001. **194**(2): p. 225-231.
54. Dreger, S.A., et al., *Profile and localization of matrix metalloproteinases (MMPs) and their tissue inhibitors (TIMPs) in human heart valves*. Journal of Heart Valve Disease, 2002. **11**(6): p. 875-880.
55. Rabkin, E., et al., *Activated Interstitial Myofibroblasts Express Catabolic Enzymes and Mediate Matrix Remodeling in Myxomatous Heart Valves*. Circulation, 2001. **104**(21): p. 2525-2532.
56. Mahler, G.J. and J.T. Butcher, *Inflammatory Regulation of Valvular Remodeling: The Good(?), the Bad, and the Ugly*. International Journal of Inflammation, 2011. **2011**: p. 13 pages.
57. Hinz, B., *The myofibroblast: Paradigm for a mechanically active cell*. Journal of Biomechanics, 2010. **43**(1): p. 146-155.
58. Tomasek, J.J., et al., *Myofibroblasts and mechano-regulation of connective tissue remodelling*. Nat Rev Mol Cell Biol, 2002. **3**(5): p. 349-363.
59. Henderson, N.C. and J.P. Iredale, *Liver fibrosis: cellular mechanisms of progression and resolution*. Clinical Science, 2007. **112**(5): p. 265-280.
60. King, T.E., A. Pardo, and M. Selman, *Idiopathic pulmonary fibrosis*. The Lancet, 2011. **378**(9807): p. 1949-1961.

61. Liu, Y., *Cellular and molecular mechanisms of renal fibrosis*. Nat Rev Nephrol, 2011. **7**(12): p. 684-696.
62. Santiago, J.-J., et al., *Cardiac fibroblast to myofibroblast differentiation in vivo and in vitro: Expression of focal adhesion components in neonatal and adult rat ventricular myofibroblasts*. Developmental Dynamics, 2010. **239**(6): p. 1573-1584.
63. Gooch, J.L., et al., *Involvement of Calcineurin in Transforming Growth Factor-beta-mediated Regulation of Extracellular Matrix Accumulation*. Journal of Biological Chemistry, 2004. **279**(15): p. 15561-15570.
64. Kagami, S., et al., *Angiotensin II stimulates extracellular matrix protein synthesis through induction of transforming growth factor-beta expression in rat glomerular mesangial cells*. The Journal of Clinical Investigation, 1994. **93**(6): p. 2431-2437.
65. Hinz, B., *Formation and Function of the Myofibroblast during Tissue Repair*. J Invest Dermatol, 2007. **127**(3): p. 526-537.
66. Barnes, J.L. and Y. Gorin, *Myofibroblast differentiation during fibrosis: role of NAD(P)H oxidases*. Kidney Int, 2011. **79**(9): p. 944-956.
67. Desmoulière, A., et al., *Apoptosis mediates the decrease in cellularity during the transition between granulation tissue and scar*. Am J Pathol., 1995. **146**(1): p. 56-66.
68. Grinnell, F., et al., *Release of Mechanical Tension Triggers Apoptosis of Human Fibroblasts in a Model of Regressing Granulation Tissue*. Experimental Cell Research, 1999. **248**(2): p. 608-619.
69. Alexopoulos, A., et al., *Bone regulatory factors NFATc1 and Osterix in human calcific aortic valves*. International Journal of Cardiology, 2010. **139**(2): p. 142-149.
70. Rajamannan, N.M., et al., *Atorvastatin Inhibits Hypercholesterolemia-Induced Cellular Proliferation and Bone Matrix Production in the Rabbit Aortic Valve*. Circulation, 2002. **105**(22): p. 2660-2665.
71. Rattazzi, M., et al., *Clones of Interstitial Cells From Bovine Aortic Valve Exhibit Different Calcifying Potential When Exposed to Endotoxin and Phosphate*. Arteriosclerosis, Thrombosis, and Vascular Biology, 2008. **28**(12): p. 2165-2172.
72. Alfieri, C.M., et al., *Wnt signaling in heart valve development and osteogenic gene induction*. Developmental Biology, 2009. **338**(2): p. 127-135.
73. Latif, N., et al., *Human Valve Interstitial Cells Demonstrate Transdifferentiation*

- Potential*. QScience Proceedings, 2012. **2012**(Heart valve biology and tissue engineering): p. 18.
74. Yang, X., et al., *Pro-Osteogenic Phenotype of Human Aortic Valve Interstitial Cells Is Associated With Higher Levels of Toll-Like Receptors 2 and 4 and Enhanced Expression of Bone Morphogenetic Protein 2*. Journal of the American College of Cardiology, 2009. **53**(6): p. 491-500.
 75. Yip, C.Y.Y., et al., *Inhibition of Pathological Differentiation of Valvular Interstitial Cells by C-Type Natriuretic Peptide*. Arteriosclerosis, Thrombosis, and Vascular Biology, 2011. **31**(8): p. 1881-1889.
 76. Monzack, E.L. and K.S. Masters, *Can valvular interstitial cells become true osteoblasts? A side-by-side comparison*. J Heart Valve Dis., 2011. **20**(4): p. 449-463.
 77. Benton, J.A., et al., *Statins Block Calcific Nodule Formation of Valvular Interstitial Cells by Inhibiting alpha-Smooth Muscle Actin Expression*. Arteriosclerosis, Thrombosis, and Vascular Biology, 2009. **29**(11): p. 1950-1957.
 78. Latif, N., et al., *Characterization of Structural and Signaling Molecules by Human Valve Interstitial Cells and Comparison to Human Mesenchymal Stem Cells*. J Heart Valve Dis., 2007. **16**: p. 56-66.
 79. Jian, B., et al., *Progression of aortic valve stenosis: TGF- β 1 is present in calcified aortic valve cusps and promotes aortic valve interstitial cell calcification via apoptosis*. Ann Thorac Surg, 2003. **75**(2): p. 457-465.
 80. Kaden, J.J., et al., *Interleukin-1 beta promotes matrix metalloproteinase expression and cell proliferation in calcific aortic valve stenosis*. Atherosclerosis, 2003. **170**(2): p. 205-11.
 81. Walker, G.A., et al., *Valvular Myofibroblast Activation by Transforming Growth Factor-beta1*. Circulation Research, 2004. **95**(3): p. 253-260.
 82. Gressner, A.M. and R. Weiskirchen, *Modern pathogenetic concepts of liver fibrosis suggest stellate cells and TGF- β as major players and therapeutic targets*. Journal of Cellular and Molecular Medicine, 2006. **10**(1): p. 76-99.
 83. Murray, L.A., et al., *TGF-beta driven lung fibrosis is macrophage dependent and blocked by Serum amyloid P*. The International Journal of Biochemistry & Cell Biology, 2011. **43**(1): p. 154-162.
 84. Leask, A. and D.J. Abraham, *TGF-beta signaling and the fibrotic response*. The FASEB

- Journal, 2004. **18**(7): p. 816-827.
85. Goumenos, D.S., et al., *Transforming Growth Factor-beta1 and Myofibroblasts: A Potential Pathway towards Renal Scarring in Human Glomerular Disease*. *Nephron*, 2001. **87**(3): p. 240-248.
 86. Igarashi, A., et al., *Regulation of connective tissue growth factor gene expression in human skin fibroblasts and during wound repair*. *Molecular Biology of the Cell*, 1993. **4**(6): p. 637-45.
 87. Gu, L., et al., *Effect of TGF-[beta]/Smad signaling pathway on lung myofibroblast differentiation*. *Acta Pharmacol Sin*, 2007. **28**(3): p. 382-391.
 88. Meyer-ter-Vehn, T., et al., *p38 Inhibitors Prevent TGF-beta-induced Myofibroblast Transdifferentiation in Human Tenon Fibroblasts*. *Investigative Ophthalmology & Visual Science*, 2006. **47**(4): p. 1500-1509.
 89. Garrett, Q., et al., *Involvement of CTGF in TGF-beta1-Stimulation of Myofibroblast Differentiation and Collagen Matrix Contraction in the Presence of Mechanical Stress*. *Investigative Ophthalmology & Visual Science*, 2004. **45**(4): p. 1109-1116.
 90. Desmoulière, A., et al., *Transforming growth factor-beta 1 induces alpha-smooth muscle actin expression in granulation tissue myofibroblasts and in quiescent and growing cultured fibroblasts*. *The Journal of Cell Biology*, 1993. **122**(1): p. 103-111.
 91. Furukawa, F., et al., *p38 MAPK mediates fibrogenic signal through smad3 phosphorylation in rat myofibroblasts*. *Hepatology*, 2003. **38**(4): p. 879-889.
 92. Horowitz, J.C., et al., *Combinatorial activation of FAK and AKT by transforming growth factor-beta1 confers an anoikis-resistant phenotype to myofibroblasts*. *Cellular Signalling*, 2007. **19**(4): p. 761-771.
 93. Kulkarni, A.A., et al., *PPAR-gamma Ligands Repress TGFbeta-Induced Myofibroblast Differentiation by Targeting the PI3K/Akt Pathway: Implications for Therapy of Fibrosis*. *PLoS ONE*, 2011. **6**(1): p. e15909.
 94. Akhmetshina, A., et al., *Activation of canonical Wnt signalling is required for TGF-beta-mediated fibrosis*. *Nat Commun*, 2012. **3**: p. 735.
 95. Shi-Wen, X., et al., *Endothelin-1 Promotes Myofibroblast Induction through the ETA Receptor via a rac/Phosphoinositide 3-Kinase/Akt-dependent Pathway and Is Essential for the Enhanced Contractile Phenotype of Fibrotic Fibroblasts*. *Molecular Biology of the Cell*, 2004. **15**(6): p. 2707-2719.

96. Vyavahare, N., et al., *Prevention of Bioprosthetic Heart Valve Calcification by Ethanol Preincubation*. *Circulation*, 1997. **95**(2): p. 479-488.
97. Miller, J.D., et al., *Lowering Plasma Cholesterol Levels Halts Progression of Aortic Valve Disease in Mice*. *Circulation*, 2009. **119**(20): p. 2693-2701.
98. Liberman, M., et al., *Oxidant Generation Predominates Around Calcifying Foci and Enhances Progression of Aortic Valve Calcification*. *Arteriosclerosis, Thrombosis, and Vascular Biology*, 2008. **28**(3): p. 463-470.
99. Miller, J.D., et al., *Dysregulation of Antioxidant Mechanisms Contributes to Increased Oxidative Stress in Calcific Aortic Valvular Stenosis in Humans*. *Journal of the American College of Cardiology*, 2008. **52**(10): p. 843-850.
100. Cushing, M.C., et al., *Fibroblast growth factor represses Smad-mediated myofibroblast activation in aortic valvular interstitial cells*. *The FASEB Journal*, 2008. **22**(6): p. 1769-1777.
101. Thayer, P., et al., *The Effects of Combined Cyclic Stretch and Pressure on the Aortic Valve Interstitial Cell Phenotype*. *Annals of Biomedical Engineering*, 2011. **39**(6): p. 1654-1667.
102. Ku, C.-H., et al., *Collagen synthesis by mesenchymal stem cells and aortic valve interstitial cells in response to mechanical stretch*. *Cardiovascular Research*, 2006. **71**(3): p. 548-556.
103. Gould, R.A., et al., *Cyclic strain anisotropy regulates valvular interstitial cell phenotype and tissue remodeling in three-dimensional culture*. *Acta Biomaterialia*, 2012. **8**(5): p. 1710-1719.
104. Olsen, A.L., et al., *Hepatic stellate cells require a stiff environment for myofibroblastic differentiation*. *American Journal of Physiology - Gastrointestinal and Liver Physiology*, 2011. **301**(1): p. G110-G118.
105. Liu, F., et al., *Feedback amplification of fibrosis through matrix stiffening and COX-2 suppression*. *The Journal of Cell Biology*, 2010. **190**(4): p. 693-706.
106. Kloxin, A.M., J.A. Benton, and K.S. Anseth, *In situ elasticity modulation with dynamic substrates to direct cell phenotype*. *Biomaterials*, 2010. **31**(1): p. 1-8.
107. Wang, H.-B., M. Dembo, and Y.-L. Wang, *Substrate flexibility regulates growth and apoptosis of normal but not transformed cells*. *American Journal of Physiology - Cell*

- Physiology, 2000. **279**(5): p. C1345-C1350.
108. Zhang, Y.-H., et al., *Substrate stiffness regulates apoptosis and the mRNA expression of extracellular matrix regulatory genes in the rat annular cells*. Matrix Biology, 2011. **30**(2): p. 135-144.
 109. Wang, H., et al., *Redirecting Valvular Myofibroblasts into Dormant Fibroblasts through Light-mediated Reduction in Substrate Modulus*. PLoS ONE, 2012. **7**(7): p. e39969.
 110. Balestrini, J.L., et al., *The mechanical memory of lung myofibroblasts*. Integrative Biology, 2012. **4**(4): p. 410-421.
 111. Wells, R.G., *The Role of Matrix Stiffness in Hepatic Stellate Cell Activation and Liver Fibrosis*. Journal of Clinical Gastroenterology, 2005. **39**(4): p. S158-S161.
 112. Dupont, S., et al., *Role of YAP/TAZ in mechanotransduction*. Nature, 2011. **474**(7350): p. 179-183.
 113. Engler, A.J., et al., *Myotubes differentiate optimally on substrates with tissue-like stiffness*. The Journal of Cell Biology, 2004. **166**(6): p. 877-887.
 114. Katsumi, A., et al., *Integrins in Mechanotransduction*. Journal of Biological Chemistry, 2004. **279**(13): p. 12001-12004.
 115. Du, J., et al., *Integrin activation and internalization on soft ECM as a mechanism of induction of stem cell differentiation by ECM elasticity*. Proceedings of the National Academy of Sciences, 2011. **108**(23): p. 9466-9471.
 116. Han, H., et al., *Elasticity-Dependent Modulation of TGF-beta Responses in Human Trabecular Meshwork Cells*. Investigative Ophthalmology & Visual Science, 2011. **52**(6): p. 2889-2896.
 117. Huang, X., et al., *Matrix Stiffness-induced Myofibroblast Differentiation Is Mediated by Intrinsic Mechanotransduction*. American Journal of Respiratory Cell and Molecular Biology, 2012. **47**(3): p. 340-348.
 118. Krepinsky, J.C., et al., *Akt Mediates Mechanical Strain-Induced Collagen Production by Mesangial Cells*. Journal of the American Society of Nephrology, 2005. **16**(6): p. 1661-1672.
 119. Masur, S.K., et al., *Myofibroblasts differentiate from fibroblasts when plated at low density*. Proc Natl Acad Sci USA, 1996. **93**(9): p. 4219-4223.

120. Hinz, B., et al., *Myofibroblast Development Is Characterized by Specific Cell-Cell Adherens Junctions*. *Molecular Biology of the Cell*, 2004. **15**(9): p. 4310-4320.
121. Pittet, P., et al., *Fibrogenic fibroblasts increase intercellular adhesion strength by reinforcing individual OB-cadherin bonds*. *Journal of Cell Science*, 2008. **121**(6): p. 877-886.
122. Lee, D.M., et al., *Cadherin-11 in Synovial Lining Formation and Pathology in Arthritis*. *Science*, 2007. **315**(5814): p. 1006-1010.
123. Valencia, X., et al., *Cadherin-11 Provides Specific Cellular Adhesion between Fibroblast-like Synoviocytes*. *The Journal of Experimental Medicine*, 2004. **200**(12): p. 1673-1679.
124. Chang, S.K., Z. Gu, and M.B. Brenner, *Fibroblast-like synoviocytes in inflammatory arthritis pathology: the emerging role of cadherin-11*. *Immunological Reviews*, 2009. **233**(1): p. 256-266.
125. Halbleib, J.M. and W.J. Nelson, *Cadherins in development: cell adhesion, sorting, and tissue morphogenesis*. *Genes & Development*, 2006. **20**(23): p. 3199-3214.
126. Hans, P.K., Birgit, Niederreiter, David, M. Lee, Esther, Jimenez-Boj, Josef, S. Smolen, Michael, B. Brenner, *Cadherin 11 promotes invasive behavior of fibroblast-like synoviocytes*. *Arthritis & Rheumatism*, 2009. **60**(5): p. 1305-1310.
127. Huang, C.-F., et al., *Cadherin-11 Increases Migration and Invasion of Prostate Cancer Cells and Enhances their Interaction with Osteoblasts*. *Cancer Research*, 2010. **70**(11): p. 4580-4589.
128. Chung, S., et al., *N-cadherin regulates mammary tumor cell migration through Akt3 suppression*. *Oncogene*, 2012.
129. Benedetto, A.D., et al., *N-cadherin and cadherin 11 modulate postnatal bone growth and osteoblast differentiation by distinct mechanisms*. *Journal of Cell Science*, 2010. **123**(15): p. 2640-2648.
130. Taipale, J. and J. Keski-Oja, *Growth factors in the extracellular matrix*. *The FASEB Journal*, 1997. **11**(1): p. 51-9.
131. Wipff, P.-J., et al., *Myofibroblast contraction activates latent TGF- beta1 from the extracellular matrix*. *J. Cell Biol.*, 2007. **179**(6): p. 1311-1323.
132. Merryman, W.D., et al., *Synergistic effects of cyclic tension and transforming growth*

- factor-beta1 on the aortic valve myofibroblast*. Cardiovascular Pathology, 2007. **16**(5): p. 268-276.
133. Hartgerink, J.D., E. Beniash, and S.I. Stupp, *Self-Assembly and Mineralization of Peptide-Amphiphile Nanofibers*. Science, 2001. **294**(5547): p. 1684-1688.
 134. Charati, M.B., et al., *Light-Sensitive Polypeptide Hydrogel and Nanorod Composites*. Small, 2010. **6**(15): p. 1608-1611.
 135. Petka, W.A., et al., *Reversible Hydrogels from Self-Assembling Artificial Proteins*. Science, 1998. **281**(5375): p. 389-392.
 136. Nuttelman, C.R., S.M. Henry, and K.S. Anseth, *Synthesis and characterization of photocrosslinkable, degradable poly(vinyl alcohol)-based tissue engineering scaffolds*. Biomaterials, 2002. **23**(17): p. 3617-3626.
 137. Bryant, S.J., et al., *Synthesis and Characterization of Photopolymerized Multifunctional Hydrogels: Water-Soluble Poly(Vinyl Alcohol) and Chondroitin Sulfate Macromers for Chondrocyte Encapsulation*. Macromolecules, 2004. **37**(18): p. 6726-6733.
 138. Martens, P.J., S.J. Bryant, and K.S. Anseth, *Tailoring the Degradation of Hydrogels Formed from Multivinyl Poly(ethylene glycol) and Poly(vinyl alcohol) Macromers for Cartilage Tissue Engineering*. Biomacromolecules, 2003. **4**(2): p. 283-292.
 139. Lutolf, M.P. and J.A. Hubbell, *Synthetic biomaterials as instructive extracellular microenvironments for morphogenesis in tissue engineering*. Nat Biotech, 2005. **23**(1): p. 47-55.
 140. Elisseeff, J., et al., *Transdermal photopolymerization for minimally invasive implantation*. Proceedings of the National Academy of Sciences, 1999. **96**(6): p. 3104-3107.
 141. Kade, M.J., D.J. Burke, and C.J. Hawker, *The power of thiol-ene chemistry*. Journal of Polymer Science Part A: Polymer Chemistry, 2010. **48**(4): p. 743-750.
 142. Metters, A. and J. Hubbell, *Network Formation and Degradation Behavior of Hydrogels Formed by Michael-Type Addition Reactions*. Biomacromolecules, 2004. **6**(1): p. 290-301.
 143. An, S.Y., et al., *Preparation of monodisperse and size-controlled poly(ethylene glycol) hydrogel nanoparticles using liposome templates*. Journal of Colloid and Interface Science, 2009. **331**(1): p. 98-103.
 144. Kloxin, A.M., M.W. Tibbitt, and K.S. Anseth, *Synthesis of photodegradable hydrogels as*

- dynamically tunable cell culture platforms*. Nat. Protocols, 2010. **5**(12): p. 1867-1887.
145. Hersel, U., C. Dahmen, and H. Kessler, *RGD modified polymers: biomaterials for stimulated cell adhesion and beyond*. Biomaterials, 2003. **24**(24): p. 4385-4415.
 146. DeLong, S.A., A.S. Gobin, and J.L. West, *Covalent immobilization of RGDS on hydrogel surfaces to direct cell alignment and migration*. Journal of Controlled Release, 2005. **109**(1-3): p. 139-148.
 147. Hern, D.L. and J.A. Hubbell, *Incorporation of adhesion peptides into nonadhesive hydrogels useful for tissue resurfacing*. Journal of Biomedical Materials Research, 1998. **39**(2): p. 266-276.
 148. He, X., J. Ma, and E. Jabbari, *Effect of Grafting RGD and BMP-2 Protein-Derived Peptides to a Hydrogel Substrate on Osteogenic Differentiation of Marrow Stromal Cells*. Langmuir, 2008. **24**(21): p. 12508-12516.
 149. Hwang, N.S., et al., *Chondrogenic Differentiation of Human Embryonic Stem Cell-Derived Cells in Arginine-Glycine-Aspartate-Modified Hydrogels*. Tissue Engineering Part A, 2006. **12**(9): p. 2695-2706.
 150. Nicodemus, G.D. and S.J. Bryant, *Cell encapsulation in Biodegradable hydrogels for tissue engineering applications*. Tissue Engineering Part B: Reviews. , 2008. **14**(2): p. 149-165.
 151. Lutolf, M.P., et al., *Synthetic matrix metalloproteinase-sensitive hydrogels for the conduction of tissue regeneration: Engineering cell-invasion characteristics*. Proceedings of the National Academy of Sciences, 2003. **100**(9): p. 5413-5418.
 152. Lin-Gibson, S., et al., *Structure-Property Relationships of Photopolymerizable Poly(ethylene glycol) Dimethacrylate Hydrogels*. Macromolecules 2005. **38**: p. 2897-2902.
 153. DeForest, C.A. and K.S. Anseth, *Photoreversible Patterning of Biomolecules within Click-Based Hydrogels*. Angewandte Chemie International Edition, 2011. **51**(8): p. 1816-1819.
 154. Kloxin, A.M., et al., *Mechanical Properties of Cellularly Responsive Hydrogels and Their Experimental Determination*. Advanced Materials, 2010. **22**(31): p. 3484-3494.
 155. Huebsch, N., et al., *Harnessing traction-mediated manipulation of the cell/matrix interface to control stem-cell fate*. Nat Mater, 2010. **9**(6): p. 518-526.

156. Cosgrove, B.D., et al., *A home away from home: Challenges and opportunities in engineering in vitro muscle satellite cell niches*. *Differentiation*, 2009. **78**(2-3): p. 185-194.
157. Bryant, S.J., J.A. Arthur, and K.S. Anseth, *Incorporation of tissue-specific molecules alters chondrocyte metabolism and gene expression in photocrosslinked hydrogels*. *Acta Biomaterialia*, 2005. **1**(2): p. 243-252.
158. Bryant, S.J., et al., *Encapsulating chondrocytes in degrading PEG hydrogels with high modulus: Engineering gel structural changes to facilitate cartilaginous tissue production*. *Biotechnology and Bioengineering*, 2004. **86**(7): p. 747-755.
159. Roberts, J.J., et al., *Incorporation of biomimetic matrix molecules in PEG hydrogels enhances matrix deposition and reduces load-induced loss of chondrocyte-secreted matrix*. *Journal of Biomedical Materials Research Part A*, 2011. **97A**(3): p. 281-291.
160. Nicodemus, G.D., S.C. Skaalure, and S.J. Bryant, *Gel structure has an impact on pericellular and extracellular matrix deposition, which subsequently alters metabolic activities in chondrocyte-laden PEG hydrogels*. *Acta Biomaterialia*, 2011. **7**(2): p. 492-504.
161. Gobin, A.S. and J.L. West, *Effects of Epidermal Growth Factor on Fibroblast Migration through Biomimetic Hydrogels*. *Biotechnology Progress*, 2003. **19**(6): p. 1781-1785.
162. Lee, S.-H., et al., *Poly(ethylene glycol) hydrogels conjugated with a collagenase-sensitive fluorogenic substrate to visualize collagenase activity during three-dimensional cell migration*. *Biomaterials*, 2007. **28**(20): p. 3163-3170.
163. Benton, J.A., B.D. Fairbanks, and K.S. Anseth, *Characterization of valvular interstitial cell function in three dimensional matrix metalloproteinase degradable PEG hydrogels*. *Biomaterials*, 2009. **30**(34): p. 6593-6603.
164. Bott, K., et al., *The effect of matrix characteristics on fibroblast proliferation in 3D gels*. *Biomaterials*, 2010. **31**(32): p. 8454-8464.
165. Hinton, R.B., et al., *Extracellular Matrix Remodeling and Organization in Developing and Diseased Aortic Valves*. *Circulation Research*, 2006. **98**(11): p. 1431-1438.
166. Veinot, J.P., et al., *CD117-positive cells and mast cells in adult human cardiac valves: observations and implications for the creation of bioengineered grafts*. *Cardiovascular Pathology*, 2006. **15**(1): p. 36-40.
167. Hajdu, Z., et al., *Recruitment of bone marrow-derived valve interstitial cells is a normal*

- homeostatic process*. Journal of Molecular and Cellular Cardiology, 2011. **51**(6): p. 955-965.
168. Deb, A., et al., *Bone marrow-derived myofibroblasts are present in adult human heart valves*. J Heart Valve Dis., 2005. **14**(5): p. 674-8.
 169. Johnson, C.M., M.N. Hanson, and S.C. Helgeson, *Porcine cardiac valvular subendothelial cells in culture: Cell isolation and growth characteristics*. Journal of Molecular and Cellular Cardiology, 1987. **19**(12): p. 1185-1193.
 170. Benoit, D.S.W., et al., *Synthesis and characterization of a fluvastatin-releasing hydrogel delivery system to modulate hMSC differentiation and function for bone regeneration*. Biomaterials, 2006. **27**(36): p. 6102-6110.
 171. Cho, I.J., et al., *E-cadherin antagonizes transforming growth factor β 1 gene induction in hepatic stellate cells by inhibiting RhoA-dependent Smad3 phosphorylation*. Hepatology, 2010. **52**(6): p. 2053-2064.
 172. Initiative, T.I.S.C., *Characterization of human embryonic stem cell lines by the International Stem Cell Initiative*. Nat Biotech, 2007. **25**(7): p. 803-816.
 173. Zhou, S., et al., *The ABC transporter Bcrp1/ABCG2 is expressed in a wide variety of stem cells and is a molecular determinant of the side-population phenotype*. Nat Med, 2001. **7**(9): p. 1028-1034.
 174. Ding, X.-w., J.-h. Wu, and C.-p. Jiang, *ABCG2: A potential marker of stem cells and novel target in stem cell and cancer therapy*. Life Sciences, 2010. **86**(17-18): p. 631-637.
 175. Ozerdem, U., et al., *NG2 proteoglycan is expressed exclusively by mural cells during vascular morphogenesis*. Developmental Dynamics, 2001. **222**(2): p. 218-227.
 176. Stallcup, W.B., *The NG2 proteoglycan: Past insights and future prospects*. Journal of Neurocytology, 2002. **31**(6): p. 423-435.
 177. Dahlke, M., et al., *The biology of CD45 and its use as a therapeutic target*. Leuk Lymphoma. , 2004. **45**(2): p. 229-36.
 178. Doyle, M.J., et al., *Abcg2 labels multiple cell types in skeletal muscle and participates in muscle regeneration*. The Journal of Cell Biology, 2011. **195**(1): p. 147-163.
 179. Wylie-Sears, J., et al., *Mitral Valve Endothelial Cells With Osteogenic Differentiation Potential*. Arteriosclerosis, Thrombosis, and Vascular Biology, 2011. **31**(3): p. 598-607.

180. Bischoff, J. and E. Aikawa, *Progenitor Cells Confer Plasticity to Cardiac Valve Endothelium*. Journal of Cardiovascular Translational Research, 2011. **4**(6): p. 710-719.
181. Gilbert, P.M. and H.M. Blau, *Engineering a stem cell house into a home*. Stem Cell Res Ther., 2011. **2**(1): p. 3.
182. Lepper, C., T.A. Partridge, and C.-M. Fan, *An absolute requirement for Pax7-positive satellite cells in acute injury-induced skeletal muscle regeneration*. Development, 2011. **138**(17): p. 3639-3646.
183. Tirelli, N., et al., *Poly(ethylene glycol) block copolymers*. Reviews in Molecular Biotechnology, 2002. **90**(1): p. 3-15.
184. Ramaswamy, S., et al., *Regulation of G1 progression by the PTEN tumor suppressor protein is linked to inhibition of the phosphatidylinositol 3-kinase/Akt pathway*. Proceedings of the National Academy of Sciences, 1999. **96**(5): p. 2110-2115.
185. Maass, A., et al., *Rational promoter selection for gene transfer into cardiac cells*. Journal of Molecular and Cellular Cardiology, 2003. **35**(7): p. 823-831.
186. Discher, D.E., D.J. Mooney, and P.W. Zandstra, *Growth Factors, Matrices, and Forces Combine and Control Stem Cells*. Science, 2009. **324**(5935): p. 1673-1677.
187. Lander, A., et al., *What does the concept of the stem cell niche really mean today?* BMC Biology, 2012. **10**(1): p. 19.
188. Lee, G.Y., et al., *Three-dimensional culture models of normal and malignant breast epithelial cells*. Nat Meth, 2007. **4**(4): p. 359-365.
189. Tilghman, R.W., et al., *Matrix Rigidity Regulates Cancer Cell Growth and Cellular Phenotype*. PLoS ONE, 2010. **5**(9): p. e12905.
190. Thannickal, V.J., et al., *Myofibroblast Differentiation by Transforming Growth Factor-beta1 Is Dependent on Cell Adhesion and Integrin Signaling via Focal Adhesion Kinase*. Journal of Biological Chemistry, 2003. **278**(14): p. 12384-12389.
191. Wang, J., et al., *Mechanical force regulation of myofibroblast differentiation in cardiac fibroblasts*. American Journal of Physiology - Heart and Circulatory Physiology, 2003. **285**(5): p. H1871-H1881.
192. Conte, E., et al., *Inhibition of PI3K Prevents the Proliferation and Differentiation of Human Lung Fibroblasts into Myofibroblasts: The Role of Class I P110 Isoforms*. PLoS ONE, 2011. **6**(10): p. e24663.

193. Cantley, L.C., *The Phosphoinositide 3-Kinase Pathway*. Science, 2002. **296**(5573): p. 1655-1657.
194. Vanhaesebroeck, B., L. Stephens, and P. Hawkins, *PI3K signalling: the path to discovery and understanding*. Nat Rev Mol Cell Biol, 2012. **13**(3): p. 195-203.
195. Vanhaesebroeck, B., et al., *The emerging mechanisms of isoform-specific PI3K signalling*. Nature Reviews Molecular Cell Biology, 2010. **11**: p. 329-341.
196. Sakamoto, K., et al., *Akt signaling in skeletal muscle: regulation by exercise and passive stretch*. American Journal of Physiology - Endocrinology And Metabolism, 2003. **285**(5): p. E1081-E1088.
197. Pardo, P.S., M.A. Lopez, and A.M. Boriek, *FOXO transcription factors are mechanosensitive and their regulation is altered with aging in the respiratory pump*. American Journal of Physiology - Cell Physiology, 2008. **294**(4): p. C1056-C1066.
198. Condorelli, G., et al., *Akt induces enhanced myocardial contractility and cell size in vivo in transgenic mice*. Proceedings of the National Academy of Sciences, 2002. **99**(19): p. 12333-12338.
199. Reif, K., et al., *Phosphatidylinositol 3-kinase signals activate a selective subset of Rac/Rho-dependent effector pathways*. Current biology : CB, 1996. **6**(11): p. 1445-1455.
200. Uhal, B.D., *The role of apoptosis in pulmonary fibrosis*. European Respiratory Review, 2008. **17**(109): p. 138-144.
201. Datta, S.R., et al., *Akt Phosphorylation of BAD Couples Survival Signals to the Cell-Intrinsic Death Machinery*. Cell, 1997. **91**(2): p. 231-241.
202. Peso, L.d., et al., *Interleukin-3-Induced Phosphorylation of BAD Through the Protein Kinase Akt*. Science, 1997. **278**(5338): p. 687-689.
203. Brunet, A., et al., *Akt Promotes Cell Survival by Phosphorylating and Inhibiting a Forkhead Transcription Factor*. Cell, 1999. **96**(6): p. 857-868.
204. Biggs, W.H., et al., *Protein kinase B/Akt-mediated phosphorylation promotes nuclear exclusion of the winged helix transcription factor FKHR1*. Proceedings of the National Academy of Sciences, 1999. **96**(13): p. 7421-7426.
205. Kulasekaran, P., et al., *Endothelin-1 and Transforming Growth Factor-beta1 Independently Induce Fibroblast Resistance to Apoptosis via AKT Activation*. American

- Journal of Respiratory Cell and Molecular Biology, 2009. **41**(4): p. 484-493.
206. Guo, W., et al., *Abrogation of TGF-beta1-induced fibroblast-myofibroblast differentiation by histone deacetylase inhibition*. American Journal of Physiology - Lung Cellular and Molecular Physiology, 2009. **297**(5): p. L864-L870.
 207. Lau, M., C. Klausen, and P. Leung, *E-cadherin inhibits tumor cell growth by suppressing PI3K/Akt signaling via beta-catenin-Egr1-mediated PTEN expression*. Oncogene, 2011. **39**(24): p. 2753-66.
 208. Bader, A. and P. Macchiarini, *Moving towards in situ tracheal regeneration: the bionic tissue engineered transplantation approach*. Journal of Cellular and Molecular Medicine, 2010. **14**(7): p. 1877-1889.
 209. Mase, V.J., et al., *Clinical application of an acellular biologic scaffold for surgical repair of a large, traumatic quadriceps femoris muscle defect*. Orthopedics, 2010. **33**(7): p. 511.
 210. Young, J.L. and A.J. Engler, *Hydrogels with time-dependent material properties enhance cardiomyocyte differentiation in vitro*. Biomaterials, 2011. **32**(4): p. 1002-1009.
 211. Tibbitt, M.W. and K.S. Anseth, *Hydrogels as extracellular matrix mimics for 3D cell culture*. Biotechnology and Bioengineering, 2009. **103**(4): p. 655-663.
 212. McIntosh, J.C., et al., *Thy1 (+) and (-) lung fibrosis subpopulations in LEW and F344 rats*. European Respiratory Journal, 1994. **7**(12): p. 2131-2138.
 213. Rice, N.A. and L.A. Leinwand, *Skeletal myosin heavy chain function in cultured lung myofibroblasts*. The Journal of Cell Biology, 2003. **163**(1): p. 119-129.
 214. Fondard, O., et al., *Extracellular matrix remodelling in human aortic valve disease: the role of matrix metalloproteinases and their tissue inhibitors*. European Heart Journal, 2005. **26**(13): p. 1333-1341.
 215. Duffield, J.S., et al., *Host Responses in Tissue Repair and Fibrosis*. Annual Review of Pathology: Mechanisms of Disease, 2012. **8**(1): p. 241-276.
 216. Hinz, B., et al., *Recent Developments in Myofibroblast Biology: Paradigms for Connective Tissue Remodeling*. The American Journal of Pathology, 2012. **180**(4): p. 1340-1355.
 217. Wynn, T.A., *Cellular and molecular mechanisms of fibrosis*. The Journal of Pathology, 2008. **214**(2): p. 199-210.

218. Biernacka, A., M. Dobaczewski, and N.G. Frangogiannis, *TGF-beta signaling in fibrosis*. Growth Factors, 2011. **29**(5): p. 196-202.
219. Niessen, C.M., D. Leckband, and A.S. Yap, *Tissue Organization by Cadherin Adhesion Molecules: Dynamic Molecular and Cellular Mechanisms of Morphogenetic Regulation*. Physiological Reviews, 2011. **91**(2): p. 691-731.
220. Bosse, T., et al., *Cdc42 and Phosphoinositide 3-Kinase Drive Rac-Mediated Actin Polymerization Downstream of c-Met in Distinct and Common Pathways*. Molecular and Cellular Biology, 2007. **27**(19): p. 6615-6628.
221. Michelle, A.U., et al., *Soluble N-cadherin stimulates fibroblast growth factor receptor dependent neurite outgrowth and N-cadherin and the fibroblast growth factor receptor co-cluster in cells*. Journal of Neurochemistry, 2001. **76**(5): p. 1421-1430.
222. Kiener, H.P., et al., *The Cadherin-11 Cytoplasmic Juxtamembrane Domain Promotes alpha-Catenin Turnover at Adherens Junctions and Intercellular Motility*. Molecular Biology of the Cell, 2006. **17**(5): p. 2366-2376.
223. Massague, J., *How cells read TGF-[beta] signals*. Nat Rev Mol Cell Biol, 2000. **1**(3): p. 169-178.
224. Khalil, N., et al., *Regulation of alveolar macrophage transforming growth factor-beta secretion by corticosteroids in bleomycin-induced pulmonary inflammation in the rat*. The Journal of Clinical Investigation, 1993. **92**(4): p. 1812-1818.
225. Flanders, K.C., et al., *Mice Lacking Smad3 Are Protected Against Cutaneous Injury Induced by Ionizing Radiation*. The American Journal of Pathology, 2002. **160**(3): p. 1057-1068.
226. Zhao, J., et al., *Smad3 deficiency attenuates bleomycin-induced pulmonary fibrosis in mice*. American Journal of Physiology - Lung Cellular and Molecular Physiology, 2002. **282**(3): p. L585-L593.
227. Renzoni, E., et al., *Gene expression profiling reveals novel TGFbeta targets in adult lung fibroblasts*. Respiratory Research, 2004. **5**(1): p. 24.
228. Chakravarti, S., et al., *Microarray Studies Reveal Macrophage-like Function of Stromal Keratocytes in the Cornea*. Investigative Ophthalmology & Visual Science, 2004. **45**(10): p. 3475-3484.
229. Serini, G., et al., *The Fibronectin Domain ED-A Is Crucial for Myofibroblastic Phenotype Induction by Transforming Growth Factor-beta1*. The Journal of Cell Biology, 1998.

- 142(3):** p. 873-881.
230. Shi-Wen, X., A. Leask, and D. Abraham, *Regulation and function of connective tissue growth factor/CCN2 in tissue repair, scarring and fibrosis*. Cytokine & growth factor reviews, 2008. **19(2):** p. 133-144.
231. Li, L., et al., *The human cadherin 11 is a pro-apoptotic tumor suppressor modulating cell stemness through Wnt/[beta]-catenin signaling and silenced in common carcinomas*. Oncogene, 2012. **31(34):** p. 3901-12.
232. Wheelock, M.J. and K.R. Johnson, *Cadherin-mediated cellular signaling*. Current Opinion in Cell Biology, 2003. **15(5):** p. 509-514.
233. Watanabe, T., K. Sato, and K. Kaibuchi, *Cadherin-mediated Intercellular Adhesion and Signaling Cascades Involving Small GTPases*. Cold Spring Harbor Perspectives in Biology, 2009. **1(3):** p. a003020.
234. Charrasse, S., et al., *N-cadherin-dependent cell-cell contact regulates Rho GTPases and beta-catenin localization in mouse C2C12 myoblasts*. The Journal of Cell Biology, 2002. **158(5):** p. 953-965.
235. Orsulic, S., et al., *E-cadherin binding prevents beta-catenin nuclear localization and beta-catenin/LEF-1-mediated transactivation*. Journal of Cell Science, 1999. **112(8):** p. 1237-1245.
236. Carthy, J.M., et al., *Wnt3a Induces Myofibroblast Differentiation by Upregulating TGF-beta Signaling Through SMAD2 in a beta-Catenin-Dependent Manner*. PLoS ONE, 2011. **6(5):** p. e19809.
237. Margadant, C. and A. Sonnenberg, *Integrin-TGF-[beta] crosstalk in fibrosis, cancer and wound healing*. EMBO Rep, 2010. **11(2):** p. 97-105.
238. Hinz, B. and G. Gabbiani, *Cell-matrix and cell-cell contacts of myofibroblasts: role in connective tissue remodeling*. Thrombosis and Haemostasis, 2003. **90(6):** p. 993-1002.
239. Zheng, G., et al., *Disruption of E-Cadherin by Matrix Metalloproteinase Directly Mediates Epithelial-Mesenchymal Transition Downstream of Transforming Growth Factor-beta1 in Renal Tubular Epithelial Cells*. The American Journal of Pathology, 2009. **175(2):** p. 580-591.
240. Hammerick, K.E., et al., *Elastic Properties of Induced Pluripotent Stem Cells*. Tissue Engineering Part A, 2011. **17(3-4):** p. 495-502.

241. Dulauroy, S., et al., *Lineage tracing and genetic ablation of ADAM12+ perivascular cells identify a major source of profibrotic cells during acute tissue injury*. Nat Med, 2012. **18**(8): p. 1262-1270.
242. Trappmann, B., et al., *Extracellular-matrix tethering regulates stem-cell fate*. Nat Mater, 2012. **11**(7): p. 642-649.
243. Gould, S.T., N.J. Darling, and K.S. Anseth, *Small peptide functionalized thiol-ene hydrogels as culture substrates for understanding valvular interstitial cell activation and de novo tissue deposition*. Acta Biomaterialia, 2012. **8**(9): p. 3201-3209.
244. Benton, J.A., H.B. Kern, and K.S. Anseth, *Substrate Properties Influence Calcification in Valvular Interstitial Cell Culture*. J Heart Valve Dis., 2008. **17**(6): p. 689-699.
245. Jiang, X., et al., *MicroRNAs and the regulation of fibrosis*. FEBS Journal, 2010. **277**(9): p. 2015-2021.